

The Exploitation of Opsin-based Optogenetic Tools for Application in Higher Plants



Doctoral thesis for a doctoral degree
in Julius-Maximilians-Universität Würzburg

Yang Zhou
From Henan, China

Würzburg, 2021



Submitted on:

Office stamp

Members of the Promotionskomitee:

Chairperson:

Primary Supervisor: Prof. Dr. Georg Nagel

Secondary Supervisor: Prof. Dr. Wolfgang Dröge-Laser

Date of Public Defense:

Date of Receipt of Certificates:

Contents

Summary	1
Zusammenfassung.....	3
1. Introduction.....	5
1.1 History of optogenetics	5
1.2 Introduction of rhodopsin	8
1.3 Channelrhodopsins.....	10
1.3.1 Light-gated cation channels	10
1.3.2 light-gated anion channels	12
1.4. Light-gated ion pumps	13
1.4.1 light-gated chloride pump	13
1.4.2 light-gated proton pump.....	14
1.4.3 light-gated sodium pump	15
1.5 Optogenetics in higher plants.....	16
1.5.1 Non-opsin-based optogenetics in higher plants	16
1.5.2 Microbial opsin-based optogenetics in higher plants.....	18
2. Results.....	20
2.1 Producing retinal and screening opsins in higher plants.....	20
2.1.1 Producing retinal in <i>N. benthamiana</i>	20
2.1.2 The expression of Ret-eYFP in transgenic <i>N. tabacum</i>	22
2.1.3 The screening of opsins in plants.....	25
2.1.4 Discussion	26
2.2 The expression and function of ACR1 in higher plants.....	30
2.2.1 Introduction.....	30
2.2.2 Expression of ACR1 in <i>N. benthamiana</i>	30
2.2.3 Expression of ACR1 in transgenic <i>N. tabacum</i>	32
2.2.4 The phenotype of transgenic <i>N. tabacum</i> plants expressing ACR1	32
2.2.5 Discussion	35
2.3 The expression and function of Chr2-XXM in higher plants.....	38
2.3.1 Introduction.....	38
2.3.2 The expression and function of XXM in <i>N. benthamiana</i>	38
2.3.3 The expression and function of XXM in the <i>N. tabacum</i>	41
2.3.4 The phenotype of Ret-XXM 2.0-expressing <i>N. tabacum</i>	43
2.3.5 Discussion	44
2.4 The expression and function of PPR (proton pump rhodopsin)	47
2.4.1 Introduction.....	47
2.4.2 The expression and function of PPR in <i>N. benthamiana</i>	47
2.4.3 The expression and function of PPR in <i>N. tabacum</i>	48
2.4.5 Discussion	49
3. Conclusion and Prospect.....	51
4. Supplementary	56
5. Materials and Methods.....	73

5.1. Molecular cloning	73
5.2 Agrobacterium transformation	73
5.3 Protoplast isolation and transformation	74
5.4 Transient expression in <i>N. benthamiana</i>	76
5.5 Aequorin-based Luminescence measurements	77
5.6 Agrobacterium-mediated transformation of <i>N. tabacum</i>	77
5.7 Growth conditions for transgenic <i>N. tabacum</i>	78
5.8 Confocal Microscopy and Image Processing.....	79
5.9 All-trans-retinal and carotenoids measurement	79
5.10 Chlorophylls extraction.....	80
5.11 Plant growth experiment	81
5.12 Cuticular wax analysis	81
5.13 Agrobacterium-mediated transformation of <i>A. thaliana</i>	82
5.14 Membrane voltage recordings in mesophyll cells	82
5.15 Chlorophyll fluorescence measurements	83
5.16 Significance analysis.....	83
6. Reference	84
Declaration of independence.....	93
Acknowledgments.....	94
Curriculum Vitae.....	95

Summary

The discovery, heterologous expression, and characterization of channelrhodopsin-2 (ChR2) – a light-sensitive cation channel found in the green alga *Chlamydomonas reinhardtii* – led to the success of optogenetics as a powerful technology, first in neuroscience. ChR2 was employed to induce action potentials by blue light in genetically modified nerve cells. In optogenetics, exogenous photoreceptors are expressed in cells to manipulate cellular activity. These photoreceptors were in the beginning mainly microbial opsins. During nearly two decades, many microbial opsins and their mutants were explored for their application in neuroscience. Until now, however, the application of optogenetics to plant studies is limited to very few reports. Several optogenetic strategies for plant research were demonstrated, in which most attempts are based on non-opsin optogenetic tools. Opsins need retinal (vitamin A) as a cofactor to generate the functional protein, the rhodopsin. As most animals have eyes that contain animal rhodopsins, they also have the enzyme - a 15, 15'-Dioxygenase - for retinal production from food-supplied provitamin A (beta-carotene). However, higher plants lack a similar enzyme, making it difficult to express functional rhodopsins successfully in plants. But plant chloroplasts contain plenty of beta-carotene. I introduced a gene, coding for a 15, 15'-Dioxygenase with a chloroplast target peptide, to tobacco plants. This enzyme converts a molecule of β -carotene into two of all-trans-retinal. After expressing this enzyme in plants, the concentration of all-trans-retinal was increased greatly. The increased retinal concentration led to increased expression of several microbial opsins, tested in model higher plants. Unfortunately, most opsins were observed intracellularly and not in the plasma membrane. To improve their localization in the plasma membrane, some reported signal peptides were fused to the N- or C-terminal end of opsins. Finally, I helped to identify three microbial opsins -- *GtACR1* (a light-gated anion channel), ChR2 (a light-gated cation channel), PPR (a light-gated proton pump) which express and work well in the plasma membrane of plants. The transgene plants were grown under red light to prevent activation of the expressed

opsins. Upon illumination with blue or green light, the activation of these opsins then induced the expected change of the membrane potential, dramatically changing the phenotype of plants with activated rhodopsins.

This study is the first which shows the potential of microbial opsins for optogenetic research in higher plants, using the *ubq10* promoter for ubiquitous expression. I expect this to be just the beginning, as many different opsins and tissue-specific promoters for selective expression now can be tested for their usefulness. It is further to be expected that the here established method will help investigators to exploit more optogenetic tools and explore the secrets, kept in the plant kingdom.

Zusammenfassung

Die Entdeckung, heterologe Expression und Charakterisierung von Channelrhodopsin-2 (ChR2) - einem lichtempfindlichen Kationenkanal, der in der Grünalge *Chlamydomonas reinhardtii* vorkommt - führte zum Erfolg der Optogenetik als leistungsfähige Technologie, zunächst in den Neurowissenschaften. ChR2 wurde eingesetzt, um in genetisch veränderten Nervenzellen durch blaues Licht Aktionspotentiale zu induzieren. Bei der Optogenetik werden exogene Photorezeptoren in Zellen exprimiert, um die zelluläre Aktivität zu manipulieren. Diese Photorezeptoren waren anfangs hauptsächlich mikrobielle Opsine. Im Laufe von fast zwei Jahrzehnten wurden viele mikrobielle Opsine und ihre Mutanten für ihre Anwendung in den Neurowissenschaften erforscht. Bis jetzt ist die Anwendung der Optogenetik in der Pflanzenforschung jedoch auf sehr wenige Arbeiten beschränkt. Es wurden mehrere optogenetische Strategien für die Pflanzenforschung aufgezeigt, wobei die meisten Versuche auf optogenetischen Werkzeugen, die nicht Opsine sind, beruhen. Opsine benötigen Retinal (Vitamin A) als Kofaktor, um das funktionelle Protein, das Rhodopsin, zu generieren. Da die meisten Tiere Augen haben, die tierische Rhodopsine enthalten, verfügen sie auch über das Enzym - eine 15, 15'-Dioxygenase - zur Retinalproduktion aus mit der Nahrung zugeführtem Provitamin A (Beta-Carotin). Höheren Pflanzen fehlt jedoch ein ähnliches Enzym, was es schwierig macht, funktionale Rhodopsine erfolgreich in Pflanzen zu exprimieren. Aber die Chloroplasten der Pflanzen enthalten reichlich Beta-Carotin. Ich führte ein Gen, das für eine 15, 15'-Dioxygenase mit einem Chloroplasten-Zielpeptid kodiert, in Tabakpflanzen ein. Dieses Enzym wandelt ein Molekül β -Carotin in zwei Moleküle all-trans-Retinal um. Nach Expression dieses Enzyms in Pflanzen wurde die Konzentration von all-trans-Retinal stark erhöht. Die erhöhte Retinalkonzentration führte zu einer verstärkten Expression von mehreren mikrobiellen Opsinen, die in höheren Modellpflanzen getestet wurden. Leider wurden die meisten Opsine intrazellulär und nicht in der Plasmamembran beobachtet. Um ihre Lokalisierung in der Plasmamembran zu verbessern, wurden

einige publizierte Signalpeptide an das N- oder C-terminale Ende der Opsine fusioniert. Schließlich trug ich dazu bei, drei mikrobielle Opsine – GtACR1 (ein lichtgesteuerter Anionenkanal), ChR2 (ein lichtgesteuerter Kationenkanal) und PPR (eine lichtgesteuerte Protonenpumpe) – zu identifizieren, die in der Plasmamembran von Pflanzenzellen gut exprimierten und zu starken Lichtsignalen führten. Die transgenen Pflanzen wurden unter rotem Licht aufgezogen, um die Aktivierung der exprimierten Opsine zu verhindern. Bei Beleuchtung mit blauem oder grünem Licht löste die Aktivierung dieser Opsine dann die erwartete Änderung des Membranpotentials aus, was den Phänotyp der Pflanzen mit aktivierten Rhodopsinen dramatisch veränderte.

Diese Studie ist die erste, die das Potenzial von mikrobiellen Opsinen für die optogenetische Forschung in höheren Pflanzen zeigt, wobei der ubq10-Promotor für die ubiquitäre Expression verwendet wurde. Ich erwarte, dass dies erst der Anfang ist, da nun viele verschiedene Opsine und gewebespezifische Promotoren für die selektive Expression auf ihre Nützlichkeit getestet werden können. Es ist davon auszugehen, dass die hier etablierte Methode Forschern helfen wird, weitere Opsin-basierte optogenetische Werkzeuge zu nutzen und die Geheimnisse zu ergründen, die im Pflanzenreich gehütet werden.

1. Introduction

1.1 History of optogenetics

From 2006, the term “optogenetics” was known by more and more biological researchers in neuroscience. Citing Prof. Nagel’s word in the foreword for the book “Optogenetics” -- “Optogenetics is an illuminating and a very simple, straightforward concept: a heterologously expressed (i.e. **genetically** encoded) protein is activated by illumination (**Opto**)” [1]. Optogenetics combines different technologies from optics, genetics, and bioengineering. Generally, this method employs microbial proteins, known as opsins (channels or pumps), to express in a specific cell type, because these opsins can be activated by light when illuminating the targeted cell with defined light parameters to achieve the control of cellular activity. Due to its advantage in temporal and spatial precision, optogenetics is applied in the research on neurons widely. However, it has experienced a long period of development before the wide application. The idea using light to control cell activity was from Francis Crick in 1979. He speculated that light could be useful to control all cells from one type in the brain in time and space [2]. Following this idea, in 1993, LC Katz and E Callaway achieved to uncage glutamate by light [3]. In the next year, Heberle and Büldt showed the ion flow induced by bacteriorhodopsin (a proton pump) with a heterologous expression upon light illumination [4], but the first light-induced current came from the bacteriorhodopsin when it was successfully expressed in *Xenopus laevis* oocytes, at the same time, the direct electrophysiological methods were applied in the research [5]. After that, in 2002 the genetically targeted method was explored to control rhodopsin-sensitized neurons in cultured *Drosophila* with light by Boris Zemelman and Gero Miesenböck [6]. Besides, Zemelman and Miesenböck also developed another method that used single inotropic channels TRPV1, TRPM8 and P2X2 to regulate activation of neurons by light [7]. Though it was irreversible, several groups used this method to alter feeding, locomotion, and behavioral resilience in laboratory animals [8-10]. However, all these methods were short of precision in time and space, and the evaluation of

potential damage to the tissue or cells was difficult. Thus, the scientists were thinking about whether there are natural proteins that could be controlled by light.

Light-sensitive proteins have been found early, but they were not used as light switches. In 1973, the bacteriorhodopsin was demonstrated that could generate and maintain a proton gradient across the cell membrane when exposed to light [11]. After that, Halorhodopsin (a chloride pump) was also discovered and was activated by light which pumps chloride to the outside of the cell [12]. However, the real turning point of optogenetics was from the discovery and functional verification of Channelrhodopsins (Channelrhodopsin-1 and Channelrhodopsin-2). When Georg Nagel was at Max Planck Institute in Frankfurt, he cooperated with Peter Hegemann who studied the light response of green algae. They found the complementary DNA sequence for a microbial opsin-related protein in an EST data bank for the green alga *Chlamydomonas reinhardtii*. This protein, when expressed in oocytes, showed characteristics of a channel selectively permeable for protons in the presence of all-trans-retinal (hereinafter referred to as retinal), and later it was proven that it also enabled permeation of other cations. They termed this protein as Channelrhodopsin-1 (ChR1) [13]. Also, to confirm the expression of the protein in the cell, they replaced the cytoplasmic tail of the algal protein with the Yellow fluorescent protein (YFP), which did not affect the function of proteins [13]. After the ChR1, another protein, termed Channelrhodopsin-2 (ChR2), was discovered [14]. ChR2 was proven as a directly blue light-switched cation-selective ion channel. This channel opened rapidly after the absorption of a photon to generate a large permeability for monovalent and divalent cations. In their publication, they commented that ChR2 “should become a useful tool to manipulate intracellular Ca^{2+} concentration or membrane potential, especially in mammalian cells” [14]. After the publication of ChR2, the revolution of optogenetics was started and the application in neurosciences began to take off. Several researchers realized the prospect of ChR2. In 2005, Karl Deisseroth's laboratory got the ChR2 clone from Georg Nagel and demonstrated the reliable, millisecond-timescale control of neuronal spiking firstly [15].

The name “optogenetics” was first proposed for the light-induced depolarization of cells via Channelrhodopsin-2 [1]. In fact, before this work, another scientist-- Zhuohua Pan of Wayne State University first observed the optical activation of retinal neurons in which ChR2 was expressed in August 2004. He reported that he achieved the successful transfection of ChR2 in retinal ganglion cells of living mice and recorded the electrical responses to photo-stimulation in retinal slice culture [16]. From 2005, there were more and more groups focused on the application of ChR2, then the related research showed blowout growth (**fig. 1**), for example, in 2005, Lynn Landmesser and Stefan Herlitze could control neuronal activity in cultured hippocampal neurons and chicken spinal cord circuits in intact developing embryos with ChR2 [17]; The groups of Alexander Gottschalk and Georg Nagel firstly used ChR2 to control the motor patterns in the *Caenorhabditis Elegans* (*C. Elegans*) by light stimulation [18]. The successful application of ChR2 made the scientists transfer their attention to the inhibition of cell activity—optogenetic inhibitors. In 2007, basis on the pre-work on Halorhodopsin, the scientists reported successful optogenetic inhibition of activity in neurons. In the work, they showed the light-induced inhibition of action potentials and the swimming of *C. elegans* [19]. In 2015, Elena G. Govorunova et al report natural light-gated anion channels from the cryptophyte alga *Guillardia theta* (*GtACRs*) which provided efficient membrane hyperpolarization and neuronal silencing, due to increased chloride conductance upon illumination [20]. Except for these light-sensitive channels or pumps, other kinds of optogenetic tools were discovered and exploited for applications, for example, a soluble light-activated adenylyl cyclase [21]. The first 8-TM enzyme rhodopsin which has the activity of light-activated production of cGMP was characterized by Dr. Shiqiang Gao in 2015 [22]. In parallel to the development of optogenetic actuators, optogenetic sensors were also developed, such as genetically encoded voltage indicators (GEVIs), eFRET-GEVIs for image activity [23-26]. So far, optogenetic sensors are used widely throughout neuroscience. In this research, I mostly focus on the application of microbial opsins (channels and pumps) in plants, so there will not be much introduction about the sensors and enzymes.

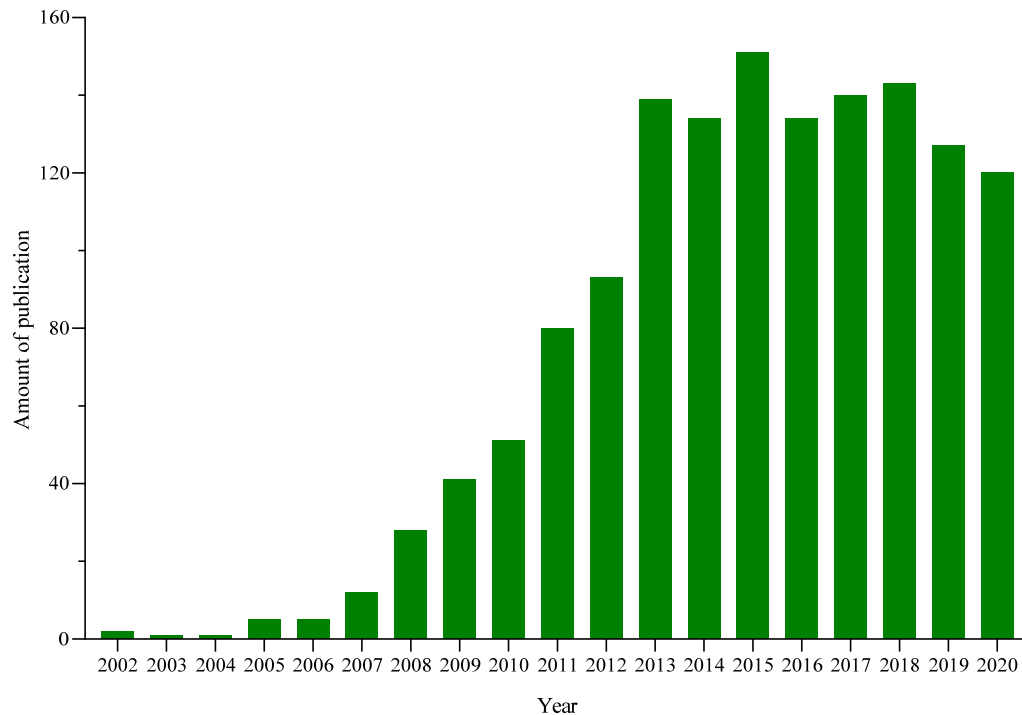


Figure. 1. A bar diagram example showed the increase of publications containing the “channelrhodopsin” as a keyword from 2002 to 2020, the search report is from the “web of science”.

1.2 Introduction of rhodopsin

From bacteria to human beings, the organism responds to light by photoreceptors called rhodopsins which consist of opsins and the light-sensitive chromophore retinal. According to the primary sequence and mode of action, opsins could be categorized as microbial opsins (type I) and animal opsins (type II). Type I opsins are from prokaryotes, algae, and fungi. Type II opsins are from animals and humans. Although the microbial-type and animal opsins share no sequence similarity, they are both seven transmembranes (TM) helices proteins and bind covalently to the retinal to mediate the response to light. The retinal binds to a lysine amino acid in the seventh TM domain by a Schiff base (RSB). Usually, the RSB is protonated ($RSBH^+$), and changes in the protonation state are integral to the signaling or transport activity of rhodopsins [27]. Microbial opsins are commonly used in optogenetics. They include pumps and channels. Microbial rhodopsins contain all-trans-retinal in the ground state. Upon illumination, the isomerization of retinal configuration is from all-trans state to 13-cis state [27, 28] (**fig. 2a**), then leads to the conformation change of opsins, which will induce the

transmembrane ionic fluxes to depolarize or hyperpolarize the cell membrane potential. These light-induced membrane potential changes result in neuronal excitation or silencing on a millisecond time scale. Animal opsins are G-protein coupled receptors (GPCR) and they only exist in eumetazoan animals [27]. They mainly participate in visual and nonvisual phototransduction, for example, the regulation of the circadian clock [29]. For the animal opsins, the chromophore is 11-cis-retinal in the ground state, the retinal configuration changes from 11-cis to all-trans [27] (**fig. 2a**). Upon illumination, they induce the protein conformational changes which result in the response to light. Due to the widespread application of microbial opsins, in this study, we mainly focus on the exploitation of optogenetic tools based on microbial opsins in plant science.

Initially, researchers tend to search for the naturally occurring opsins, but elucidation of the crystal structure of opsin proteins makes more and more available optogenetic tools be generated by genetic engineering. These engineered opsins have different properties, such as specific ion conductance, faster kinetics, higher light sensitivity, red-shifted spectrum, and so on. At present, optogenetics is added to novel techniques for exploring the mystery in the brain and it improved the development of neuroscience tremendously.

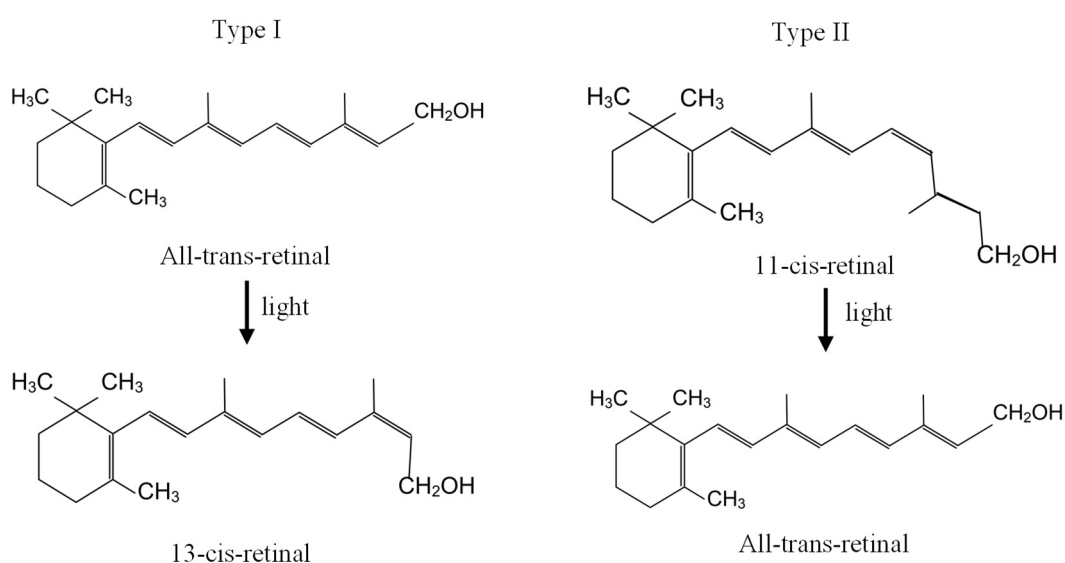


Figure. 2: Retinal and its photoisomerization in type I and type II opsins, respectively

1.3 Channelrhodopsins

1.3.1 Light-gated cation channels

Channelrhodopsins are light-sensitive proteins from fresh green algae *Chlamydomonas reinhardtii*, such as *CrChR1* [13]. and *CrChR2* [14] (*Cr* represents the genus *Chlamydomonas* and species *reinhardtii* of the organism from which the rhodopsin originates, followed by the gene number or possible mutations. In the next text, their common abbreviation will be given). In the algae, the ChRs act as photoreceptors that localize in the “eyespot” to find the optimal light conditions for photosynthesis [30]. At present, ChR2 is the superstar in neuroscience, in our study, we also focus on its application in plants. ChR2 has a 7-TM structure (**fig. 3a**) in which a large C-terminal is in the cytoplasm and the N-terminal domain is outside of the cell. The truncation of ChR2 from 737 amino acids to 315 would not affect the function of the protein. This is the first improvement of natural ChR2 as an optogenetic tool [14, 31]. When YFP was fused to the C-terminal domain of ChR2, ChR2 still could show the normal function [18].

After the discovery and application of ChR2, the natural and engineered ChRs came out rapidly (**fig. 3b**). However, many of these new optogenetic tools did not improve the application. In the following content, some important variants or discovered natural ChRs which are valuable for the users will be introduced.

The first mutant of ChR2 is H134R (histidine to arginine mutation at position 134) which causes larger stationary photocurrents in comparison to wild-type ChR2 (ChR2-wt) [18]. Expression in the HKE-cells, this mutant could induce a large and fast light-induced membrane depolarization. Besides, when it was expressed in muscles or mechanosensory neurons of *C. elegans*, the worm showed body contractions in the defined times and behavioral response under light illumination. So far, this mutant is still one of the widely used optogenetic tools. Another important mutant of ChR2, I

think, is the T159C (threonine is replaced by cysteine) [32], which enhances resistance to degradation in the absence of retinal. In some expression systems, there is not enough retinal for the function of opsins, such as *C. elegans* and *D. melanogaster* [31, 33]. The ChR2-wt needed all-trans-retinal to function. In the absence of retinal, ChR2-T159C still could induce a large photocurrent and showed an increased affinity for endogenous all-trans-retinal [34]. Though these mutants were better than ChR2-wt, there were a lot of application constraints in living adult animals. For example, H134R mediated large photocurrent in larvae, but there was not much improvement in adult flies and the ChR2-wt has the same situation as H134R [35-38]. Other variants, such as C128T [39], red-shifted ChRs – ReaChR [40], also encountered problems to some extent when they were employed in flies. In 2014, the mutant ChR2-D156C (Aspartic acid was replaced with Cysteine at position 156), termed XXL, was engineered. Compared with other variants, this mutant is more sensitive to light and displays increased expression, improved subcellular localization, elevated retinal affinity, an extended open-state lifetime, and photocurrent amplitudes, which made it the most appropriate optogenetic tool in the research of flies [41]. As the extension of the application, ChRs with higher Ca^{2+} conductance are demanded. Although XXL had been successfully applied, however, it only influenced slightly Na^+ and Ca^{2+} conductance. In 2017, a mutant ChR2-D156H (Aspartic acid was replaced with Histidine at position 156), showed strong expression without retinal supplementation in *Xenopus* oocytes and had larger photocurrents and medium open state. It could evoke normal activity in *dCirl^{KO}* larvae [42]. XXM showed enhanced Na^+ and Ca^{2+} conductance, so it could be employed as a powerful optogenetic tool for Ca^{2+} manipulation [43]. Afterward, based on the XXL and XXM mutants, some new double mutants combining H134 and D156 point mutants were engineered in Nagel's group, termed XXL 2.0 and XXM 2.0 (data not published). These double mutants have improved characteristics compared to point mutants, and this is also the one reason why we choose the XXL 2.0 and XXM 2.0 as the ultimate tools for the application in plants in this study.

1.3.2 light-gated anion channels

Except for the cation channelrhodopsins introduced above, some channelrhodopsins were applied as optogenetic tools to hyperpolarize membrane potential. At first, chloride pumps—*NpHR* was employed to inhibit neuronal firing as the optogenetic tool, which hyperpolarizes the membrane potential by inducing Cl^- influx [19]. However, pumps have limited efficiency, in which there is only one charge per captured photon. Though they are utilized as light-inhibited tools to silence neurons in live animals, they needed very high-density expression and intense light [44-46]. To overcome these disadvantages, new mutants from cation ChRs with anion permeability were created as inhibitory tools [47-50]. However, these mutants still keep some cation conductance and have no high light sensitivity [47, 48].

In 2015, the naturally occurring anion channelrhodopsins (ACRs) were discovered from the cryptophyte algae *Guillardia theta* (termed *GtACRs*) (**fig. 3a**). Compared with previous inhibitory tools, *GtACRs* have obvious advantages, such as the fast photocycle, the strict anion-selectivity, and the higher sensitivity [20]. *GtACRs* showed robust inhibition of behavioral responses in live *Drosophila* in lower light intensity [51], meanwhile, they showed more efficient inhibition of action potential than that induced by archaeorhodopsin-3 (Arch, a proton pump) [52]. Even though 20 families had been confirmed and characterized as anion-selective channels, in the study, two constructs generated photocurrents when they were expressed in HEK293 cells, termed *GtACR1* (ACR1 for short) and *GtACR2* (ACR2 for short). ACR1 has the maximal sensitivity to green light (515 nm), while ACR2 is sensitive to blue light (best in 470 nm). They have the permeability sequence $\text{NO}_3^- > \text{I}^- > \text{Br}^- > \text{Cl}^- > \text{F}^- > \text{SO}_4^{2-} = \text{Asp}^-$. Considering the importance of Cl^- for plant cells, they could be employed as optogenetic tools in the plant system. In our study, we just tried three ACRs -- *GtACR1*, *GtACR2* [20], and ZipACR (an anion channelrhodopsin from *Proteomonas sulcata*) [53, 54]. The report showed that ACR2 was a better optogenetic tool than ACR1 in animal cells, on the contrary, from our result in plant cells, ACR1 is better than ACR2 and ZipACR as

optogenetic tool in the plant system.

1.4. Light-gated ion pumps

As mentioned above, except for the light-activated ion channels, some light-gated pumps also are used as optogenetic tools. At present, there are three different light-activated ion pumps (H^+ , Na^+ , and Cl^- pumps), which could be used to inhibit the neural firing [12, 55-57]. The channelrhodopsins and ion pump rhodopsins have similar structures (**fig. 3a**), but the transport through ion pump rhodopsins is active, in contrast, the transport through channelrhodopsins is passive [58]. Here, I just introduce some representative pumps.

1.4.1 light-gated chloride pump

Halorhodopsins, derived from *Natromonas pharaonic* (*NpHR*), is a light-gated inward chloride pump as an optogenetic tool (**fig. 3a**). It has an excitation maximum of 590nm[59]. In 2007, scientists found that it could inhibit the activity of mammalian neurons and regulate the behavior of *C. elegans* [19]. Besides, it could mediate the sleep of mice when it was expressed in the orexin/hypocretin neurons of the mouse brain [60]. However, wild-type *NpHR* has limited expression levels and only produces low photocurrents in neurons. To improve protein trafficking ability to the PM, some enhanced versions were engineered (*eNpHR2.0*, *eNpHR3.0*) [61-63]. The expression of *eNpHRs* was high and safe for the neurons, the currents induced by light were larger and the inhibition for the neural firing was augmented. Furthermore, under optimized photo-stimulation conditions, the temporal stability of *eNpHR3.0* could be improved, such as co-application of yellow and blue light, green and violet light, or blue light alone [64]

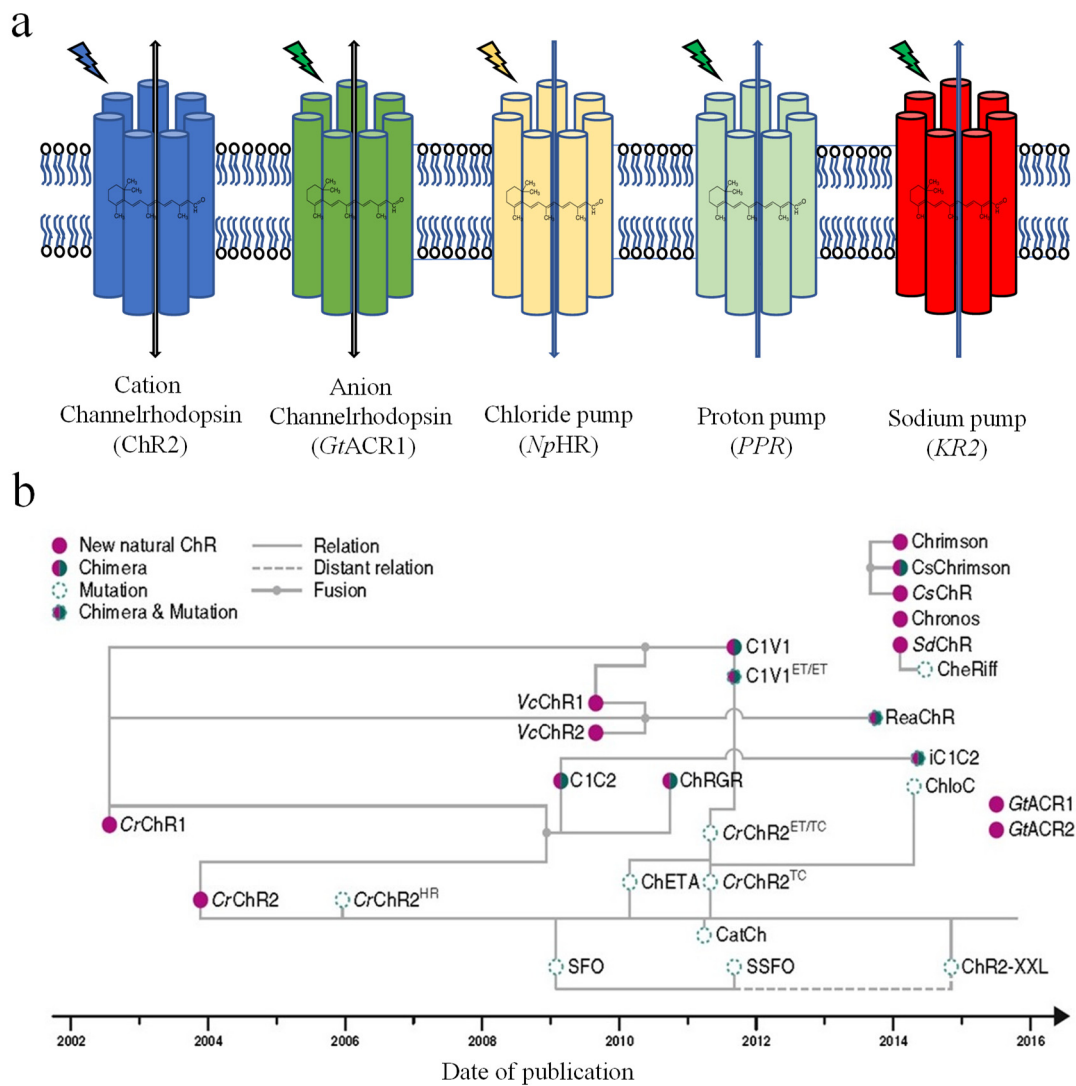


Figure 3. a, Cartoon of microbial rhodopsins consisting of a 7TM helix, binding to all-trans-retinal, the names only are the examples in the families. **b**, An ancestral chart of a part of engineered and newly discovered ChRs from 2002 to 2016 [65].

1.4.2 light-gated proton pump

The proton pump is another kind of optogenetic tool to inhibit neural activity through hyperpolarization. They transport the proton from the cytoplasmic to the extracellular side by light illumination (**fig. 3a**). The fast recovery from inactivation and high light-driven currents makes them desirable tools for altering chloride pumps. The first ion pump is bacteriorhodopsin (BR) from *Halobacterium salinarum* [11]. The studies on BR aid in the research of other novel rhodopsins as a paradigm [5, 66-68]. Its enhanced

version eBR shows robust efficiency in neuron inhibition [62]. In 2010, people found another ion pump -- Archaeorhodopsin-3 (Arch) from *Halorubrum sodomense* had a similar mechanism to that of BR. It could be a better neural silencer in mammalian neurons. Upon yellow light, it enables near ~100% silencing of neurons in the awake brain in the mouse cortex. Also, it could produce photocurrent both at a low and high light intensity [69, 70]. Now it and its variants are widely used as optogenetics tools in neuroscience research [71]. CvRh from *Chlorella vulgaris* is another outward light-gated proton pump (**fig. 3a**) [72, 73], although there is no more report about it, we proved that it had a better expression on the PM in the plant system, we named it PPR in our study. In addition to the outward proton pumps introduced above, people also found natural inward proton pumps, like *NsXeR* (proton pump from the *nanohalosarchaeon Nanosalina*) [74], *PoXeR* (proton pump from a deep-ocean marine bacterium, *Parvularcula oceanifrom*) [75]. As inward proton pumps, they will depolarize the membrane which is in a weak position compared to the most light-gated channels as optogenetic tools, therefore, they did not attract too much attention, at least temporarily.

1.4.3 light-gated sodium pump

In 2013, a light-driven sodium pump was discovered from marine bacterium *Krokinobacter eikastus* by K. Inoue and co-workers, they named it KR2 which pumps sodium ions outward of the cell [56] (**fig. 3a**). Based on the analysis of the structure of KR2 [76], the potassium channel was also engineered by targeted mutagenesis [77, 78], which enriched the weapon depots in optogenetics. Soon after KR2, similar proteins were found with light-driven Na⁺ ion transport activity [79-81].

Compared with ion channels, these light-gated pumps have some disadvantages, such as low expression level, one ion per photocycle, however, they could be eligible tools for their strict permeability which is not limited by the physiological ionic gradients. Besides, to a greater extent, the cellular pH will not be changed upon the function of

proton pumps.

1.5 Optogenetics in higher plants

Plants grow in a changeable environment. Unlike animals, plants do not possess a neural system, but they have both electrical and chemical signals to respond to the stimuli [82]. Compared with chemical signals, electrical signals transfer information faster and over long distances [83]. More and more physiological effects of electrical signals were discovered, so this rapid transmission is important to plants [84-86]. In plants, the types of electrical signals mainly consist of action potential (AP), variation potential (VP), and systemic potential (SP) [87]. All the electrical signals must involve membrane potential changes. While the membrane potential changes are induced by fluxes of ions such as H^+ , K^+ , Cl^- , Na^+ , and Ca^{2+} through the diverse ion channels or pumps in the membrane systems, such as PM, tonoplast, chloroplast membrane, and so on. Reacting to the stimuli (such as wounding, ice, heating, and so on), the ion channels open and the ions go across the membrane with the density gradient. Therefore, the regulation of ionic flow may be an effective method to research information transport in the plants. While the control of ionic flow must be achieved by the manipulation of ion channels or pumps within the plant system. In higher plant cells, there are many essential ion channels for the permeability of diverse ions, such as ligand-gated channels, voltage-gated channels, and mechanically-gated channels [88, 89]. These ion channels are important for the physiological function of plant cells. However, due to the characteristics of these channels, it is difficult to manipulate them precisely. Thus, in the research on plants, the optogenetic tools may play potential roles with their spatial and temporal precision. In recent years, several optogenetic strategies are utilized in plant research, including non-opsin-based and opsin-based.

1.5.1 Non-opsin-based optogenetics in higher plants

In plants, many kinds of photoreceptors can respond to a specific light spectrum from sunlight. Such as phytochrome for red/far-red, cryptochrome and phototropin for blue

light, and so on. Upon absorbing the specific light wavelength, plants can regulate the physiological activity, like flowering, photosynthesis, seed germination, directional growth [90]. With the extension of optogenetic tools, these photoreceptors are also engineered as optogenetic tools to be employed in plants [91]. The first optogenetic tool applied in higher plants was engineered based on phytochrome B (PhyB) and its interacting factors (PIF6) from *A. thaliana*. In the plant protoplasts, under red light, the PhyB was activated to (P_{fr}) active state and bound to PIF6, which led to the downstream gene expression (**fig. 4a**). Upon far-red light, the PhyB goes back to the inactive state (P_r) and is disassociated with PIF6, which ceases the gene expression [92]. However, because the PhyB-PIF6 system is from plants, the endogenous PHY system may interfere with the activity of this system. In 2018, another optogenetic method was made to control gene expression in protoplasts (**fig. 4b**). The light-sensitive bacterial transcription factor CarH was engineered and fused to the Herpes simplex transactivation domain VP16. Expressed in *A. thaliana* protoplasts, with green light illumination, this system could inhibit gene expression [93]. In the CarH-VP16 system, Vitamin B12 is required as the chromophore, while it is short of this cofactor in plants. The drawbacks of PhyB-PIF6 and CarH-VP16 limit the application in plant research. To overcome these disadvantages, a new strategy was developed, known as plant usable light-switch elements (PULSE) (**fig. 4c**). In this system, a blue light repressor -- EL222 which is from the LOV-based transcription factor [94], and the red-light switch engineered from the PHYB-PIF6 are combined. In normal growth conditions (white light, blue light, far-red light, and darkness), the gene of interest is in inhibition, only in red light, the system could be activated to induce gene expression [95]. Except for controlling gene expression, a blue light-induced K⁺ channel fused with LOV2-Jα photoswitch (called BLINK1) [96] was engineered to minimize the opening and closing of stomata [97]. In darkness, the BLINK1 is in the closing state. Upon blue light, it induces K⁺ influx across the plasma membrane. In *A. thaliana*, it could enhance the stomatal opening kinetics and improve carbon assimilation, water use, and plant growth (**fig. 4d**).

1.5.2 Microbial opsin-based optogenetics in higher plants

In 2020, ChR2-XXL was transiently expressed in *N. benthamiana* and demonstrated that it could induce the depolarization of plasma membrane potential with exogenous retinal addition under blue light (**fig. 4e**). In transgenic *A. thaliana* expressing ChR-XXL, the investigators demonstrated the plasma membrane H⁺-ATPase is a major driver of membrane repolarization by depolarizing PM with ChR2-XXL [98]. Although this is a successful attempt for the expression of microbial opsin in higher plants, it did not change the fundamental problem for the optogenetic application in plants. The exogenous retinal addition is still the weak part. Retinal addition not only costs money but also retinal will degrade easily which makes the experiment difficult to control in practical condition. New methods are needed for the improvement of microbial opsin-based optogenetic tools in plant research. In this study, I will introduce a new method in which a dioxygenase was expressed to produce retinal in plants (**fig. 3b**). With this method, many microbial opsins were transiently expressed in the model plants -- *Nicotiana benthamiana* (*N. benthamiana* for short), *Nicotiana tabacum* (*N. tabacum* or tobacco for short) and *Arabidopsis thaliana* (*A. thaliana*) successfully.

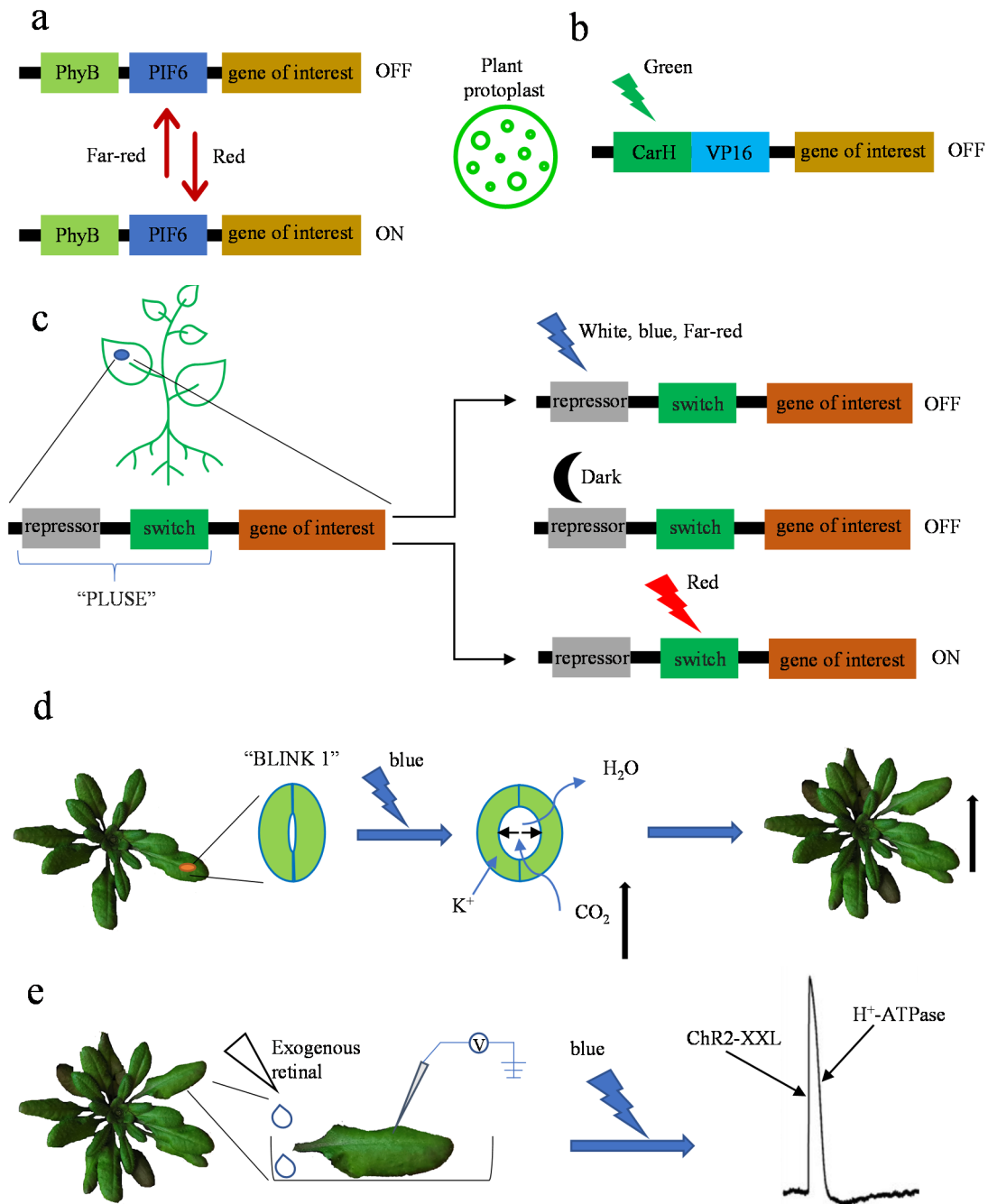


Figure 4. The current optogenetic application in higher plants

a, The schema of CarH-VP16 which could control gene expression in *A. thaliana* protoplasts upon green light. **b**, The schema of the PhyB-PIF6 system that was employed to control gene expression in tobacco protoplasts. The system could be activated in red light and inhibited in far-red light. **c**, The schema of plant usable light-switch elements (PULSE). PULSE combines a blue-light-regulated repressor with a red-light-inducible switch. Gene expression is only activated under red light and remains inactive under white light, blue light, far-red or darkness. **d**, The schema of BLINK1 in plants. BLINK1 was expressed in the stomata of *A. thaliana*. Illuminated by blue light, BLINK1 induced K^+ influx, which enhances stomatal opening and improves CO_2 assimilation further. However, the balance of H_2O is retained, finally leading to the accumulation of biomass. **e**, The schema of Chr2-XXL-based optogenetics in plants. Under blue light illumination and exogenous retinal, it induced the changes of plasma membrane potential. which indicated that the plant plasma membrane H^+ -ATPase was the major driver of membrane potential repolarization control during plant electrical signaling.

2. Results

2.1 Producing retinal and screening opsins in higher plants

2.1.1 Producing retinal in *N. benthamiana*

Before this research, no methods were found to express microbial opsins on the PM of plant cells. The PM, as a barrier keeping the constituents of the cell, also is a gate allowing ions to transport into or out of the cell. Keeping exploration, we found a method that could express different opsins in plants. In higher plants, there is no enzyme for retinal production. In this method, we introduced a gene from a marine bacterium coding a β -carotene 15, 15'-Dioxygenase (MbDio) (**fig. 5a, fig. 5b**) [99] for retinal production in plants. The enzyme could cleave β -carotene at its central double bond (15, 15') to yield all-trans-retinal. In the first attempt with transient expression of MbDio in the cytosol of *N. benthamiana* leaves, only a very little amount of retinal was produced (**fig. 5c**). Thus, we targeted MbDio into the chloroplast where most of its substrate, β -carotene, resides. An optimized chloroplasts transit signal peptide RC2 [100] targeted enhanced yellow fluorescent protein -- eYFP exceptionally well to *N. benthamiana* chloroplasts (**fig. 5b, d**). Therefore, the fusion construct of RC2-MbDio together with eYFP as a reporter was generated – RC2-MbDio-eYFP (**fig. 5b**), while the localization of this construct is not in the chloroplast (**suppl fig. 1**), so a P2A self-cleaving peptide [101, 102] was put between the RC2: MbDio and eYFP (**fig. 5b**). This fused construct, named Ret-eYFP, could produce retinal efficiently in *N. benthamiana* (**fig. 5c**), whereas in wild-type (WT) and empty *Agrobacterium*-infiltrated leaves (Agro + WT) no retinal was detected (**fig. 5c**).

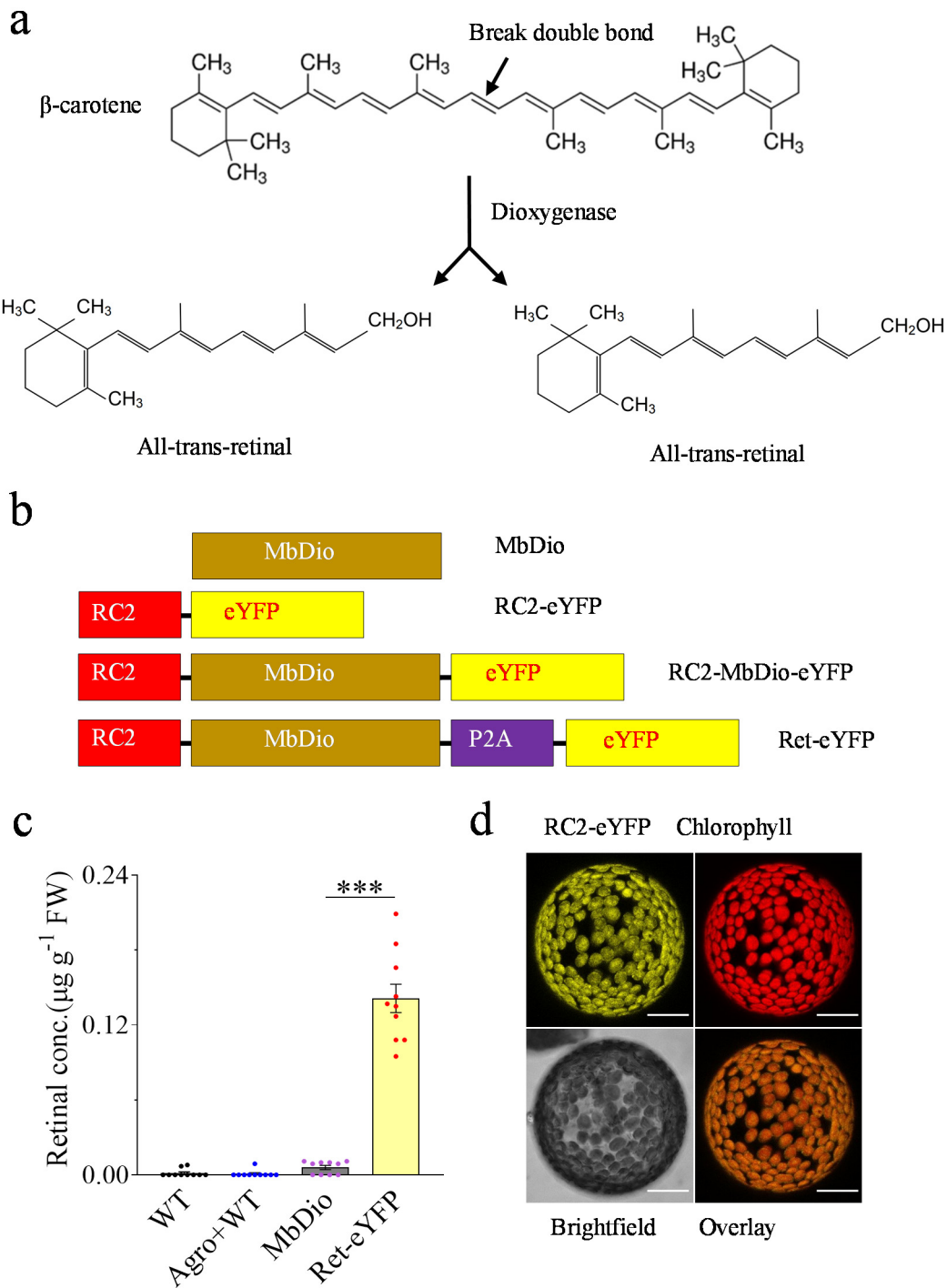


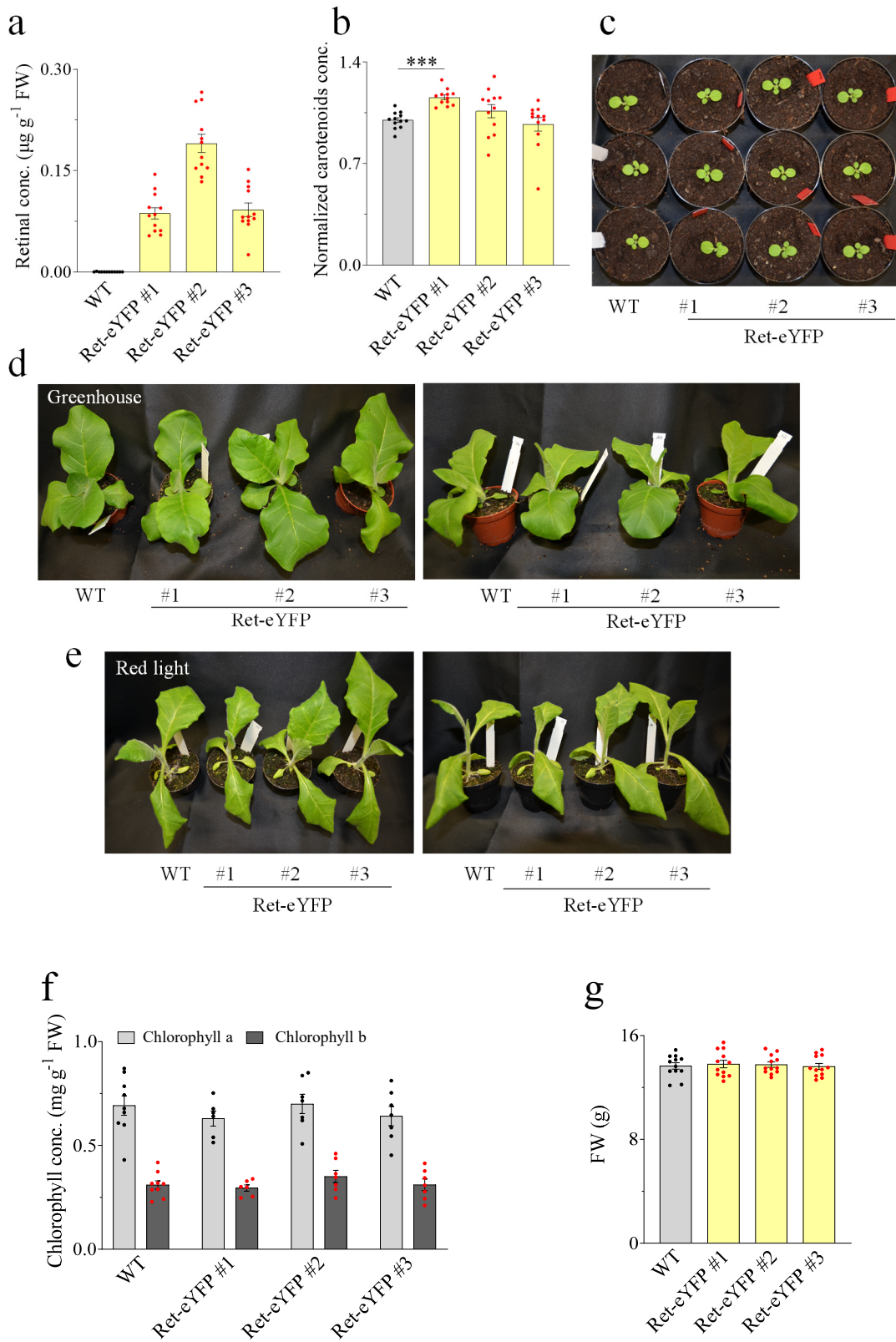
Figure 5. Retinal producing in *N. benthamiana*

a Schema of conversion from β -carotene to all-trans-retinal. Under the catalysis of dioxygenase, a molecule of β -carotene could be converted to two molecules all-trans-retinal; **b**, Schema of constructs—MbDio, RC2-eYFP, RC2-MbDio-eYFP, and Ret-eYFP, all the constructs are driven by UBQ10 promoter. MbDio, a β -carotene 15,15'-dioxygenase from a marine bacterium; RC2, a synthetic chloroplast transit peptide; eYFP, enhanced yellow fluorescent protein; P2A, the self-cleaving peptide from porcine teschovirus. **c**. Retinal contents of *N. benthamiana* leaves expressing MbDio and Ret-eYFP transiently in wild type (WT) and plants infiltrated with empty GV3101 *Agrobacterium* as controls; measurements are performed on the third day after *Agrobacterium* infiltration by UPLC-MS/MS. Error bars = s.e.m., $n = 10$. One-way analysis of Variance (ANOVA)

followed by a Tukey test was performed for the significance analysis, $P = 0.3 \times 10^{-6}$ for MbDio vs. Ret-eYFP. **d**, Confocal images of *N. benthamiana* protoplasts expressing RC2-eYFP. The images were taken 24h after transient transformation, scale bar = 20 μm .

2.1.2 The expression of Ret-eYFP in transgenic *N. tabacum*

To make sure whether retinal will have effects on the plants, or not, we stably transformed Ret-eYFP in *N. tabacum*. In contrast to the WT tobacco leaves that had no detectable retinal, the three Ret-eYFP-expressing tobacco lines showed considerable retinal production (**fig. 6a**), at the same time, these three lines of Ret-eYFP-expressing plants showed WT-comparable levels of carotenoids (**fig. 6b**) and the phenotype of them in the greenhouse and red light was also like WT plants (**fig. 6c, d, e**). Besides, other physiological indexes between Ret-eYFP-expressing plants and WT plants also keep the same levels, including chlorophyll concentration (**fig. 6f**), the fresh weight (FW) of 40-day-old plants (**fig. 6g**) and dry weight (DW) of 40-day-old plants (**fig. 6h**), the effective quantum yield of photochemical energy conversion (**fig. 6i**) and Photochemical quenching (**fig. 6j**). Even though the plants grew to the mature phase, they also kept similar plant size (**fig. 6k**) and seed weight (**fig. 6l**). All these data showed that the retinal production in plants will not affect the normal growth and basic physiological characteristics



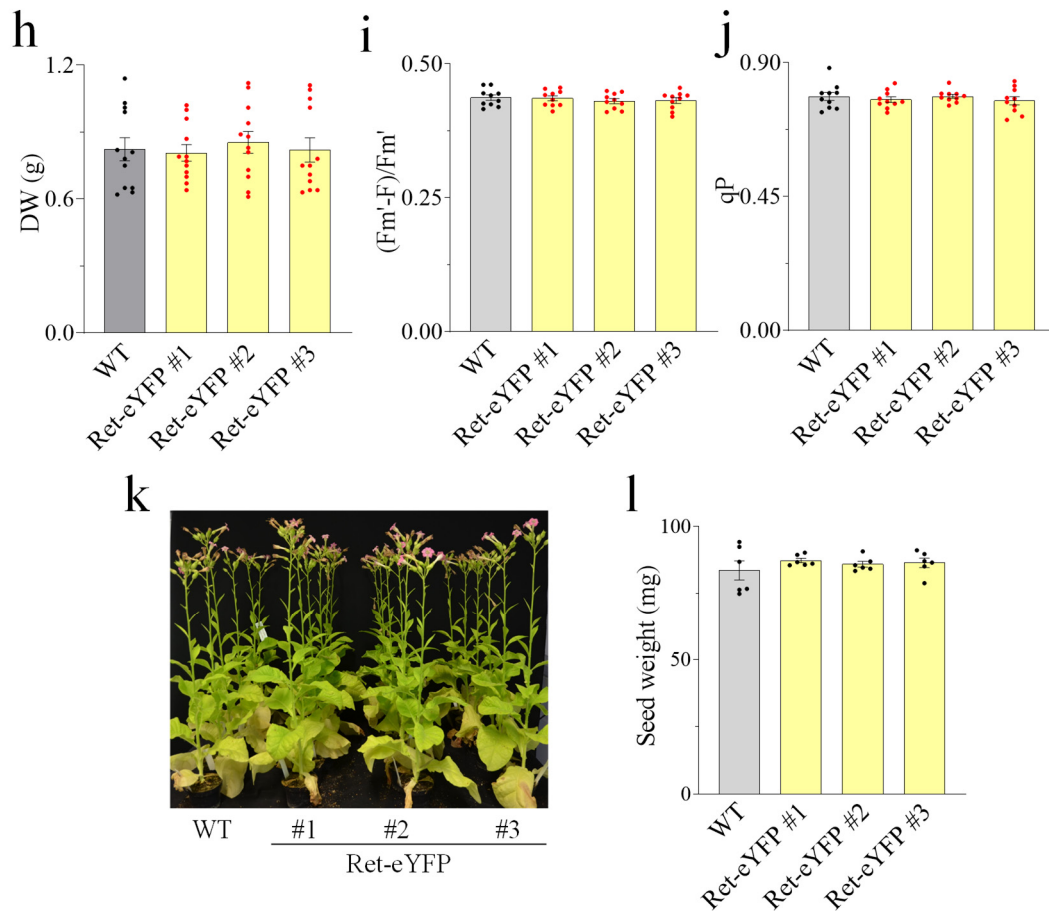


Figure 6: Ret-eYFP-expressing *N. tabacum* plants produce retinal and grow like WT plants
a, Retinal concentrations measured in extracts from WT *N. tabacum* and 3 Ret-eYFP-expressing *N. tabacum* lines; leaves are collected after 45 days' growth in red light. Error bars = s.e.m., n = 12. **b.** Carotenoid concentrations measured from the same batch samples as in (a). Data is normalized to the WT carotenoid content. Error bars= s.e.m., n = 12. One-way ANOVA followed by Tukey test performed the significance analysis, $P = 4 \times 10^{-6}$ for the indicated significance analysis. **c.** WT, and 3 lines of Ret-eYFP expressing transgenic tobacco plants grown in the greenhouse for 27 days. **d,** WT, and 3 lines of Ret-eYFP-expressing tobacco plants grown in the greenhouse for 37 days. **e,** WT and 3 lines of Ret-eYFP expressing tobacco plants grew in red light for 37 days. **f,** Chlorophyll contents of WT and 3 lines of Ret-eYFP-expressing transgenic *N. tabacum* leaves. Error bars = s.e.m., n = 6-9. One-way ANOVA followed by the Tukey test was performed, which showed no significant difference between WT and Ret-eYFP-expressing *N. tabacum*. **g,** Fresh weight (FW) of plants' aboveground part. WT *N. tabacum* and 3 lines of Ret-eYFP-expressing *N. tabacum* grew in the greenhouse for 40 days. Error bar = s.e.m., n = 12. One-way ANOVA followed by the Tukey test was performed and showed no significant difference between WT and Ret-eYFP-expressing *N. tabacum*. **h,** Dry weight (DW) of plants' aboveground part. WT *N. tabacum* and 3 lines of Ret-eYFP-expressing *N. tabacum* grew in the greenhouse for 40 days. Error bar = s.e.m., n = 12. One-way ANOVA followed by the Tukey test was performed, which showed no significant difference between WT and Ret-eYFP expressing *N. tabacum*. **i,** Effective quantum yield of photochemical energy conversion of WT and retinal-producing transgenic tobacco (Ret-eYFP #1, #2, and #3) leaves. All plants grew in the greenhouse for 40 days. Error bars = s.e.m., n = 10. One-way ANOVA followed by the Tukey test was performed, which showed no significant difference between WT and Ret-eYFP-expressing *N. tabacum*. **j,** Photochemical quenching (qP) of WT and retinal-producing transgenic tobacco (Ret-eYFP #1, #2 and #3) leaves. All plants grew in the greenhouse for 40 days. Error bars = s.e.m., n = 10. One-way ANOVA followed by the Tukey test was performed, which showed no significant difference between WT and Ret-eYFP-expressing *N. tabacum*. **k,** Pictures of mature WT and 3 lines of retinal-producing tobacco plants grown in the

greenhouse. **1**, 1000 seeds weight from WT, Ret-eYFP-expressing *N. tabacum* growing under red light condition. Error bars = s.e.m., n = 6. One-way analysis of Variance (ANOVA) followed by Tukey test was performed for the significance analysis, there is no significant difference among these groups.

2.1.3 The screening of opsins in plants

Now that the retinal production did not affect the plants, we began to express different opsins in plants. Before that, we first expressed two opsins -- ACR1 and Chr2-XXL (hereinafter “XXL” for short) in plants. We generated different constructs based on these two opsins (**fig. 7a**), in which ACR1 or XXL was fused to N/C-terminal of Ret, and eYFP was the reporter to monitor the expression in plants. To improve the expression on the PM, we fused different signal peptides, including trafficking signal peptide (named “T”) [62], endoplasmic reticulum (ER) export signal peptide (named “E”) [103] to the C-terminal of ACR1 or XXL. These peptides could improve the transport from the Golgi apparatus and ER to the PM of plant cells. Through the transient expression in *N. benthamiana* leaves, we found that it had a better expression level in the epidermal cells of *N. benthamiana* leaves when ACR1 or XXL was fused to the C-terminal of Ret (**fig. 7b**), comparing with WT and the constructs which have no Ret (XXL-eYFP, ACR1-TYE) and ACR1 or XXL was fused in N-terminal of Ret (ACR1-TY-Ret, XXL-Ret) (**fig. 7b**). Finally, we confirmed the architecture of the construct, in which the opsins were fused to the C-terminal of Ret with P2A linking them.

In the next work, we transiently expressed many opsins in *A. thaliana* protoplasts (**suppl table 1, suppl fig. 2**) and *N. benthamiana* leaves (**suppl. fig. 3**). We found that all the opsins we tried could express in these two systems, though some of them did not present an exciting expression level. Totally, this method producing retinal in plants could be the key to open the research in plants with microbial opsin-based optogenetic tools.

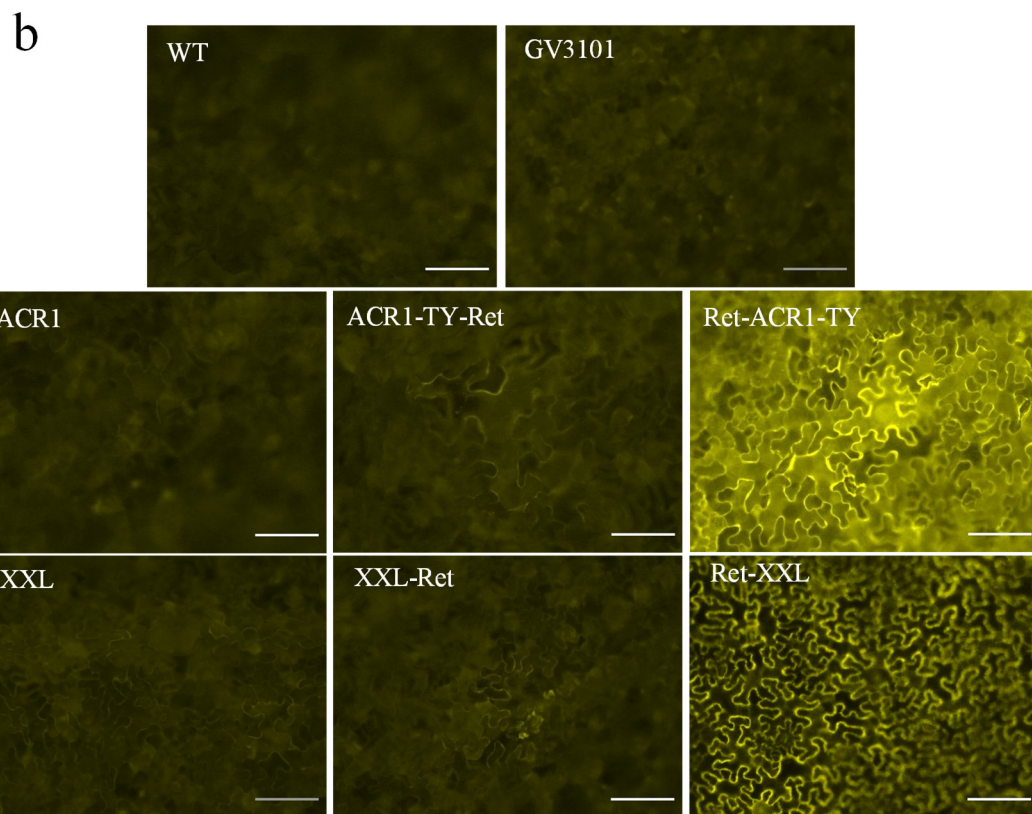
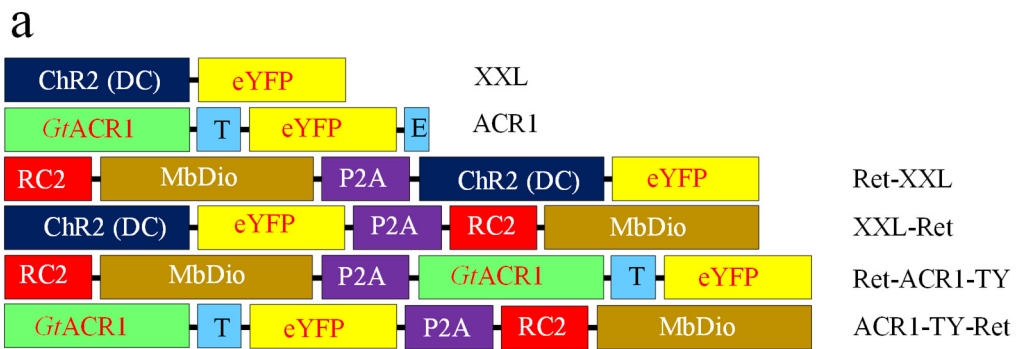


Figure 7. Transient expression of constructs based ACR1 and XXL in *N. benthamiana*
 a, Schema of fusion constructs of XXL, ACR1, Ret-XXL, XXL-Ret, Ret-ACR1-TY, and ACR1-TY-Ret. ChR2 (DC), mutant of channelrhodopsin-2 on position 156 from Aspartic acid to Cysteine; ACR1, *Guillardia theta* anion channelrhodopsin-1; T, the PM trafficking signal from Kir2.1; E, the endoplasmic reticulum (ER) export signal from Kir2.1. b, Images of epidermal cells of *N. benthamiana* transiently expressing different constructs in (a), the images were taken on the third day after infiltration with Leica DMI 8 microscopy system. WT plants and plants infiltrated with empty GV3101 *Agrobacterium* as controls. Scale bars = 100 μ m.

2.1.4 Discussion

Retinal is the prerequisite for the function and expression of opsins. Retinal is present in photosynthetic microorganisms and vertebrate animals. In higher plants, there is no enzyme for retinal production. When we expressed ACR1 and XXL in the *N.*

benthamiana leaves transiently, the expression level is very low. Retinal addition in the bath solution in the study could solve this problem, however, this approach is not feasible for whole living plants, as retinal is too unstable and expensive when “feed” it to growing seedlings and whole plants. Many factors should be considered, such as dosage, loss, assimilation, and so on. Therefore, it will be a time and material-consuming process, and the experiments will be more complicated. Thus, the effective method is to produce retinal in plants.

It is a common site that retinal is one of the many forms of vitamin A, and vertebrate animals get retinal from meat, or they produce retinal from carotenoids which are rich in vegetables. It reported that β -carotene 15,15'-dioxygenase could catalyze one molecule of β -carotene into two molecules of all-trans-retinal. In plants, β -carotene is the active component of chloroplasts [104]. To produce endogenous retinal in plants, we expressed a β -carotene 15,15'-dioxygenase from an uncultured Marine Bacterium in plants [99, 105]. Although we expressed the β -carotene 15,15'-dioxygenase in the plant, the content in plants is still low. There may be two main reasons: on the one hand, maybe the protein could not work in plants; on the other hand, the content of β -carotene was limited in the cytoplasm, which means that the enzyme did not have enough substrate. First, it had been proved that the expression of the exogenous gene in plants was available under suitable promoters [106]. The most possible reason is the limited substrate.

As we know, chloroplasts use β -carotene to transfer electrons in the photosynthetic system. To make the enzyme express in the chloroplast, the enzyme with signal peptide -- RC2 was co-expressed in plants. From the expression in *N. benthamiana* protoplasts, it could prove that the RC2 enables target eYFP to the chloroplasts well. However, the fusion protein RC2-MbDio-eYFP did not show good expression in the chloroplasts. It was understandable. After all, RC2 only has 255 bp, when it was co-expressed with MbDio (828 bp) and eYFP (717 bp), the targeting ability was affected. After we inserted

a self-cleaving P2A linker, the leaves produced more retinal successfully. It indicated that the fusion protein Ret had expressed in the chloroplast and the enzyme worked well. Although the content of retinal in the *N. tabacum* plants was more than that in the WT plant, it did not influence the normal growth of the plants and other physiological indexes of retinal-producing plants. It suggested that we could alter eYFP with opsins to express in plants. This makes the expression of opsins possible.

Considering the effect on the function and localization of opsins in plants, we designed different constructs in which ACR1 and XXL were fused to the N/C-terminal of Ret, respectively, and some reported signal peptides were also fused to opsins to improve the expression on the PM. The expression level in the *N. benthamiana* leaves showed that the constructs that the opsin was fused in the C-terminal of Ret are better than the constructs that the opsin was fused in the N-terminal of Ret. The worse expression may be attributed to the short sequence of RC2. In the cleavage of the P2A peptide, the bond breaks between the Proline (P) and Glycine (G) in the C-terminal of the 2A peptide, resulting in the gene located upstream of the 2A peptide having extra amino acids on its C-terminal end while the gene located downstream the 2A peptide will have an extra Proline on its N-terminal end. In the constructs ACR1-TY-Ret and XXL-Ret, the Proline will be left in the N terminal of RC2, the extra P maybe changed the sequence of RC2 and led to incorrect targeting, and further affected the retinal production in the plant cells. This is also the reason why the expression had no difference between the constructs ACR1-TY-Ret and ACR1-TYE (without retinal production), XXL-eYFP-Ret and XXL-eYFP (without retinal production).

To improve the expression level and localization of opsins on the PM. We tried many signal peptides in the C/N-terminal of opsins, it proved that the signal peptides -- trafficking signal (T) and ER export (ER) in the C-terminal of opsins would not only improve the localization, but also the expression level of opsins on the PM. Also, from the expression of different constructs based on Chrimson (a red-shifted

channelrhodopsin) [107] which were fused with different signal peptide sequences [108-114] in the N/C-terminal of Chrimson in *A. thaliana* protoplasts (**suppl fig. 4**), we found that T and ER export signal peptide had more universal applicability. Therefore, real tools could stand the test of practice. Furthermore, according to the results in *Xenopus laevis* oocytes (data not shown), for some opsins, the expression was better on the PM when opsins were fused with more T signal peptides in the oocytes. Based on a series of results above, we confirmed the final construct structure in the study -- Ret-P2A-LR- (opsins gene)-T (or 2T)-YFP-E.

2.2 The expression and function of ACR1 in higher plants

2.2.1 Introduction

ACR1 is a natural light-gated anion channelrhodopsin, which takes all-trans-retinal as the chromophore. It provided high light-sensitive and efficient membrane potential manipulation, so it was used for neuronal silencing. ACR1 conducted anions strictly, completely excluding protons and larger cations. In plants, there are many anion channels, they play important roles in cell signaling, osmoregulation, plant nutrition, and metabolism. The PM potential of resting cells is highly negative in plant cells (about -100 to -200 mV), which is determined by the H-ATPase. While there is a low abundance of extracellular cations as the counterions for the negative potential. The anion channels can permeate anions across the PM to regulate the membrane potential [115]. However, these anion channels in plants are voltage-dependent or mechanosensitive channels. As the tools for the study of plants, there is no advantage in temporal and spatial control. ACR1, as a light-gated anion channel, has many advantages in the plant study. Firstly, the opening and closing can be manipulated by light, and the kinetics is very fast. Secondly, ACR1 permeates anions completely (mainly Cl⁻), which could replace the anion channels in plants. At last, ACR1 has a good expression on the PM, which could induce the membrane potential changes by regulation of anions fluxes across the cell membrane.

2.2.2 Expression of ACR1 in *N. benthamiana*

To further improve the expression of ACR1 on the PM, except for trafficking and ER export signal peptides, lucy and rhodopsin peptide (LR) [116] was fused to the N-terminal of ACR1, so the constructs about ACR1 were improving (**fig. 8a**), in which the best one is Ret-ACR1 2.0. When transiently expressed in *N. benthamiana*, compared with other constructs -- ACR1 and Ret-ACR1, Ret-ACR1 2.0 showed the best expression in the epidermal cells of *N. benthamiana* leaves (**fig. 8b**), and the highest light-induced depolarization in the mesophyll cells of *N. benthamiana* leaves

(Fig. 8c, d). Higher light intensities evoked stronger depolarization (fig. 8e, f) which were associated with endogenous counter forces to repolarize the membrane potential during and shortly after illumination (Fig. 8e).

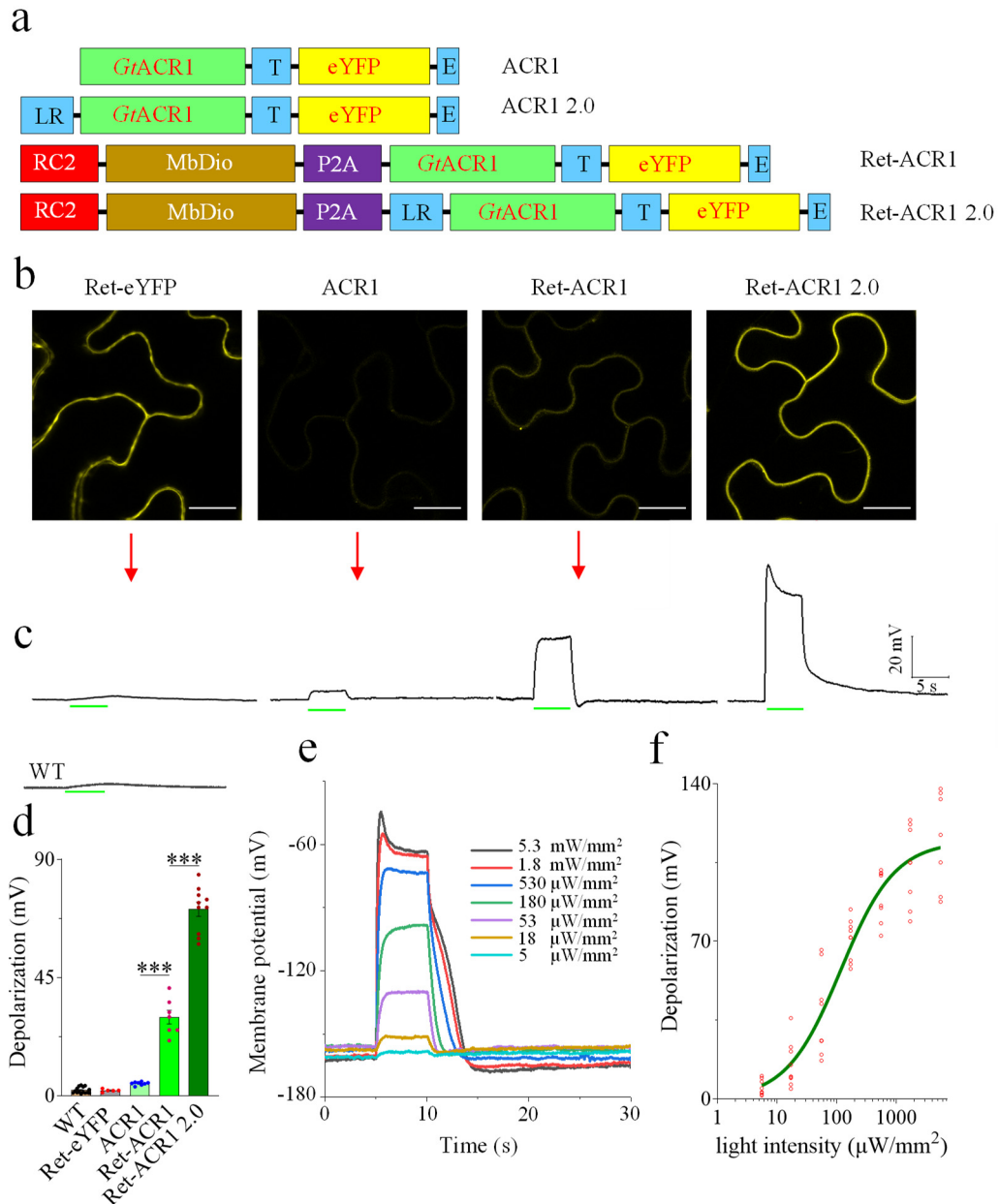


Figure 8. Transient expression of ACR1 in *N. benthamiana*

a, schematic diagram of constructs -- ACR1, ACR1 2.0, Ret-ACR1, and Ret-ACR1 2.0. LR, the cleavable N-terminal signal peptide Lucy-Rho; **b**, Representative confocal images of Agrobacterium-infiltrated *N. benthamiana* leaf epidermal cells transiently expressing Ret-eYFP, ACR1, Ret-ACR1, and Ret-ACR1 2.0. Pictures were taken on the third day post Agrobacterium infiltration (dpi), scale bar = 200 μm . **c**, Representative voltage recording traces of *N. benthamiana* mesophyll cells transiently expressing Ret-eYFP, ACR1, Ret-ACR1, and Ret-ACR1 2.0. 5 s 180 $\mu\text{W}/\text{mm}^2$ (864 $\mu\text{mol}/\text{m}^2/\text{s}$) green (532 nm) light illumination were indicated by the green bars; Representative voltage recording trace of WT *N. benthamiana* mesophyll cell illuminated with 5 s 180 $\mu\text{W}/\text{mm}^2$ (864 $\mu\text{mol}/\text{m}^2/\text{s}$) lasting green light (532 nm) pulse was shown in the lower left side.

d, Comparison of light-induced membrane potential changes in the mesophyll cells of WT, and Ret-eYFP, ACR1, Ret-ACR1, and Ret-ACR1 2.0-expressing *N. benthamiana*. Illumination was performed with 5 s 180 $\mu\text{W}/\text{mm}^2$ (864 $\mu\text{mol}/\text{m}^2/\text{s}$) green (532 nm) light. Error bars = s.e.m., n = 5 - 15. One-way ANOVA followed by a Games-Howell's Post Hoc Test was performed for significance analysis. For ACR1 vs. Ret-ACR1, $P = 4 \times 10^{-4}$; Ret-ACR1 vs. Ret-ACR1 2.0, $P = 1.8 \times 10^{-7}$; e, Membrane potential changes of mesophyll cells transiently expressing Ret-ACR1 2.0 when illuminated with different intensities of 5 s green light (532 nm) pulses; f, Ret-ACR1 2.0-expressing *N. benthamiana* mesophyll cell depolarizations induced by different intensities of 532 nm green light. All individual data points are shown, n = 7 - 9

2.2.3 Expression of ACR1 in transgenic *N. tabacum*

Taking the Ret-eYFP as the reference, the constructs -- ACR1 and Ret-ACR1 2.0 were transferred into the cDNA of *N. tabacum* with the Agrobacterium-mediated transformation. In **fig. 9a and suppl fig. 5a**, it showed the confocal images of epidermal cells in the transgenic *N. tabacum* leaves expressing Ret-eYFP, ACR1, and Ret-ACR1 2.0 with the same situation of transient expression in *N. benthamiana*, the Ret-ACR1 2.0-expressing tobacco still had the best expression on the epidermal cells and highest expression level. 5s green light (180 $\mu\text{W}/\text{mm}^2$, 532 nm) already evoked $\sim 100\text{mV}$ membrane potential change (**fig. 9b, c, suppl fig. 5b, 5c**), and the depolarization also increased with the light intensity (**fig. 9c, d, suppl fig. 5c, 5d**). The cell could also produce hyperpolarization even more negative values when the illumination was stopped (**fig 9d, suppl fig. 6**), it is likely caused by the activation of endogenous H^+ -ATPase, which was shown to be activated by membrane depolarization [117].

2.2.4 The phenotype of transgenic *N. tabacum* plants expressing ACR1

Under greenhouse (white light) as well as red light conditions, due to very weak expression and activity (**Fig. 8d, 9b**), ACR1-only plants (without the retinal producing enzyme) grow similarly to the Ret-eYFP-expressing and WT plants (**fig. 10a**), as retinal is missing. In 650 nm red light conditions, ACR1 is not activated, so Ret-ACR1 2.0 lines grew like WT and Ret-eYFP plants (**Fig. 10a**), but red light-grown Ret-ACR1 2.0 plants wilted dramatically upon transition into white light (greenhouse condition that activated the light-gated anion channel, **fig 10b**).

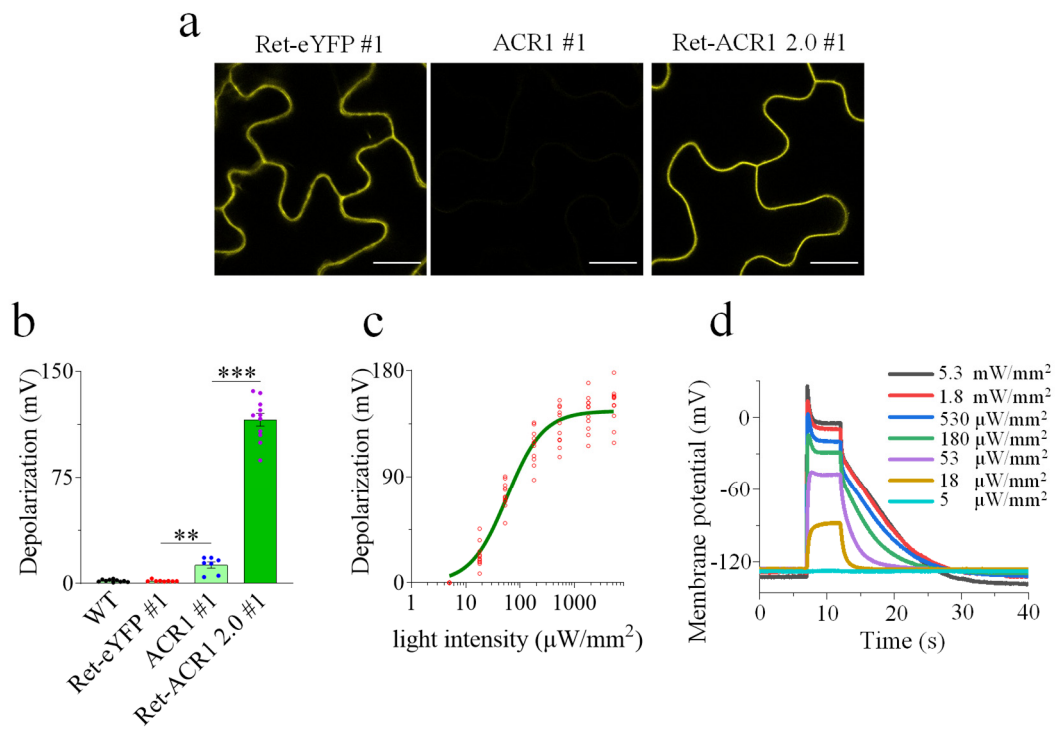
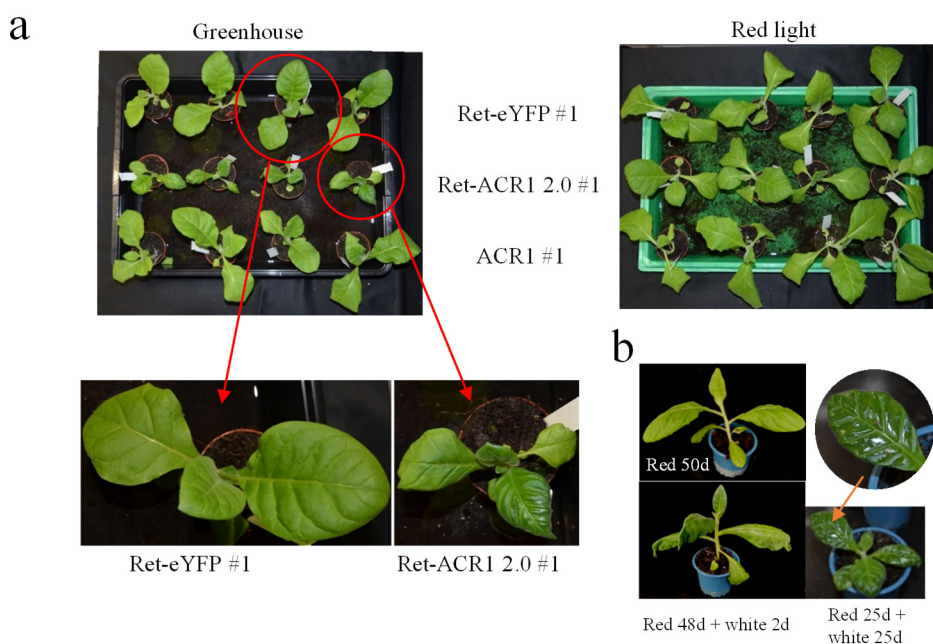


Figure 9. Functional expression of improved ACR1 2.0 in *N. tabacum*.

a, Representative confocal images of transgenic *N. tabacum* leaf epidermal cells expressing Ret-eYFP (line #1), ACR1 (line #1) and Ret-ACR1 2.0 (line #1). Scale bar = 200 μm . **b**, 5 s 180 $\mu\text{W}/\text{mm}^2$ green (532 nm) light-induced mesophyll cell membrane potential changes (depolarizations) in WT, Ret-eYFP, ACR1, and Ret-ACR1 2.0-expressing transgenic tobacco plants (line #1 was used for all). Error bars = s.e.m., $n = 7 - 11$. One-way ANOVA followed by a Games-Howell's Post Hoc Test was performed for significance analysis. $P = 0.008$ for Ret-eYFP vs. ACR1; $P = 4.5 \times 10^{-11}$ for ACR1 vs Ret-ACR1 2.0. **c**, Mesophyll cell depolarizations of transgenic Ret-ACR1 2.0 *N. tabacum* #1 induced by 532 nm light with different intensities. Individual data points are shown, $n = 11$. **d**, The membrane potential recording traces of transgenic Ret-ACR1 2.0 tobacco #1 mesophyll cells illuminated with 5 s 532 nm light pulses of different intensities.



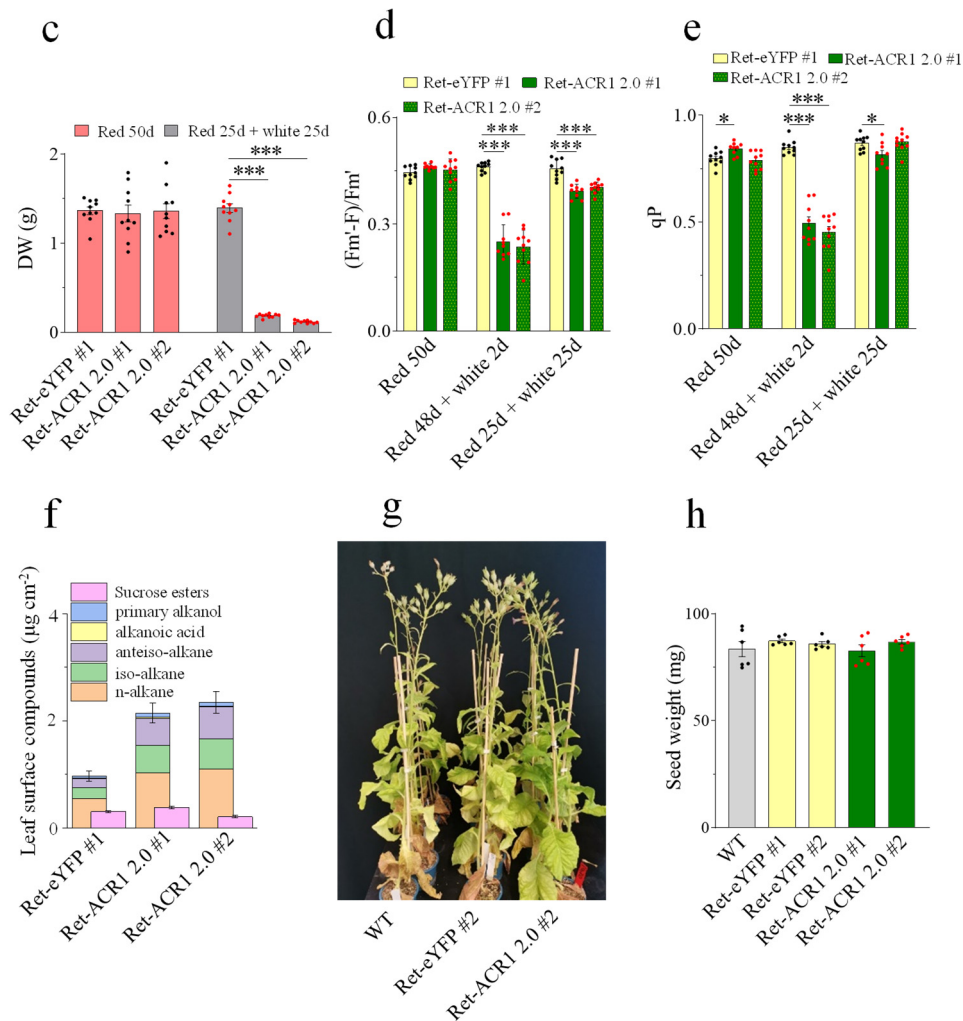


Figure 10. Phenotype of Ret-ACR1 2.0-expressing *N. tabacum*

a, Comparison on the phenotypes of *N. tabacum* expressing Ret-eYFP (line #1, up row of two pictures above), Ret-ACR1 2.0 (line #1, the middle row of two pictures above) and ACR1 (line #1, down row of two pictures above) growing for 12 days in red (650 nm LED) light + 25 days in the greenhouse (left panel) or 37 days in red light (right panel). Representative pictures (two pictures below) of Ret-eYFP #1 and Ret-ACR1 2.0 #1 plants growing firstly for 12 days in red light and then 25 days in the greenhouse. **b**, Phenotypes of Ret-ACR1 2.0 expressing tobacco plants (line #1) growing in red light for 50 days (upper) or firstly growing in red light for 48 days and then moved to the greenhouse (white light) for 2-3 days (lower), right part showed the phenotype of Ret-ACR1 2.0 tobacco grown firstly 25 days in red light and then 25 days in the greenhouse. **c**, Comparison on the dry weight (DW) of transgenic *N. tabacum* expressing Ret-eYFP (line #1) and Ret-ACR1 2.0 (line #1 and #2) which grew in different conditions as indicated. Error bars = s.e.m., n = 10. One-way ANOVA followed by the Tukey performed for the significance analysis. There is no significant difference among the “Red 50d” group; in “Red 25d + White 25d” group, $P = 5.1 \times 10^{-9}$ and 5.1×10^{-9} for Ret-eYFP #1 vs. Ret-ACR1 2.0 #1 and #2, respectively. **d**, Effective quantum yield of energy conversion of Ret-eYFP line #1 and Ret-ACR1 2.0 lines #1 and #2 tobacco leaves grown under different conditions as indicated. Error bars = s.e.m., n = 9-10. One-way ANOVA followed by Tukey test was performed for the significance analysis. There is no significant difference in Group “Red 50d”; in Group “Red 48d + white 2d”, $P = 5.1 \times 10^{-9}$ and 5.1×10^{-9} for Ret-eYFP #1 vs. Ret-ACR1 2.0 #1 and #2, respectively; in Group “Red 25d + white 25d”, $P = 1 \times 10^{-6}$ and 1.4×10^{-5} for Ret-eYFP #1 vs. Ret-ACR1 2.0 #1 and #2, respectively. **e**, Photochemical quenching (qp) of Ret-eYFP (line #1) and two lines of Ret-ACR1 2.0 tobacco leaves grown under different conditions as indicated. Error bars = s.e.m., n = 9-10. One-way ANOVA followed by Tukey test was performed

for the significance analysis: in group “Red 50d”, $P = 0.023$ for Ret-eYFP #1 vs. Ret-ACR1 2.0 #1 and there is no significant difference between Ret-eYFP #1 and Ret-ACR1 2.0 #2; in group “Red 48d + white 2d”, $P = 5.3 \times 10^{-9}$ and 5.1×10^{-9} for Ret-eYFP #1 vs. Ret-ACR1 2.0 #1 and #2, respectively; in group “Red 25d + white 25d”, $P = 0.039$ for Ret-eYFP #1 vs. Ret-ACR1 2.0 #1 and there is no significant difference between Ret-eYFP #1 and Ret-ACR1 2.0 #2. **f**, Leaf cuticular waxes and sucrose esters of Ret-eYFP line #1 and two Ret-ACR1 2.0 lines #1 and #2 growing 25 days in red light and 25 days in white light. Error bars= s.e.m., $n = 6$. One-way ANOVA followed by Tukey test was performed for the significance analysis between Ret-eYFP #1 and two lines of Ret-ACR1 2.0-expressing plants on different wax compound classes and sucrose esters: *n*-alkanes, $P = 3.6 \times 10^{-5}$ and 9×10^{-6} for Ret-eYFP #1 vs. Ret-ACR1 2.0 #1 and #2, respectively; *iso*-alkanes, $P = 1.3 \times 10^{-8}$ and 6.5×10^{-9} for Ret-eYFP #1 vs. Ret-ACR1 2.0 #1 and #2, respectively; *anteiso*-alkanes, $P = 3.4 \times 10^{-5}$ and 1×10^{-6} for Ret-eYFP #1 vs. Ret-ACR1 2.0 #1 and #2, respectively; alkanolic acids, $P = 3.4 \times 10^{-4}$ and 0.013 for Ret-eYFP #1 vs. Ret-ACR1 2.0 #1 and #2, respectively; primary alkanols, $P = 9 \times 10^{-7}$ and 1.8×10^{-5} for Ret-eYFP #1 vs. Ret-ACR1 2.0 #1 and #2, respectively; sucrose esters, $P = 0.068$ and 0.013 for Ret-eYFP #1 vs. Ret-ACR1 2.0 #1 and #2, respectively. **g**. WT, Ret-eYFP #2, and Ret-ACR1 2.0 #2 tobacco plants grown in red light for 3 months and generated seeds. **h**, 1000 seeds weight from WT, Ret-eYFP (two lines), and Ret-ACR1 2.0-expressing (two lines) *N. tabacum* growing under red light condition. Error bars = s.e.m., $n = 6$. One-way analysis of Variance (ANOVA) followed by Tukey test was performed for the significance analysis, there is no significant difference among these groups.

At the same time, due to the activation of ACR1 in white light, the growth of Ret-ACR1 2.0-expressing tobacco was inhibited and the biomass is much lower than that of tobacco grown in red light (**fig. 10c**). Then the normal photosynthesis is strongly impaired, indicated by the reduction of effective quantum yield (**fig. 10d**) and photochemical quenching (**fig. 10e**), shown by chlorophyll fluorescence measurements. Also, Ret-ACR1 2.0 plants showed about 2 times higher cuticular wax load (**fig. 10f**), which is probably to counteract wilting and reduce excessive water loss. Growing in red light all the time, Ret-ACR1 2.0-expressing tobacco could reproduce normally (**Fig. 10g, h**).

2.2.5 Discussion

The balance of membrane potential is maintained by the cations and anions in a wide variety of environments. The ion flux across the PM is essential for the plant to grow healthily. Therefore, the control of ion flux is important for the plant system. Although there are many ion channels on the membrane system of plants, it is difficult to manipulate them in time and space. We heterogeneously expressed ACR1 -- a light-gated anion channelrhodopsin on the PM in *N. tabacum*. With green light illumination, ACR1 could induce the Cl^- outflux of cells and depolarize the membrane potential of

the cell. This change could disturb the ion balance of the intra/extracellular environment. Although ACR1 has excellent light sensitivity, plants also have light absorption near green light [118], so the effects of ACR1 activation by green light must be proved by comparing with appropriate control plants.

To improve the ability of ACR1 targeting on the membrane, the plasmid of Ret-ACR1 2.0 was constructed. Due to the role of LR, T, and E, the ACR1 could be expressed on the PM very well. Meanwhile, upon the green light illumination, it could induce the depolarization of mesophyll cells in the bath solution (10 mM MES-Tris, 1 mM KCl, 1 mM CaCl₂). From the trace of membrane potential recording, it showed that the permeability of ACR1 is positively related to the light intensity. When the light intensity is too high, the response from plants would decrease the effect of ACR1, maybe this response is from the activation of other voltage-dependent channels or chloride-related channels. Besides, when the membrane potential turns to resting potential, it will appear the hyperpolarization which may be a normal physiological response to protect the plant from the stress by H⁺-ATPase which extrudes H⁺ into the apoplast. Furthermore, membrane depolarization induced by the ion flux may also lead to a net salt loss, further driving water movements, and participating in cell osmoregulation. That is the reason why the transgenic plants expressing Ret-ACR1 2.0 showed evident phenotype (leaf wilting) in the greenhouse. Except for the leaf wilting, the content of wax on the surface of leaves expressing Ret-ACR1 2.0 was much higher than that of *N. tabacum* expressing Ret-eYFP and only ACR1. The increase of wax indicated that plants began to reflect the light for reducing water loss. As the sensitive crops to chloride [119, 120], maybe this is also one triggered protection mechanism for tobacco plants to keep themselves away from the harmful stimulus.

In the flowering phase, because of the interference of membrane potential, the buds always were easy to fall when the plants grew in the greenhouse (data not shown). Interestingly, the plants could recover to normal growth if they were moved to red light

in which ACR1 would not be activated. And the phenotype on the leaves (water loss, wax aggregation) also disappeared. Furthermore, they also could bear fruits normally. In this process, maybe the regulation of homeostasis in the plant system plays a key role, and it also indicated that the higher plants could survive in a tough environment.

As an optogenetic tool, ACR1 could be available in the plant system. Under the light condition, it could change the membrane potential with the control of Cl⁻ flux across the PM. Due to the importance of anions for the plants, ACR1 could be employed in the research of anion's effect on the plant system. Except for ACR1, there also are another two anion channelrhodopsins trying in our study -- *GtACR2* and *ZipACR*, which have better application in neurons. In the plant system, ACR1 had a distinct expression and function than *GtACR2* and *ZipACR*. Maybe this is related to the fine distinction among them on the sequence homology. Compared with ACR1, *GtACR2* has blue-light sensitivity and *ZipACR1* has faster kinetics. These characteristics may make *GtACR2* and *ZipACR* backup tools in the future. The function of ACR1 is limited, more optogenetic toolkits are needed to explore for the plant study.

2.3 The expression and function of ChR2-XXM in higher plants

2.3.1 Introduction

Light-gated cation channels can induce a fast depolarization of neurons upon light stimulation directly. Natural channelrhodopsins were discovered in green algae *Chlamydomonas reinhardtii*. ChR1 is activated by blue light and permits (mainly proton) influx into the cell [13]. ChR2 is the first widely adopted optogenetic tool in neurons, and it is also activated by blue light [14]. ChR2, as a non-selective cation channel, is preferred over ChR1 in the application, because ChR2 has higher conductance at physiological pH and expresses well on the PM. After ChR2, more novel ChRs had been identified from other algal species. Besides, new synthetic variants also were developed to enhance the family of ChRs with the genetic engineering methods, e.g ChR2 (H134R) [32], ChR2 (D156C) -- XXL [41], ChR2 (D156H) -- XXM [42, 43] (hereinafter XXM for short). Among the variants, it reported that XXL had extra high expression and long open state, and reduced dependence on retinal addition. This mutant could evoke synaptic transmission, and activate neuronal networks at very low irradiance, even did not require dietary retinal supplementation in the study. Compared with ChR2-wt and XXL, the XXM showed a superior photostimulation efficiency with faster kinetics than XXL, and it also had enhanced Na⁺ and Ca²⁺ conductance [42, 43]. For the plant, Ca²⁺ plays a central role in the information transmission system, so the manipulation of Ca²⁺ flux will affect physiological activities. As the widely used optogenetic tool, ChR2 or its mutants will provide new optogenetic tools for plant research. XXM has high Ca²⁺ permeability, so it is an ideal tool employing in plants. In the next study, we focus on the expression and function of XXM in plants.

2.3.2 The expression and function of XXM in *N. benthamiana*

According to the modification on ACR1, the constructs about XXM were improved by fused LR, T, and E signal peptides (**fig. 11a**). Though with the same modification

strategy as Ret-ACR1 2.0, Ret-XXM 1.0 is still expressed in ER, to some extent (**fig. 11b**). Thus, we generated the construct Ret-XXM-ER (**fig. 11a**), in which the ER retention signal sequence was fused to the C terminal of XXM (**fig. 11a**) to make the protein only expressed in ER as the positive control in the next study. To future improve the expression of XXM on the PM, 11 amino acid residues in the N- terminal of XXM were truncated and made the construct -- Ret-XXM 2.0. Compared with other constructs, Ret-XXM 2.0 showed a clear profile of epidermal cells and no expression in ER which is a hint for the expression on the PM (**fig. 11b**), while for the plants expressing Ret-XXM-ER, it is difficult to recognize the epidermal cells (**fig. 11b**). Upon the blue light, activation of Ret-XXM 2.0 could induce depolarization of the PM, and the amplitude increased following the light intensity (**fig. 11c**). Also, the permeability of Ret-XXM 2.0 for Ca^{2+} was demonstrated again through a luminescence experiment. Ret-XXM 2.0 and 10 μM coelenteron were co-expressed in *N. benthamiana* expressing aequorin by agro-infiltration. For the WT plants, illuminated by blue light, the plants could produce a response, even for 5s blue light illumination (**fig. 11d**), while there was no obvious response when the plants were upon green light, even in different illumination duration (**fig. 11d**). Therefore, to decrease the effect of the plant itself, we chose green light to activate XXM. Upon 5s green light illumination, the plants transiently expressing Ret-XXM 2,0 produced strong Ca^{2+} fluctuation (**fig. 11e**), comparing with the response from the plants expressing Ret-eYFP (**fig. 11e**). According to these data from the transient expression in *N. benthamiana*, by and large, we identified the function of XXM in plants.

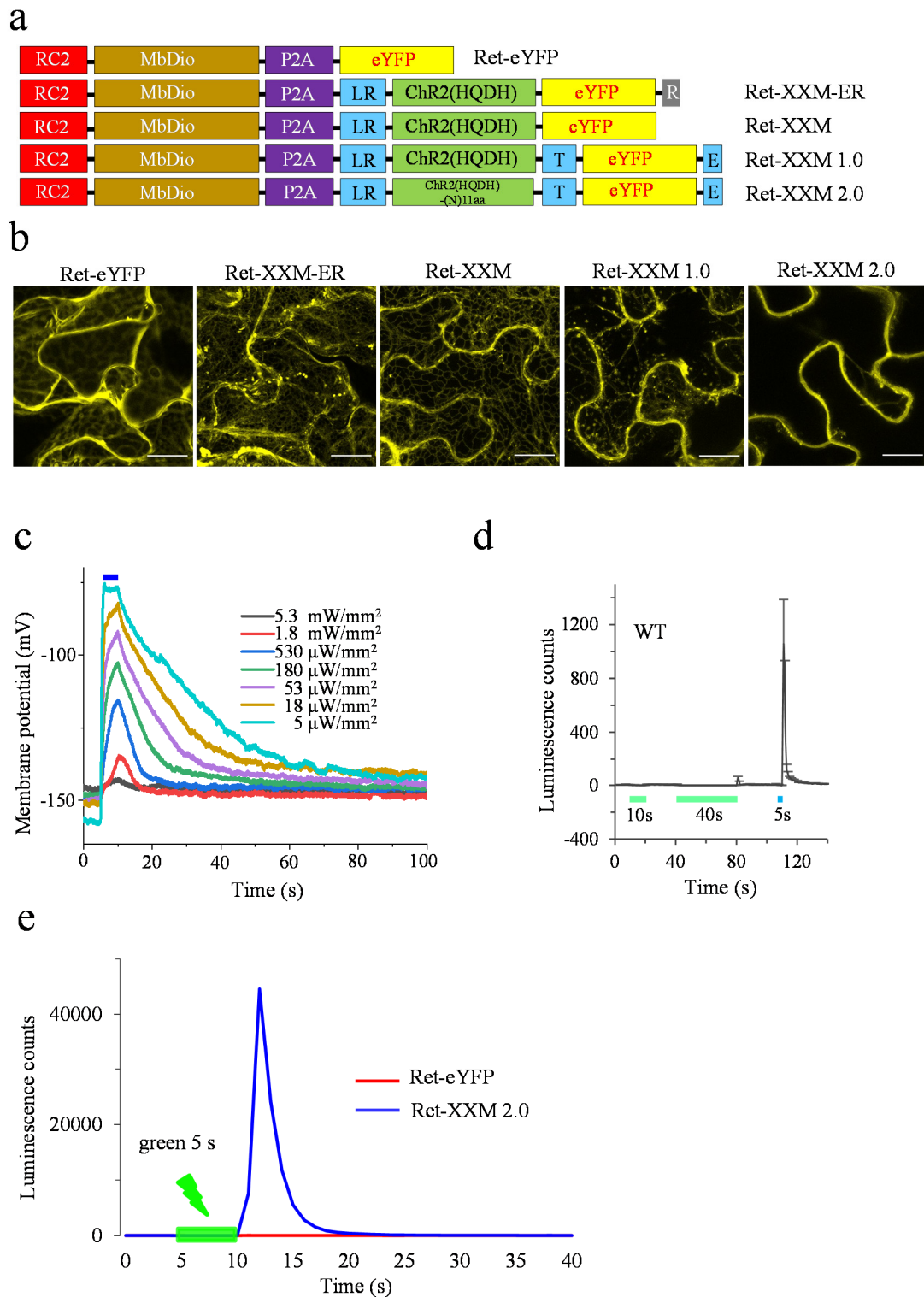


Figure 11. Expression of XXM in *N. benthamiana*

a, Schematic diagram of constructs-Ret-eYFP, Ret-XXM-ER, Ret-XXM, Ret-XXM 1.0, and Ret-XXM 2.0. ChR2 (HQDH), double mutants of channelrhodopsin-2 at the position 134 from Histidine to Glutamine and position 156 from Aspartic Acid to Histidine; ChR2 (HQDH)-(N)11aa, double mutants of channelrhodopsin-2 at the position 134 from Histidine to Glutamine and position 156 from Aspartic Acid to Histidine and truncated 11 amino acids in the N-terminal. R, Endoplasmic reticulum retention signal sequence (5'-aaatataactctctgaagaaacgaac-3'); **b**, Representative superimposed confocal images of epidermal cells in *N. benthamiana* transiently expressing Ret-

eYFP, Ret-XXM-ER, Ret-XXM, Ret-XXM 1.0, and Ret-XXM 2.0, scale bar = 200 μm . **c**, Membrane potential recording of mesophyll cells in *N. benthamiana* leaves transiently expressing Ret-XXM 2.0 with different blue light (473 nm) intensity for 5 s. **d**, Aequorin-based Luminescence measurements for wild-type *N. benthamiana* infiltrated by empty GV3101 upon different time duration of green (10 s, 40 s) and blue light (5 s). **e**, Aequorin-based Luminescence measurements for *N. benthamiana* transiently expressing Ret-eYFP and Ret-XXM 2.0 upon green light for 5 s.

2.3.3 The expression and function of XXM in the *N. tabacum*

To study the function in plants deeply, the *N. tabacum* plants stably expressing Ret-XXM 2.0 were cultured. The plants expressing Ret-eYFP, Ret-XXM and Ret-XXM-ER were as control. In the transgenic *N. tabacum* plants, the plants expressing Ret-XXM-ER had no clear expression on PM (**fig. 12a, suppl. fig. 7a**) and the response to the 5s 180 $\mu\text{W}/\text{mm}^2$ green light illumination is the same to WT plants and Ret-eYFP-expressing plants (**fig. 12b, c, suppl. fig. 7b**), which shows that little protein is expressed on the PM. The plants expressing Ret-XXM had a better expression on PM (**fig. 12a, b, suppl. fig. 7a**) and could depolarize the membrane potential (**fig. 12b, c, suppl. fig. 7b**), but the expression on ER still is strong. Among these transgenic *N. tabacum*, Ret-XXM 2.0-expressing plants had the best expression on PM (**fig. 12a, suppl. fig. 7a**) and had the highest light-induced membrane potential changes in mesophyll cells of transgenic *N. tabacum* (**fig. 12b, c, suppl. fig. 7b**). As the best constructs, in the Ret-XXM 2.0-expressing tobacco higher light intensities evoked stronger depolarizations under blue light (**fig. 12d, f, suppl. fig. 7c, e**) and green light (**fig. 12e, f, suppl. fig. 7d, e**). While, Different from ACR1, very strong depolarization did not lead to hyperpolarization when the potential went back to resting state (**fig. 12g**).

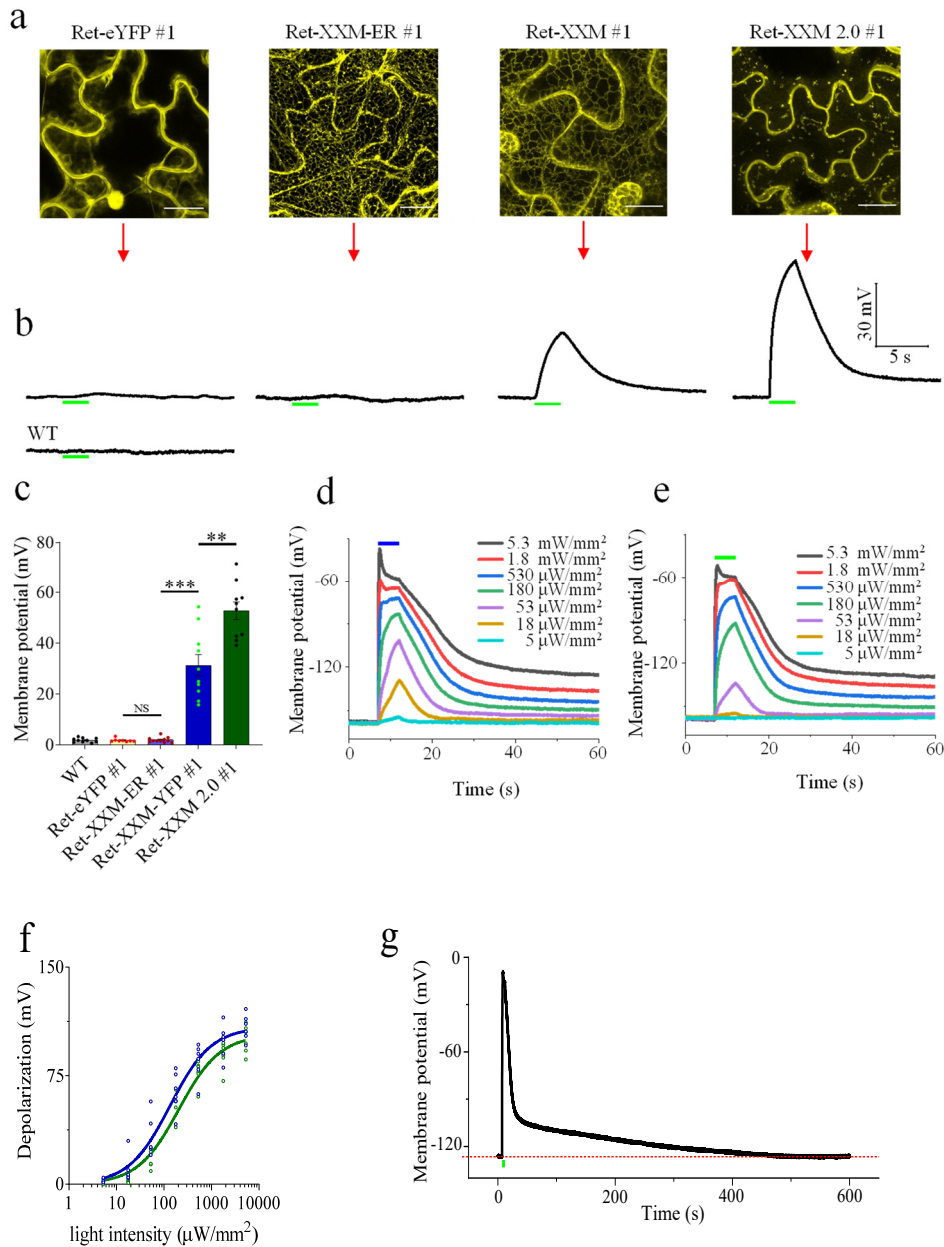


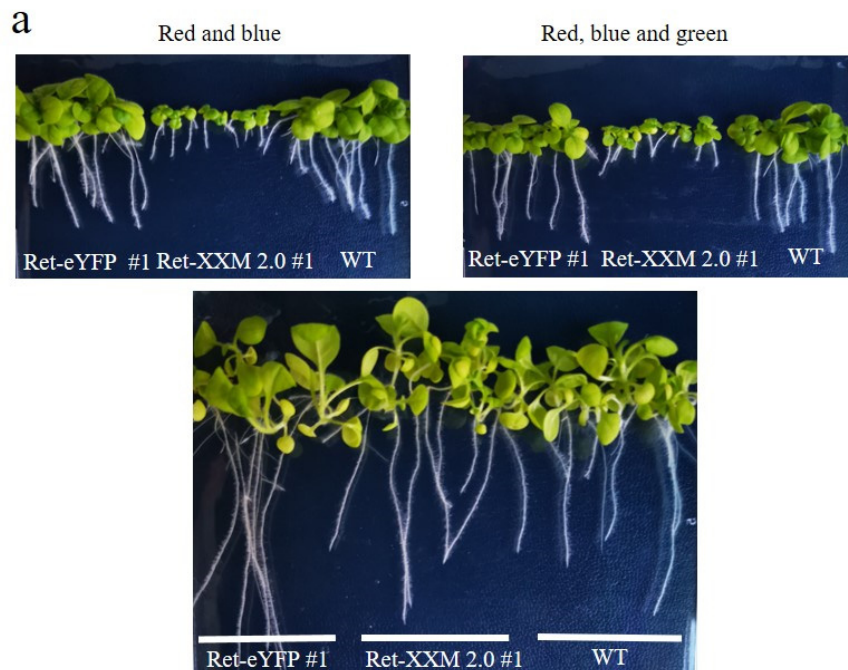
Figure 12. Functional expression of Ret-XXM 2.0 in *N. tabacum*

a, Representative superimposed confocal images of epidermal cells in transgenic *N. tabacum* expressing Ret-eYFP #1, Ret-XXM-ER #1, Ret-XXM #1 and Ret-XXM 2.0 #1, scale bar = 200 μm . **b**, Representative voltage recording trace of transgenic *N. tabacum* mesophyll cells expressing Ret-eYFP #1, Ret-XXM-ER #1, Ret-XXM #1 and Ret-XXM 2.0 #1, 5 s 180 $\mu\text{W}/\text{mm}^2$ (864 $\mu\text{mol}/\text{m}^2/\text{s}$) green (532 nm) light illumination were indicated by the green bars; Representative voltage recording trace of wild type (WT) *N. tabacum* mesophyll cell illuminated with 5 s 180 $\mu\text{W}/\text{mm}^2$ (864 $\mu\text{mol}/\text{m}^2/\text{s}$) lasting green light (532 nm) pulse was shown in the lower left side. **c**, Comparison of light-induced membrane potential changes in the mesophyll cells of WT, and Ret-eYFP #1, Ret-XXM-ER #1, Ret-XXM #1 and Ret-XXM 2.0 #1-expressing *N. tabacum*. illumination was performed with 5 s 180 $\mu\text{W}/\text{mm}^2$ (864 $\mu\text{mol}/\text{m}^2/\text{s}$) green (532 nm) light. Error bar = s.e.m. n = 8 - 11. One-way ANOVA analysis followed by a Games-Howell's Post Hoc Test was performed for significance analysis. For Ret-eYFP #1 vs. Ret-XXM-ER #1, there is no significant difference; for Ret-XXM-ER #1 vs. Ret-XXM #1, $P = 2.9 \times 10^{-5}$; Ret-XXM #1 vs. Ret-XXM 2.0, $P = 0.002$. **d**, Membrane potential recording of mesophyll cells in transgenic *N. tabacum* expressing Ret-XXM 2.0 #1 with blue (473 nm) light in different light intensity for 5 s. **e**, Membrane potential recording

of mesophyll cells in transgenic *N. tabacum* expressing Ret-XXM 2.0 #1 with green (532 nm) light in different light intensity for 5 s. **f**, Ret-XXM 2.0-expressing *N. tabacum* mesophyll cell depolarization induced by different intensities of 473 nm blue light and 532 nm green light. all individual data are shown, n = 6. **g**, Example of a long-time membrane potential recording trace of in transgenic Ret-XXM 2.0-expressing *N. tabacum* (line #1) mesophyll cell, illuminated with 5 s 5.3 mW/mm² (25.4 mmol/m²/s) green light (532 nm, green bar).

2.3.4 The phenotype of Ret-XXM 2.0-expressing *N. tabacum*

When the plants were grown under different light conditions, compared with the WT tobacco and Ret-eYFP-expressing plants (**fig. 13a**), the growth of Ret-XXM 2.0 plants would be inhibited (**fig 13a, suppl fig. 8**). The main reason is the activation of Ret-XXM 2.0 under blue light and green light (**fig. 12d, e, suppl fig. 7c, d**). However, it is different from ACR1 on the leaf phenotype. For the plants expressing Ret-ACR1 2.0, there was a layer of wax on the surface of leaves when the plants grew in the greenhouse. On the contrary, for the transgenic *N. tabacum* expressing Ret-XXM 2.0, there would be many necroses on the surface of the leaves when the plants grew in the greenhouse for about 24 h (**fig. 13b**). If the plants grow in white light condition for a long time, they will die (**suppl fig. 8**). But it is strange that the Ret-XXM 2.0-expressing seedlings would not die, even though they grew in white light condition for a long time and just grew slower than WT plants and Ret-eYFP-expressing plants (**fig. 13a**).



b



Figure 13. The phenotype of Ret-XXM-2.0-expressing *N. tabacum*

a, Comparison on the growth of wild-type *N. tabacum* with the transgenic *N. tabacum* expressing Ret-eYFP #1 and Ret-XXM 2.0 #1 on the plate containing MS medium in different light (red 650 nm LED, blue 465 nm LED and green 532 nm LED) conditions (red, 12:12 h; red and blue, 12: 12 h; red, blue and green, 12: 12 h, respectively) for 45 days. **b**, The phenotype of 3 lines of Ret-eYFP-expressing and 3 lines of Ret-XXM 2.0-expressing *N. tabacum* in the greenhouse for 10 days, respectively.

2.3.5 Discussion

Different from the ACR1, Chr2, the widely employed optogenetic tool, has a big potential in the plant system. As cation channels, it has high permeability for Ca^{2+} , H^+ et al which is important for the regulation of biological characteristics in plants. To find an available cation channel for the plant study, we expressed XXL (**suppl fig. 9a**) and XXM in plants. Although Ret-XXL 2.0 (**suppl fig. 9a**) showed the obvious expression on the PM and ability as an optogenetic tool, which could induce the depolarization of plant cells (**suppl fig. 9b**), it had less permeability on Ca^{2+} , compared to Ret-XXM 2.0. At last, we decided XXL as the ultimate tool for study. Certainly, Ret-XXL 2.0 may be the potential tool for different research. Except for Chr2 mutants, we also tried *PsChR* which also has high Ca^{2+} conductance [43], according to the expression in epidermal cells of *N. benthamiana* (**suppl fig. 3**), *PsChR* had a lower expression level than XXL

2.0. Maybe the construct about *PsChR* could be engineered more to improve the expression of the PM in the future. At least, at present, XXM is the best one as a Ca^{2+} flux regulator in plant research.

In consideration of photoreceptors in plants, blue light which activated XXM 2.0 can also affect the plant system, and blue light has higher energy than green light at the same light intensity. Thus, we compared the effect of blue light (473 nm) and green light (532 nm) on plants under lone-time illumination (60 s and 600 s) (**suppl fig. 10a, b**). Compared with blue light, the effect of green light on plants was weaker (**suppl fig. 10a, b**). In the short illumination (5 s), compared with Ret-XXM 2.0, the effect of green light on the plants could be neglected. Different from ACR1, XXM depolarizes the membrane potential by Ca^{2+} and H^+ influxes. What's more, the Ret-XXM 2.0 could not induce the hyperpolarization of the membrane potential when the membrane potential recovers to the resting state, which is also different from the response from ACR1. Ca^{2+} and H^+ are the initial response to the external stresses, thus the plants have a different mechanism to balance the ionic changes across the PM. The same point for Ret-XXM 2.0-expressing and Ret-ACR1 2.0-expressing tobacco is the response under the illumination by high light intensity. Under strong light intensity (5.3 mW/mm^2) the voltage changes induced by Ret-XXM 2.0 and Ret-ACR1 2.0 could activate the voltage-gated channels to equilibrate the ionic distribution. Due to the different ion permeability, the channels induced in plants maybe were also different.

Although the activation of Ret-ACR1 2.0 and Ret-XXM 2.0 both could depolarize the membrane potential, due to the different ion permeability, the tobacco expressing Ret-XXM 2.0 presented a much different phenotype from the tobacco expressing Ret-ACR1 2.0. Ret-XXM 2.0-expressing tobacco could not survive when the plants grew in white light for a long time, which indicated the importance of Ca^{2+} balance in the plant system. Besides, the phenotype of Ret-XXL 2.0-expressing tobacco is similar to the phenotype of Ret-XXM 2.0-expressing tobacco (**suppl fig. 8**). In my opinion, on the one hand, this

is the result of different characteristics of the anion channel and cation channel. On the other hand, the similar phenotype between Ret-XXL 2.0 and Ret-XXM 2.0-expressing tobacco is ascribed to the similar ion permeability. We compared the Ca^{2+} permeability of Ret-XXL 2.0 and Ret-XXM 2.0 by luminescence experiment (**suppl fig. 11**), it showed that Ret-XXL 2.0 also has a permeability to Ca^{2+} which is a little lower than Ret-XXM 2.0, but in a long-time white light condition, the effects should be similar. Because of the importance of Ca^{2+} in plant systems, especially for information transport, Ret-XXM 2.0 could be a good tool for the research, and with precise temporal and spatial manipulation, it will play an important role in plant research. In short, Ret-XXM 2.0 and Ret-XXL 2.0 could be used as the new optogenetic tools for plant research in different aspects.

2.4 The expression and function of PPR (proton pump rhodopsin)

2.4.1 Introduction

After ChR2, the light-gated proton pumps are used as optogenetic tools in neuroscience. The efflux of protons elicited by these proton pumps under illumination will result in hyperpolarization of the plasma membrane. However, there is a shortcoming in these proton pumps, as they can transport only one proton per absorbed photon. Besides, to increase the efficiency, usually higher light intensity is required for the activation. Therefore, the expression level of these pumps is important.

In plant cells, the circuits are driven by proton gradients that mediate secondary active transport of compounds across the PM or endosomal membranes, and the regulation of endosomal acidification is critical for endocytic and secretory function [121]. There are many proton pumps in the membrane system in plants, but their activity is not easy to control, which just depends on the changing environment. In the process of screening the available light-driven proton pump, we found that a proton pump from *Chlorella vulgaris* (CvRh, called PPR in next content) had a good expression in the *Xenopus* oocytes. Under green light illumination, it could induce high photocurrent (data not shown). Based on our method for the expression of opsins in plants, Ret-PPR 2.0 was constructed and expressed on the PM successfully with a high expression level. The high expression deleted the drawback of single H⁺ transport and made it beneficial for the research in plant systems.

2.4.2 The expression and function of PPR in *N. benthamiana*

According to the study on ACR1 and XXM, the construct Ret-PPR 2.0 was made, but different from Ret-ACR1 2.0 and Ret-XXM 2.0, two “T” were fused to the C-terminal of PPR (**fig. 14a**), because it demonstrated in *Xenopus* oocytes that more “T” could future improve the expression level of PPR (data not shown). We transiently expressed Ret-PPR 2.0 in *N. benthamiana*, from the confocal image of *N. benthamiana* epidermal

cells leaves (**fig. 14b**), we could find that the expression of Ret-PPR 2.0 was on the PM and had a high expression level. Because PPR is outward proton rhodopsin, when we recorded the membrane potential changes in mesophyll cell, upon 5s, 180 $\mu\text{W}/\text{mm}^2$ green (532 nm) light, it could induce the hyperpolarization of membrane potential which has a positive correlation with the light intensity (**fig. 14c**).

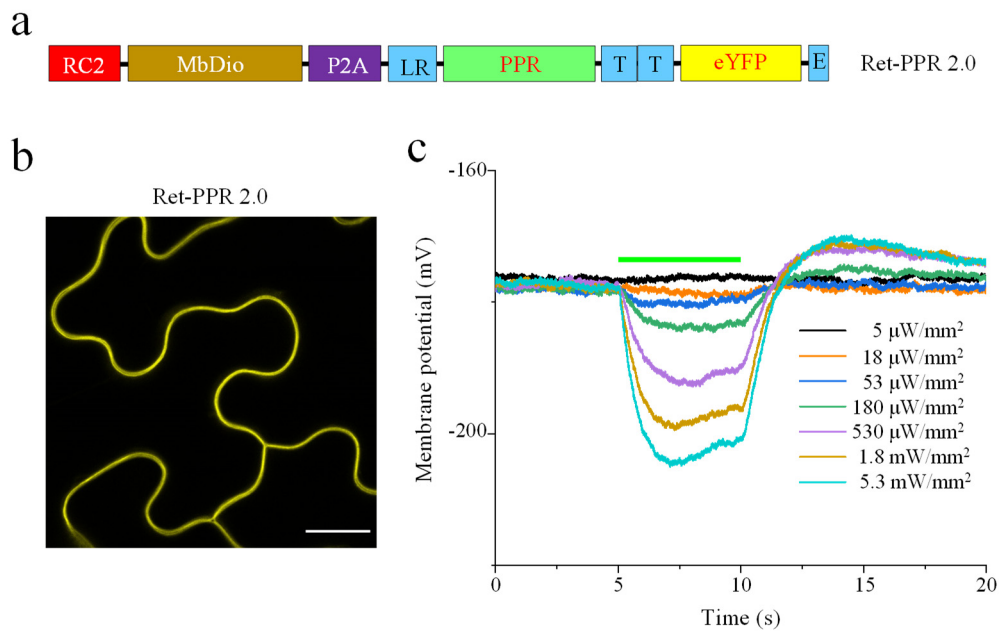


Figure 14. Functional expression of Ret-PPR 2.0 in *N. benthamiana*

a, Schematic diagram of construct Ret-PPR 2.0. PPR, proton pump rhodopsin. **b**, Representative confocal image of the epidermal cells in the *N. benthamiana* leaves expressing Ret-PPR 2.0 transiently. scale bar = 200 μm . **c**, Membrane potential recording trace in mesophyll cell of *N. benthamiana* expressing Ret-PPR 2.0 transiently in different green (532 nm) light intensities for 5 s.

2.4.3 The expression and function of PPR in *N. tabacum*

Due to the good localization on the PM, we transferred Ret-PPR 2.0 into *N. tabacum*. Also, there was a high expression on the PM (**fig. 15a**). The hyperpolarization induced by activation of PPR is correlative with light intensity (**fig. 15b**), and higher light intensity evoked stronger hyperpolarization (**Fig. 15c**). Unfortunately, a distinct phenotype was not observed in Ret-PPR 2.0-expressing *N. tabacum* (**fig. 15d**).

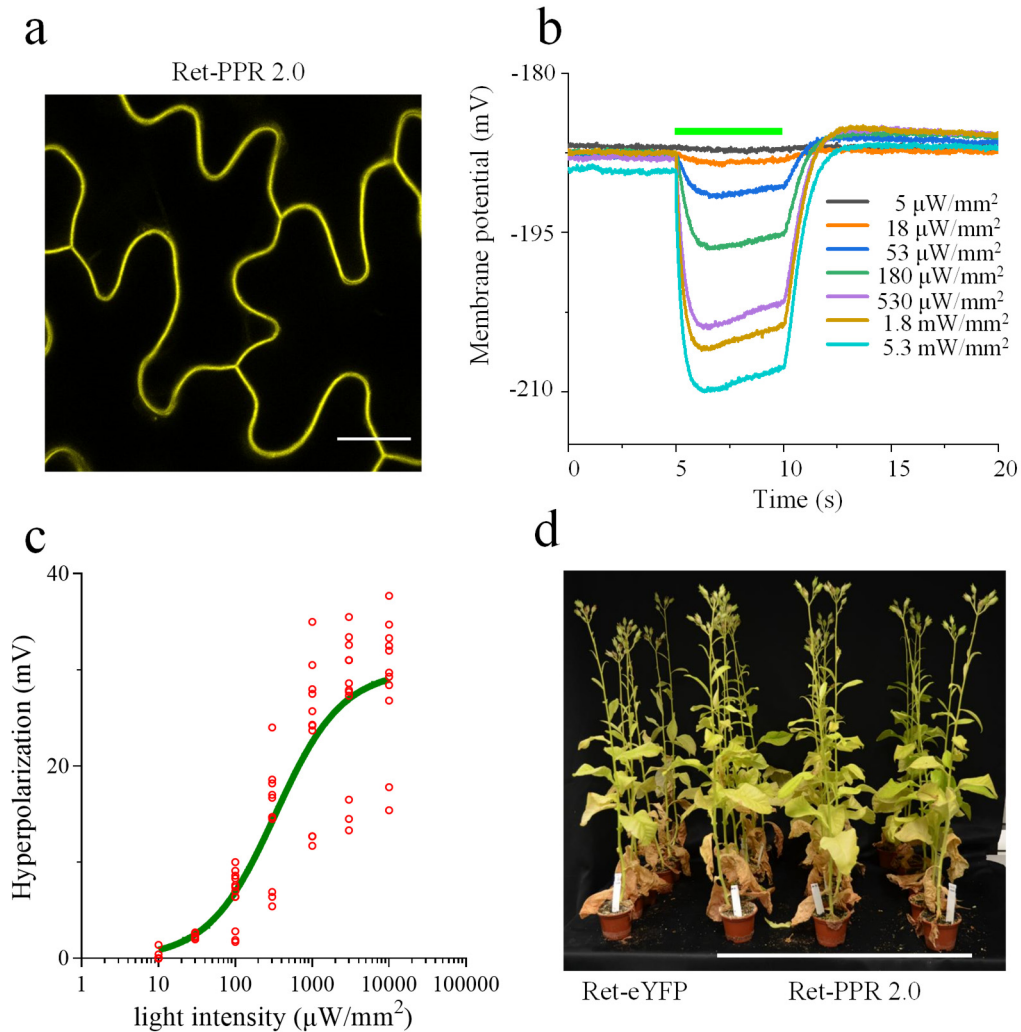


Figure 15. Functional expression of Ret-PPR 2.0 in *N. tabacum*

a, Representative confocal image of transgenic *N. tabacum* leaf epidermal cells expressing Ret-PPR 2.0, scale bar = 200 μm . **b**, Membrane potential recording trace of *N. tabacum* mesophyll cell expressing Ret-PPR 2.0 in different green (532 nm) light intensities for 5 s. **c**, Mesophyll cells hyperpolarization of transgenic Ret-PPR 2.0 *N. tabacum* induced by green (532 nm) light with different intensities. $n = 7-12$, all individual data points are shown. **d**, The phenotype of Ret-eYFP and Ret-PPR 2.0-expressing *N. tabacum* in the greenhouse for 3 months.

2.4.5 Discussion

There was no obvious phenotype in the different phases of *N. tabacum* expressing Ret-PPR2.0 stably, compared with the plants expressing Ret-eYFP. Upon the light stimulation, activated PPR only pumps one proton out of the cell, which is more modest than Ret-ACR1 2.0 and Ret-XXM 2.0. Even though Ret-PPR2.0 has a high expression level on the PM of *N. tabacum*, however, due to the low efficiency for the H^+ permeability, the plant system could equilibrium the effect which was induced by the

hyperpolarization from the Ret-PPR 2.0. After all, the effect on the membrane potential is weaker than that from channels. Except for the expression on the PM, Ret-PPR2 0 also showed a good expression on the PM of guard cell (**suppl fig. 12**), which provides a good tool for the research on stomata. Given protons are important in the plant system, Ret-PPR 2.0 can be employed as an ideal optogenetic tool to study ionic transport in a much precise way without hurting plants. There are many light-driven H⁺ pumps, in which some have been identified and used in neuroscience and maybe some will be identified as new optogenetic tools. Thus, there will be more perfect tools than PPR for the plant study. In our study, we will continue to explore the potential of Ret-PPR 2.0 in plant research.

3. Conclusion and Prospect

Since the discovery of ChR2, optogenetics began to be used for the manipulation of neuronal activity and improved the development of neuroscience greatly. At present, more new opsins were identified from new species and variants also were engineered based on the current opsins. In our study, we mainly focus on microbial opsins which are widely used as optogenetic tools. Rhodopsin is the opsin that is bound with its chromophore which in microbial opsins usually is all-trans-retinal. Despite the great success of optogenetics in neuroscience, the application in plants is still at a standstill. From 2016, some engineered optogenetic tools were employed in the manipulation of gene expression or guard cell activity [92, 93, 95, 97], but the microbial opsins still are not applied in plant research. In 2020, ChR2-XXL was expressed in *N. benthamiana* and *A. thaliana*. With exogenous retinal addition, it could depolarize the membrane potential under blue light. However, this attempt did not provide an effective method for the microbial opsins to express in the plant cell widely. The method of exogenous retinal addition cannot solve the fundamental problems in the application of microbial opsins in plants.

Retinal can be synthesized in most vertebrate tissues and can be easily provided through food to animals that do not synthesize it naturally. There is very little retinal in plant tissues which was certified in our study by UPLC-MS/MS. For the isolated tissues, the researcher could add retinal into the bath solution, but for research in the whole plant, it will be useless to add retinal. First, it can't make sure whether the extra retinal will transport to every tissue or cell. Secondly, even though the extra retinal could be transported in plant systems, the retinal is unstable and expensive. Therefore, the addition of exogenous retinal is not a solution for plant studies. At least, in my opinion, this method is a helpless action for the researchers. Considering the importance of retinal for the expression and function of opsins, we introduced a gene coding a β -carotene 15, 15'-Dioxygenase from a marine bacterium (MbDio) into plant tissues.

This enzyme can convert a molecule of β -carotene into two molecules of all-trans-retinal. As we know, there is an amount of β -Carotene applied for photosynthesis in plants. This is the reason why finally we express this enzyme in the chloroplast. When fusion protein “Ret” was expressed in plants, the concentration of all-trans-retinal increased greatly. In the next experiments, we proved that the heterologous expression of Ret did not affect the growth of plants. In the whole research, the conversion of β -carotene into all-trans-retinal is the most important step, which clears the way for the expression of opsins in plants.

Next, we encountered another problem - poor PM localization. Although these opsins express on the PM in the original species. Maybe they indeed have a low expression on the PM in the tissues of other species, but they cannot function fully. Therefore, the improvement of expression on the PM is another problem that must be solved in plant study. It is important to design the constructs about the fusion of Ret with opsins. Firstly, we determined which promoter would be better for the constructs. After comparing *UBQ10* with *35S* promoters, the *UBQ10* promoter was chosen to drive the constructs. Unlike the *35S*-driven construct, expression under the *UBQ10* promoter remained for a longer time [122], though the expression had no difference for the constructs driven by these two promoters (**suppl fig.13**). Under the driving of the *UBQ10* promoter, various combinations -- Ret-ACR1-TY vs. ACR1-TY-Ret and Ret-XXL vs. XXL-Ret were expressed in *N. benthamiana*, and when the opsins were fused to the C-terminal of Ret, the opsins could have a higher expression level in plants. Maybe the epibiotic amino acids from the cleavage of the P2A linker disturbed the orientation function of “Ret”, which led to the uneven and low expression on the PM. Secondly, according to reference about improving opsins PM localization in neurons, we also fused LR, T, and E signal peptides to N/C-terminals of opsins, in which LR is for the improvement of expression, T is the Golgi trafficking signal for the transport from Golgi apparatus peptide and E is for the transport from ER. With the help of these peptides, the expression level and localization of opsins on the PM were improved indeed. Based on

the retinal production in plants and the methodology used in neuroscience, a series of microbial opsin-based optogenetic tools were made.

Compared to the expression level, we found that Ret-ACR1 2.0, Ret-XXM 2.0, and Ret-PPR 2.0 had the best expression on PM, regardless of expressing in plants transiently and stably. Corresponding to the expression level, the membrane potential changes induced by these channels or pumps were larger. In the transgenic *N. tabacum* expressing Ret-ACR1 2.0, when the plant is grown in the greenhouse for a few days, there would be dehydration in the leaves and the reproductive growth also was disturbed which the buds always dropped before fertilization. Different from the plants expressing Ret-ACR1 2.0, some neuroses appeared on the leaves of transgenic *N. tabacum* expressing Ret-XXM 2.0 in the greenhouse. Growing in the greenhouse for a long time, the vegetative growth of plants would be affected and die. While the *N. tabacum* expressing Ret-PPR 2.0 could grow normally, which did not have any distinct phenotype. In theory, the overexpression of the proton pump could change the biological characteristics of plants [123, 124], but we did not find a similar phenomenon in *N. tabacum*. However, we cannot deny the potential role of Ret-PPR 2.0 in the future, because it has a good expression on the PM, including the PM guard cell. Also, for the Ret-ACR1 2.0 and Ret-XXM 2.0-expressing *N. tabacum*, the opsins have a good expression on the PM of the guard cell (**suppl fig. 12**). Foreseeably, they will be useful optogenetic tools for the research on the biological characteristics of stomata. Except for *N. benthamiana* and *N. tabacum*, in *A. thaliana*, another model plant in biological research, Ret-ACR1 2.0, Ret-XXM 2.0, and Ret-PPR 2.0 also exhibited the capacity as optogenetic tools (**suppl fig. 14a-c, suppl fig. 15a-d, suppl fig. 16a-b**). The plants expressing these opsins have distinct phenotype changes when these opsins were activated. More and more studies on *A. thaliana* expressing these opsins will be done in the next work.

Optogenetics had pushed neuroscience into a new era. The development of optogenetics

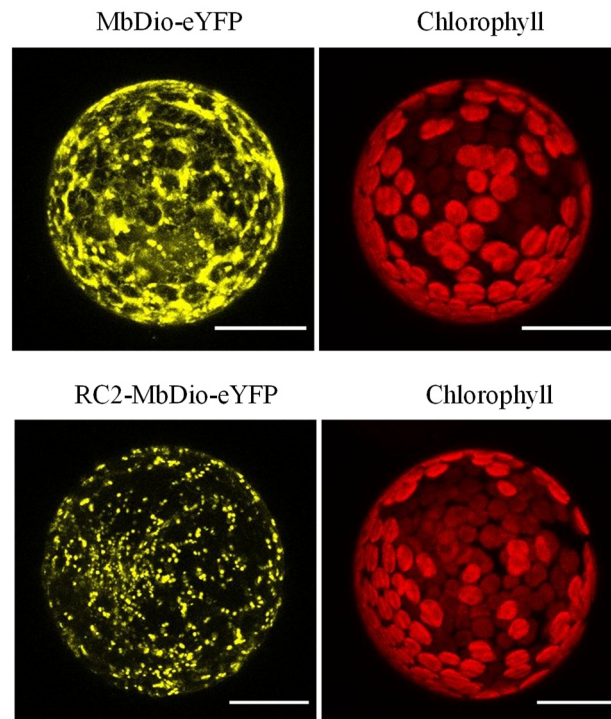
is also the development of optogenetic toolkits, especially microbial opsins. In recent years, optogenetics has been extended to plant research. Producing retinal endogenously in plants makes the opsin-based toolkits could be employed in plants and to selectively study the effect of ion transport on the plant physiology. Except choosing appropriate for the research, it is also important to select the most suited plant system for the purpose, such as Arabidopsis, moss, liverworts. More new methods that enable the expression of different opsins in plants are needed in the future. Because in a different system, the same tools may not still work well, the investigators need to adjust the strategy in the practical experiment. In neuroscience, the optogenetic toolkits with higher light sensitivity and red-shifted properties are demanded in noninvasive research *in vivo*. Though plants are penetrable to light, they have various photoreceptors that are sensitive to light. the activation of optogenetic tools also may induce the response from photoreceptors in plants. To overcome this problem, more opsin-based or non-opsin-based toolkits are needed, after all, the existing tools always can't meet the demand of progress. The rapid expansion of optogenetics in neuroscience, in these two decades, gives us sufficient confidence to develop plant optogenetics in the future.

Where is the future of plant optogenetics?

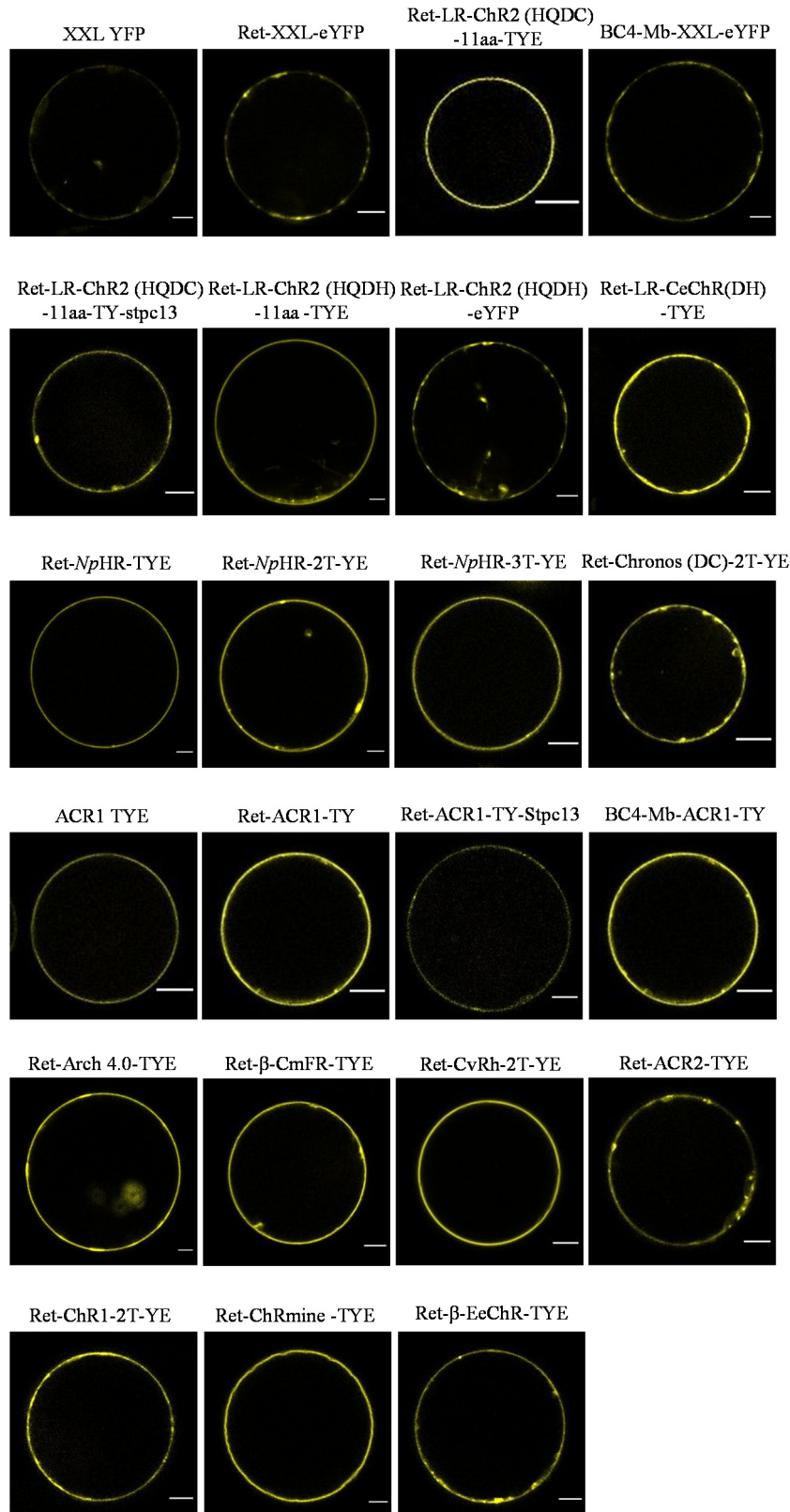
In plants, the ion transport across the membrane could affect diverse physiological activity, such as abiotic and biotic tolerance. Existing experimental methods have limited ability to measure ion fluxes at a detailed quantitative level [125]. Optogenetics is the dawn. The expression of these opsins could be utilized to regulate the hormone secretion or signal transmission in plants. Rhodopsin-based voltage sensors also could be powerful tools to monitor signal pathways, the light-activated enzyme could be used to manipulate the chemical signals transmission. Subcellular localization on the membrane systems in plants, like on mitochondrial membrane, chloroplast membrane or tonoplast, will affect the metabolism and energy conversion in plants. Depending on this novel plant optogenetic approach, more opsin-based tools will be engineered and employed in the future and assemble an “artificial nervous system” for plants.

In short, in this study, through producing retinal in plants, a series of optogenetic tools were explored and applied in the plant study. From the application of optogenetics in bioresearch, this is the first time to employ the opsin-based optogenetic tools in the plant in a real sense and open the gate to the plant study with precise time and space resolution. This is just the beginning, and we are convinced that more and more optogenetic toolkits will be exploited and employed for plant research with this method. The secrets keeping in the plant kingdom also will be unlocked with optogenetics in the future. The application of optogenetics in the plant is endless.

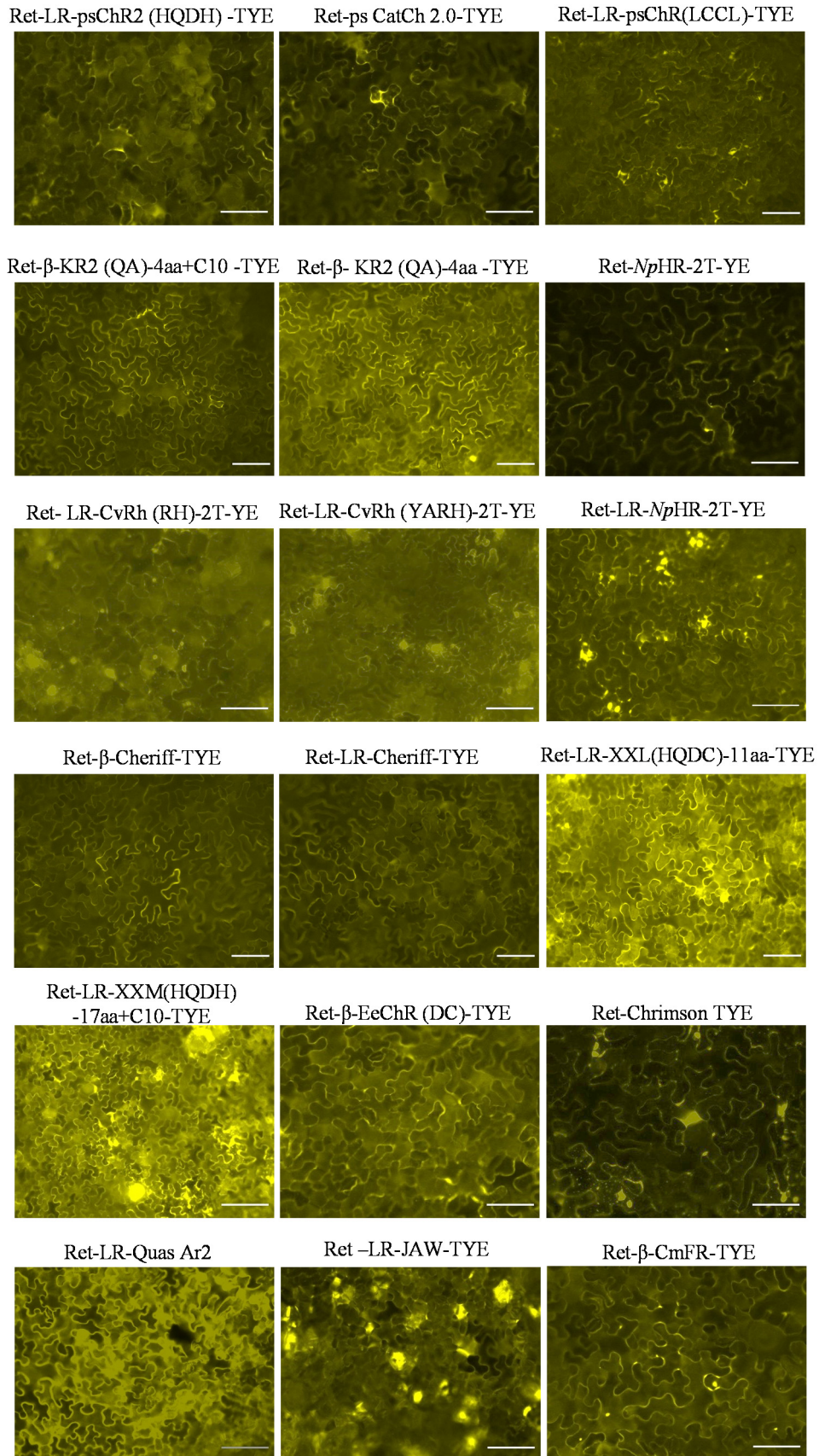
4. Supplementary

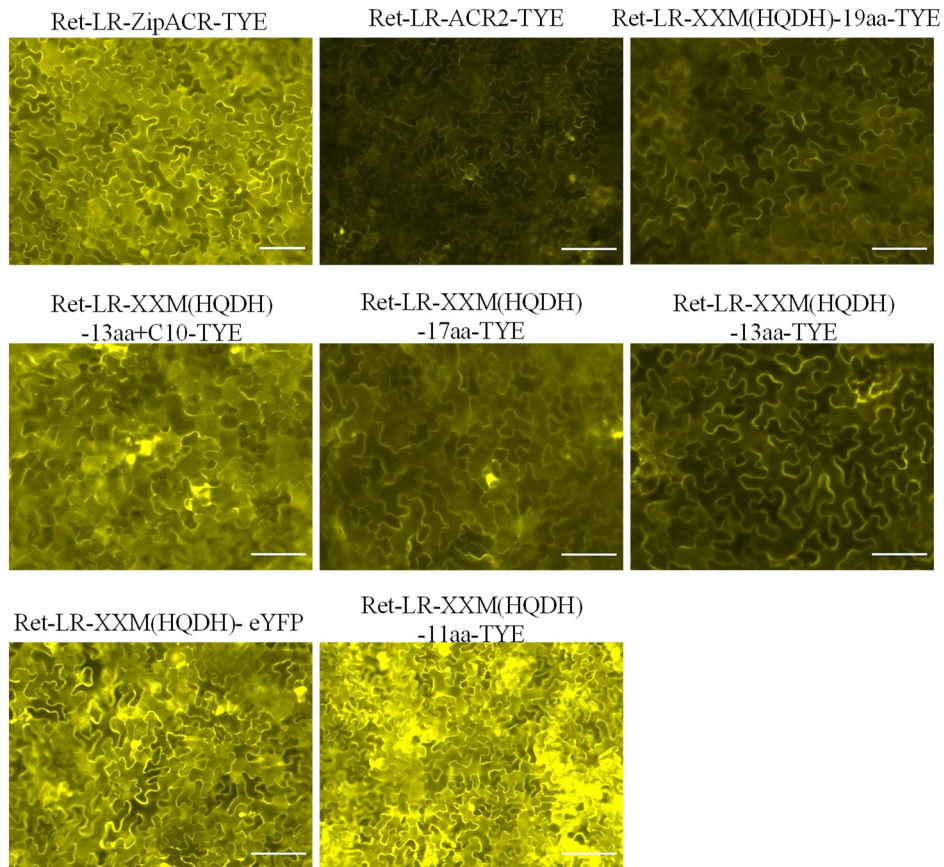


Suppl Figure. 1. Representative superimposed confocal images of *N. benthamiana* protoplasts transiently expressing MbDio-eYFP and RC2-MbDio-eYFP, scale bar = 20 μm.

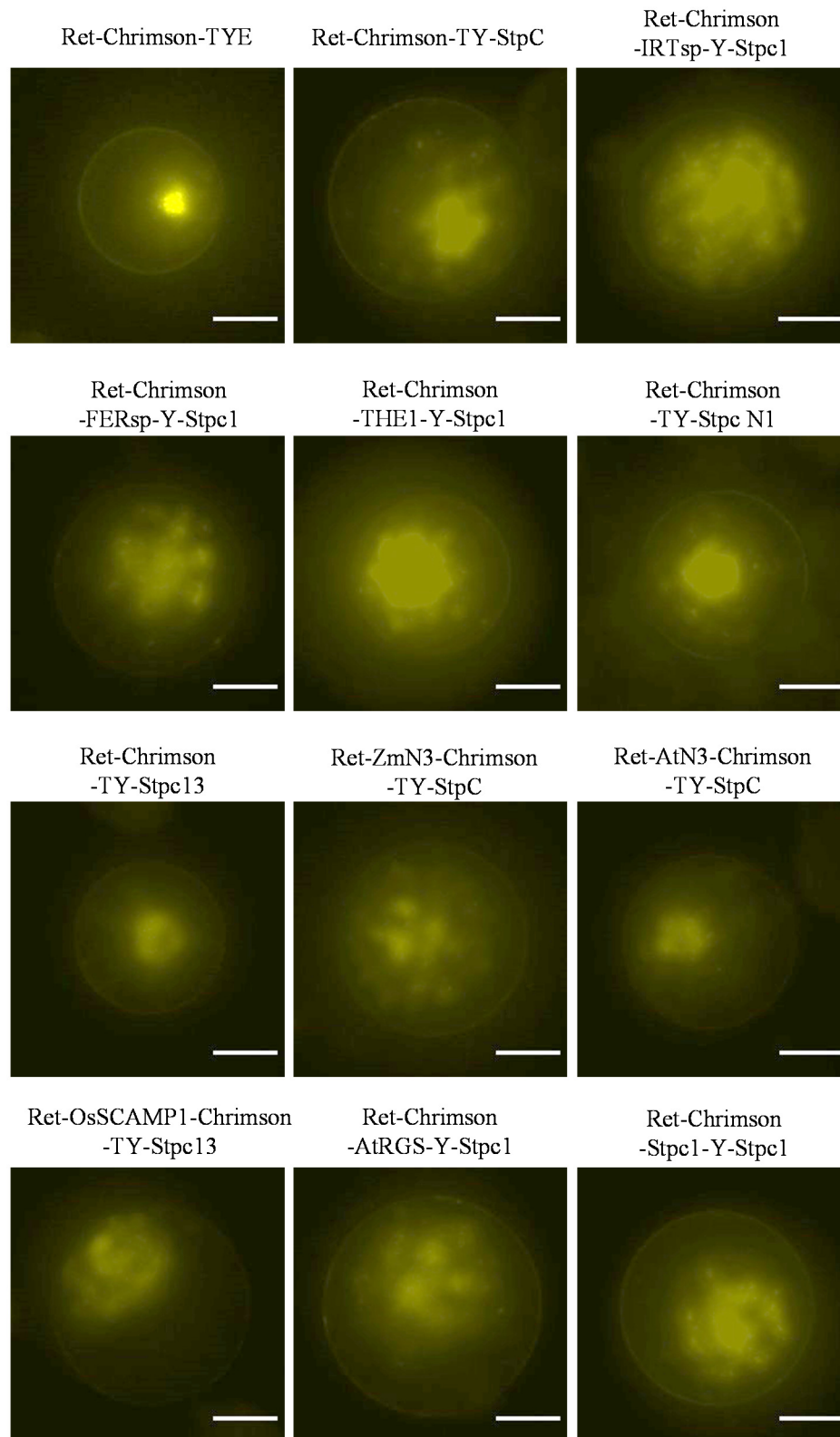


Suppl figure. 2. Representative confocal images of *A. thaliana* protoplasts transiently expressing different opsins, scale bar = 20 μm . **LR**, the cleavable N-terminal signal peptide Lucy-Rho; **β** , β -helix -- 105-amino-acid N-terminal fragment of the β subunit of the rat gastric H^+ , K^+ -ATPase [126]. The images were taken on the third day after transformation.

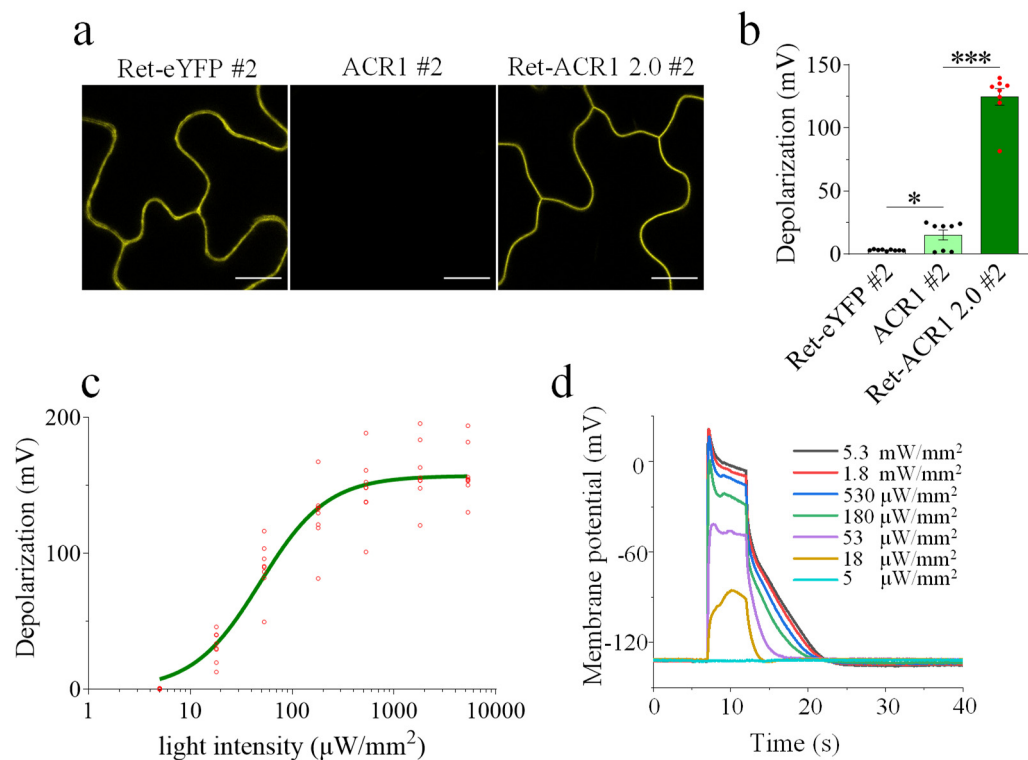




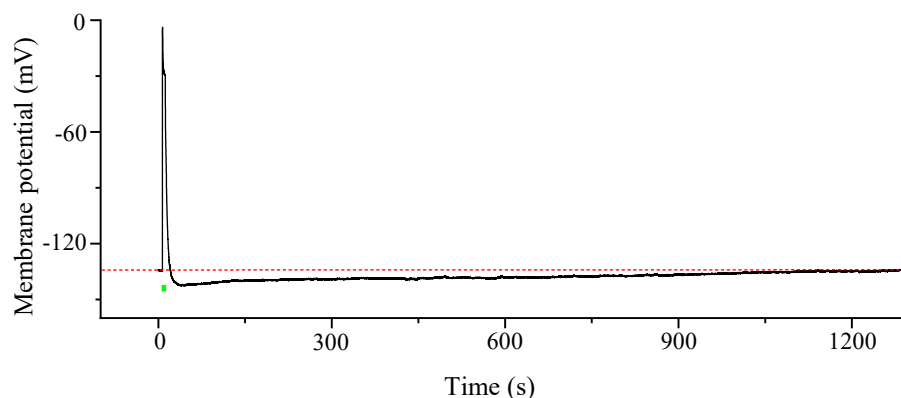
Suppl figure. 3. The representative images of *N. benthamiana* leaf epidermal cells transiently expressing different opsins, scale bar = 200 μ m, the images were taken on the third day after Agro-infiltration.



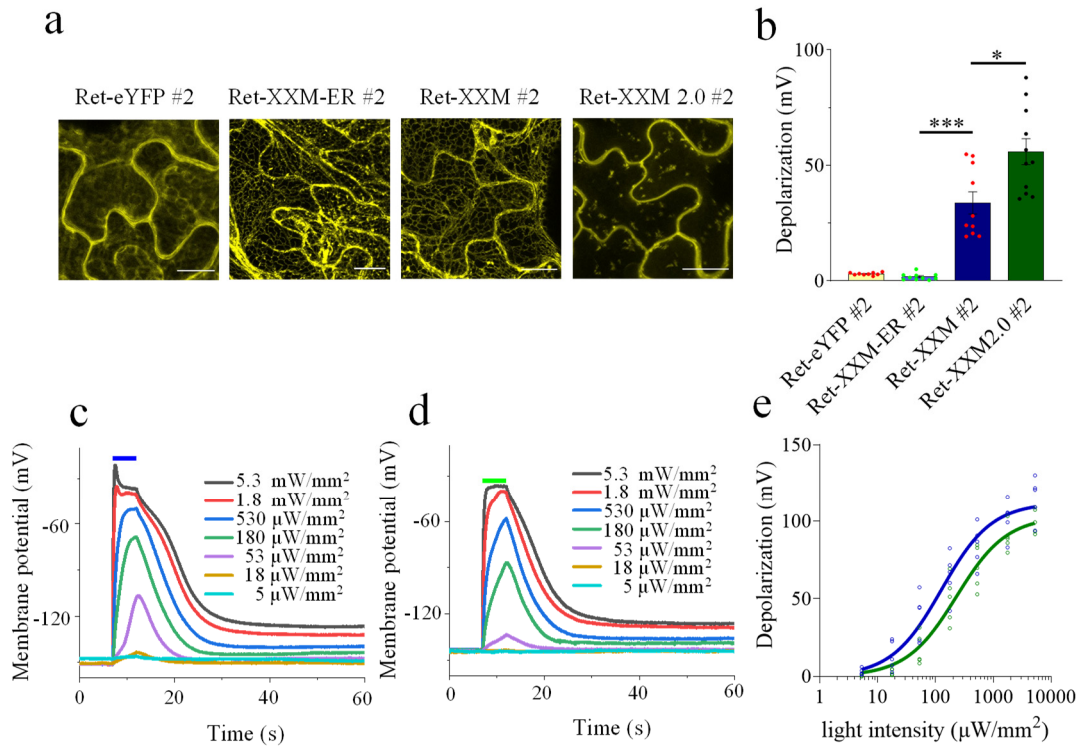
Suppl figure. 4. Representative superimposed confocal images of *A. thaliana* protoplasts transiently expressing different constructs based on Chromimson with different reported signal peptides for targeting PM, scale bar = 20 μ m. The images were taken on the third day after transformation.



Suppl figure. 5. Functional characterization of Ret-ACR1 2.0 in transgenic *N. tabacum* line #2. **a**, Representative confocal images of transgenic *N. tabacum* leaf epidermal cells expressing Ret-eYFP (line #2), ACR1 (line #2) and Ret-ACR1 2.0 (line #2). Scale bar = 200 μm . **b**, 5 s 180 $\mu\text{W}/\text{mm}^2$ (864 $\mu\text{mol}/\text{m}^2/\text{s}$) green (532 nm) light-induced mesophyll cell membrane potential changes (depolarizations) in the second lines of Ret-eYFP, ACR1 and Ret-ACR1 2.0-expressing transgenic tobacco plants. Error bars = s.e.m., $n = 8 - 9$. One-way ANOVA followed by a Games-Howell's Post Hoc Test was performed for significance analysis. $P = 0.041$ for Ret-eYFP #2 vs. ACR1 #2; $P = 3.9 \times 10^{-8}$ for ACR1 #2 vs. Ret-ACR1 2.0 #2. **c**, Membrane potential recording traces of Ret-ACR1 2.0 #2 transgenic tobacco mesophyll cells illuminated with 5 s 532 nm light pulses of different intensities. **d**, Mesophyll cell depolarizations of transgenic Ret-ACR1 2.0 tobacco #2 induced by 532 nm light with different intensities, $n = 8$, all individual data points are shown.

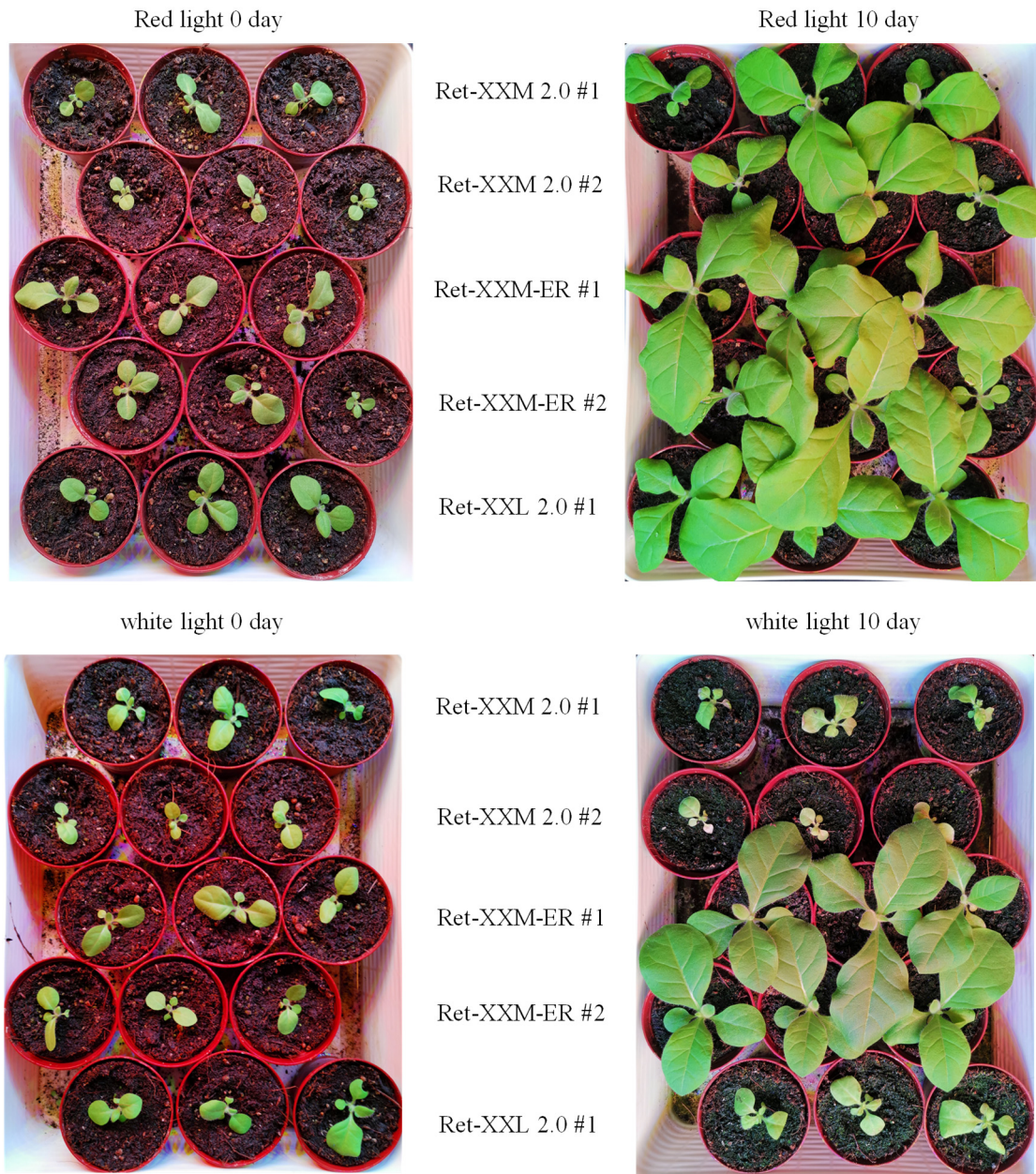


Suppl figure. 6. Example of a long-term membrane potential recording trace of the Ret-ACR1 2.0-expressing *N. tabacum* (line #1) mesophyll cell, illuminated with 5 s 1.8 mW/mm^2 (8640 $\text{mmol}/\text{m}^2/\text{s}$) green (532 nm) light (green bar).

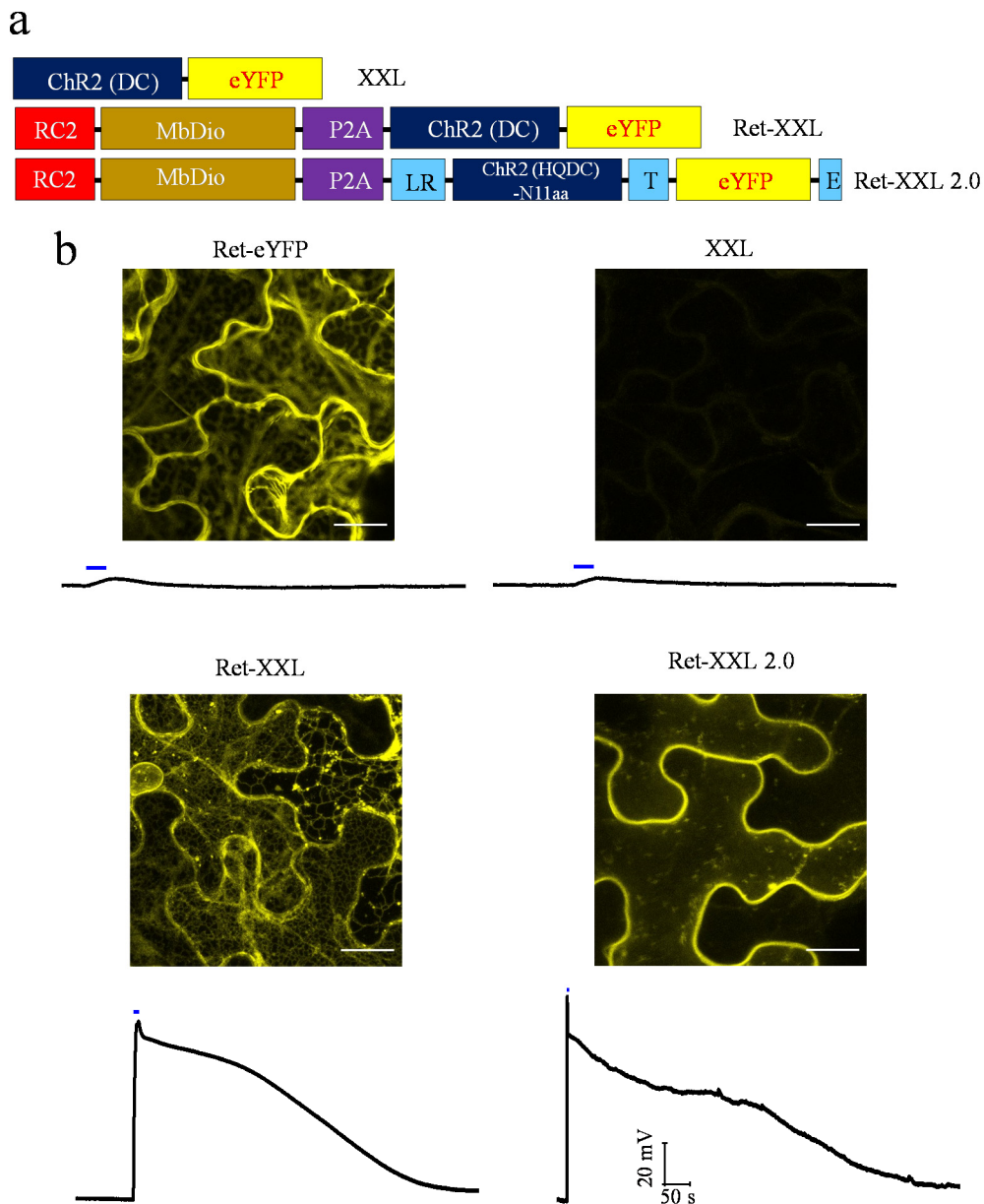


Suppl figure. 7. Expression and function of Ret-XXM 2.0 in transgenic *N. tabacum* line #2.

a, Representative superimposed confocal images of transgenic *N. tabacum* epidermal cells expressing Ret-eYFP #2, Ret-XXM #2, Ret-XXM #2 and Ret-XXM 2.0, scale bar = 200 μm ; **b**, comparison of light-induced membrane potential changes in the mesophyll cells of WT, and Ret-eYFP #2, Ret-XXM-ER #2, Ret-XXM #2 and Ret-XXM 2.0 #2-expressing *N. tabacum*. illumination was performed with 5 s 180 $\mu\text{W}/\text{mm}^2$ (864 $\mu\text{mol}/\text{m}^2/\text{s}$) green (532 nm) light. Error bar = s.e.m. $n = 9 - 11$. One-way ANOVA analysis followed by a Games-Howell's Post Hoc Test was performed for significance analysis. For Ret-eYFP #2 vs. Ret-XXM-ER #2, there is no significant difference; for Ret-XXM-ER #2 vs. Ret-XXM #2, $P = 4.06 \times 10^{-4}$; for Ret-XXM #2 vs. Ret-XXM 2.0 #2, $P = 0.033$. **c**, Membrane potential recording of mesophyll cells in transgenic *N. tabacum* expressing Ret-XXM 2.0 #2 with blue (473 nm) light in different light intensity for 5 s. **d**, Membrane potential recording of mesophyll cells in transgenic *N. tabacum* expressing Ret-XXM 2.0 #2 with green (532 nm) light in different light intensity for 5 s. **e**, Ret-XXM 2.0-expressing *N. tabacum* (line #2) mesophyll cell depolarization induced by different intensities of 473 nm blue light and 532 nm green light. $n = 5$, all individual data are shown.

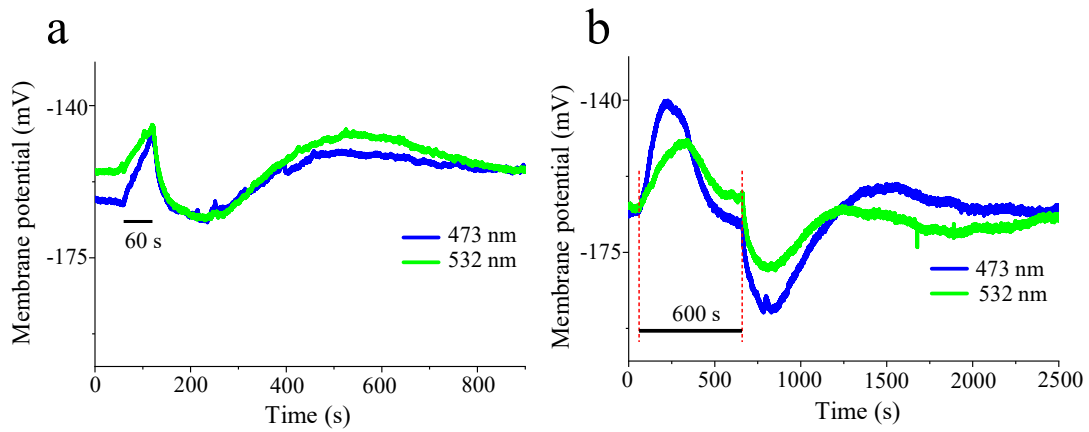


Suppl figure. 8. Phenotype of transgenic *N. tabacum* expressing Ret-XXM 2.0 (line #1 and line #2), Ret-XXM-ER (line #1 and line #2), and Ret-XXL 2.0 (line #1) in different light condition for 10 days.

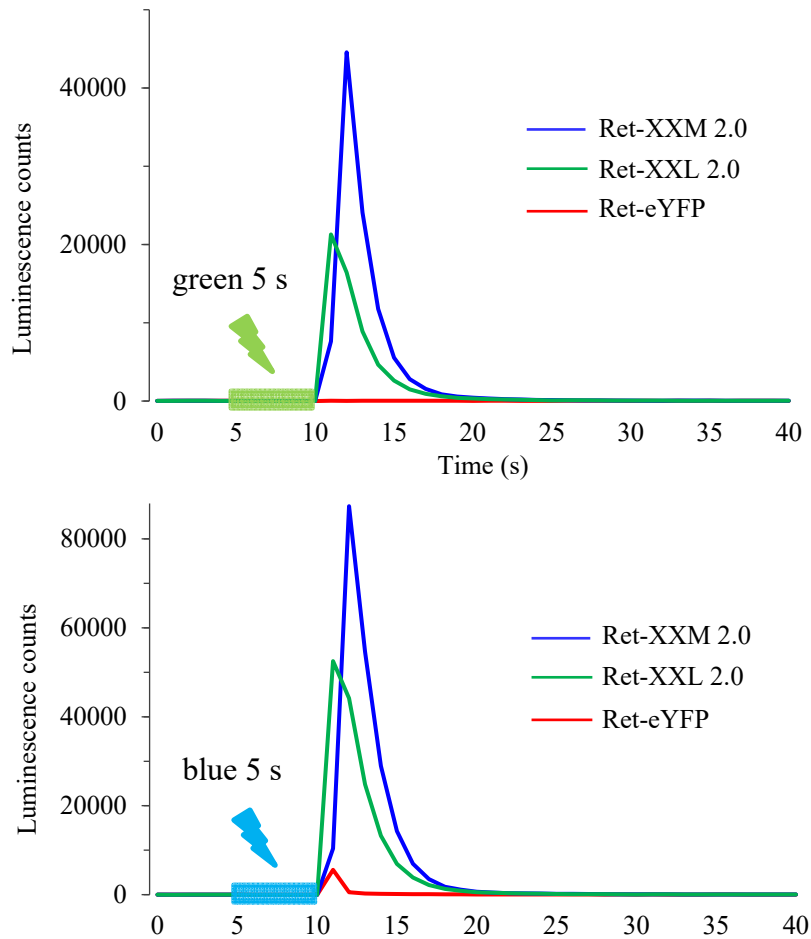


Suppl Figure. 9. Transient expression of XXL in *N. benthamiana*.

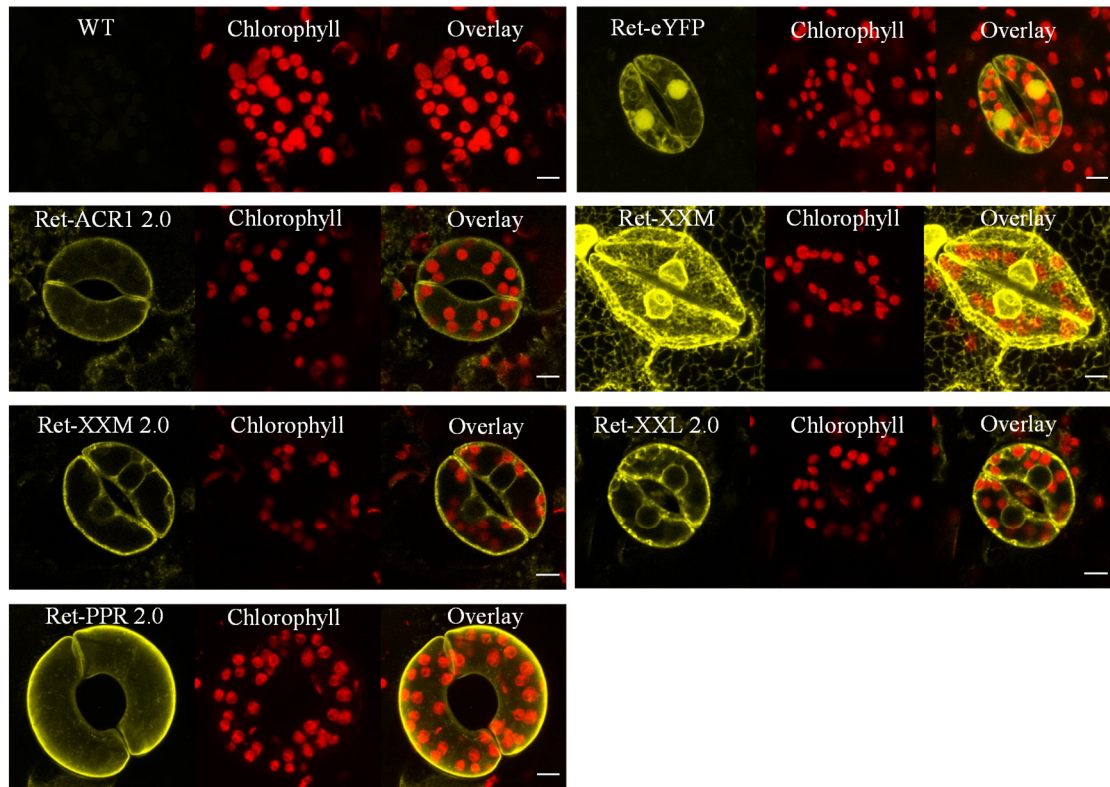
a, Schematic diagram of construct XXL, Ret-XXL, and Ret-XXL 2.0. ChR2 (HQDC)-(N)11aa, double mutants of channelrhodopsin-2 at the position 134 from Histidine to Glutamine and position 156 from Aspartic Acid to Cysteine and truncated 11 amino acids in the N-terminal. **b**, Representative confocal images of *N. benthamiana* leaf epidermal cells transiently expressing Ret-eYFP, XXL, Ret-XXL, and Ret-XXL 2.0 and corresponding membrane potential recording trace from *N. benthamiana* mesophyll cells transiently expressing XXL, Ret-XXL, and Ret-XXL 2.0. The images were taken on the third day after agro-infiltration in leaves, the scale bar = 200 μm , and the membrane potential recording was upon blue (473 nm) light in $550\mu\text{W}/\text{mm}^2$ for 5s.



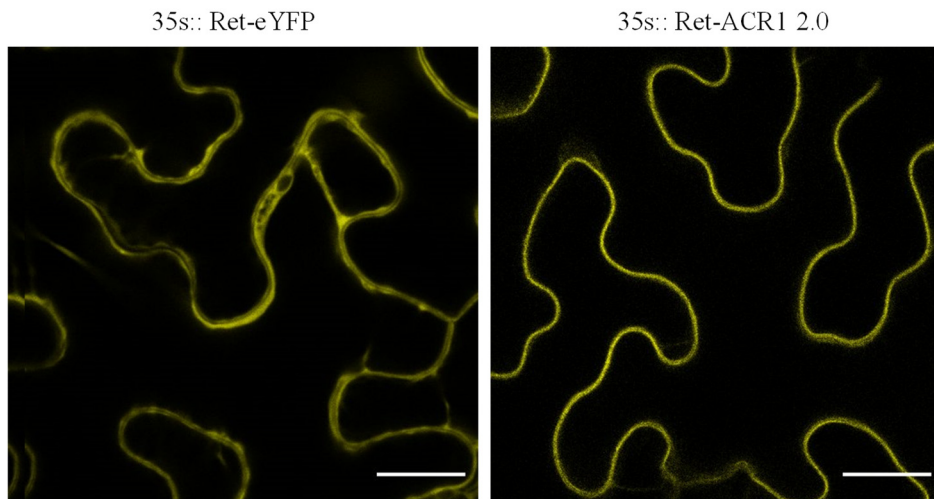
Suppl figure. 10. The response of WT *N. tabacum* to blue light (473 nm) and green light (532 nm) **a**, Membrane potential recording of mesophyll cells in WT *N. tabacum* under 60 s, 1.8 mW/mm² light illumination; **b**, Membrane potential recording of mesophyll cells in WT *N. tabacum* under 600 s, 1.8 mW/mm² light illumination.



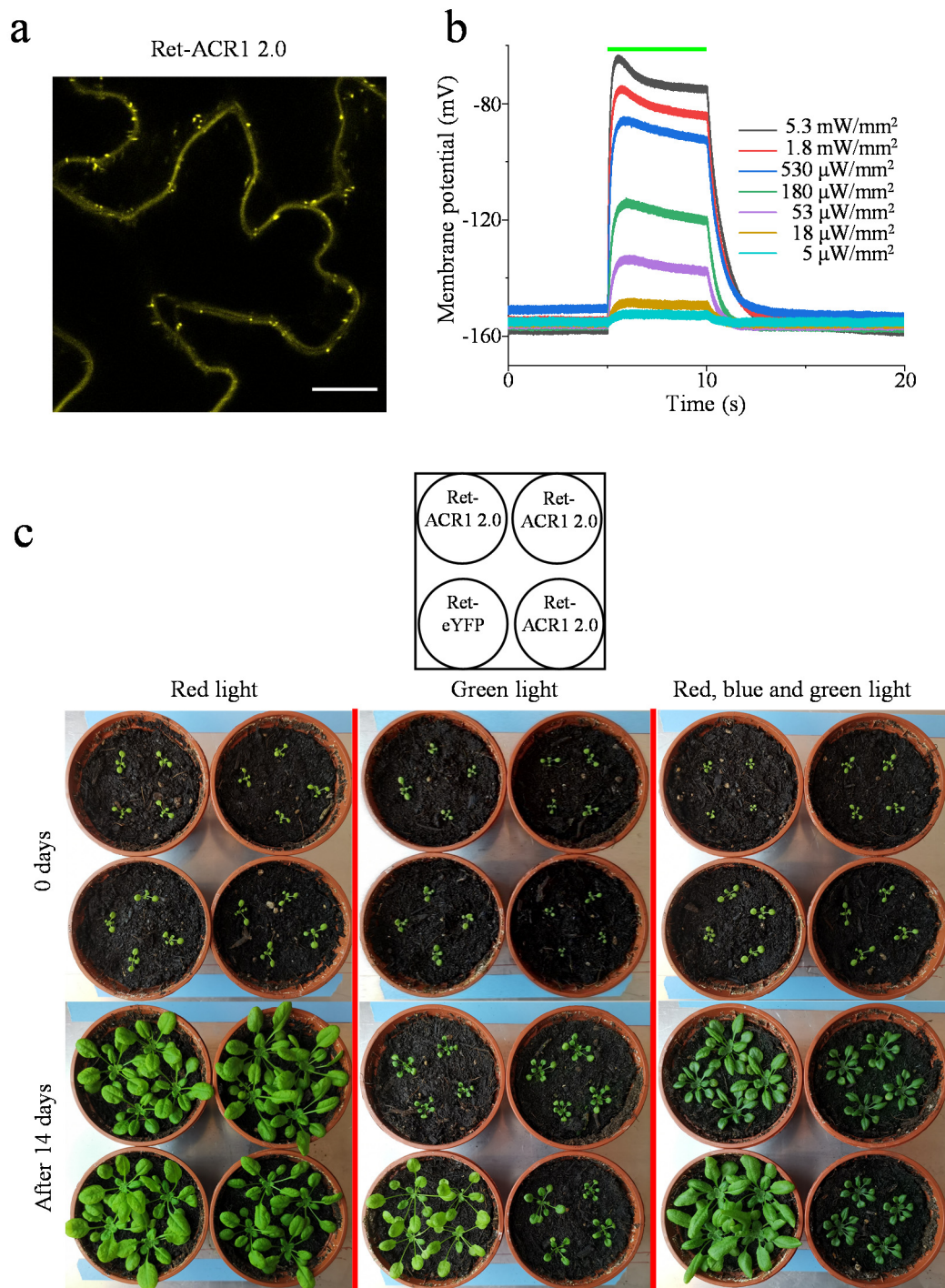
Suppl figure. 11. The comparison of Aequorin-based Luminescence measurements for *N. benthamiana* transiently expressing Ret-eYFP, Ret-XXL2.0, and Ret-XXM 2.0 upon blue light and green light for 5 s. The detection was done on the third day after agro-infiltration in leaves.



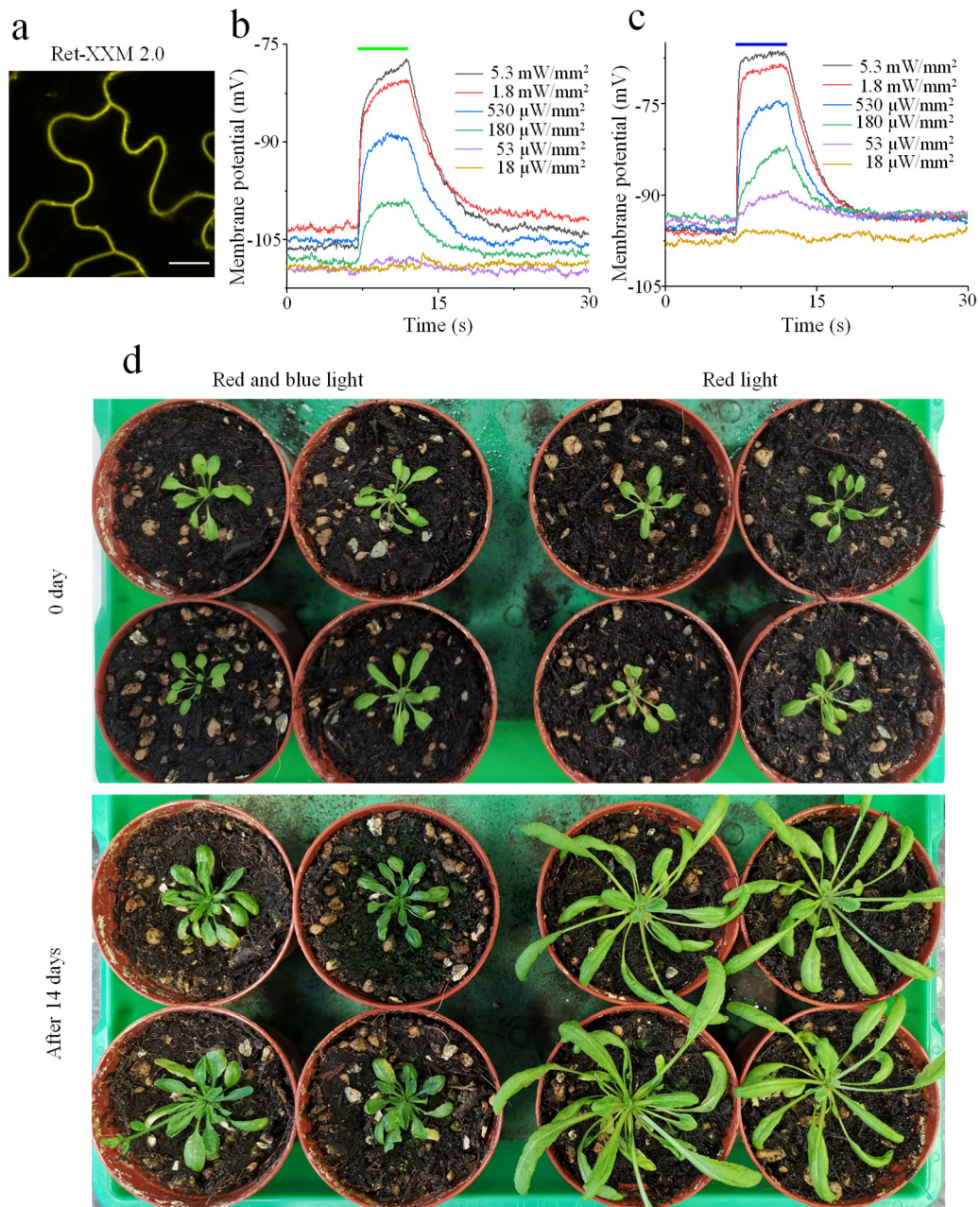
Suppl figure. 12. The representative confocal images of stomata in wild type and transgenic *N. tabacum* expressing Ret-eYFP, Ret-ACR1 2.0, Ret-XXM, Ret-XXM 2.0, Ret-XXL 2.0 and Ret-PPR 2.0, Scale bar = 20 μ m.



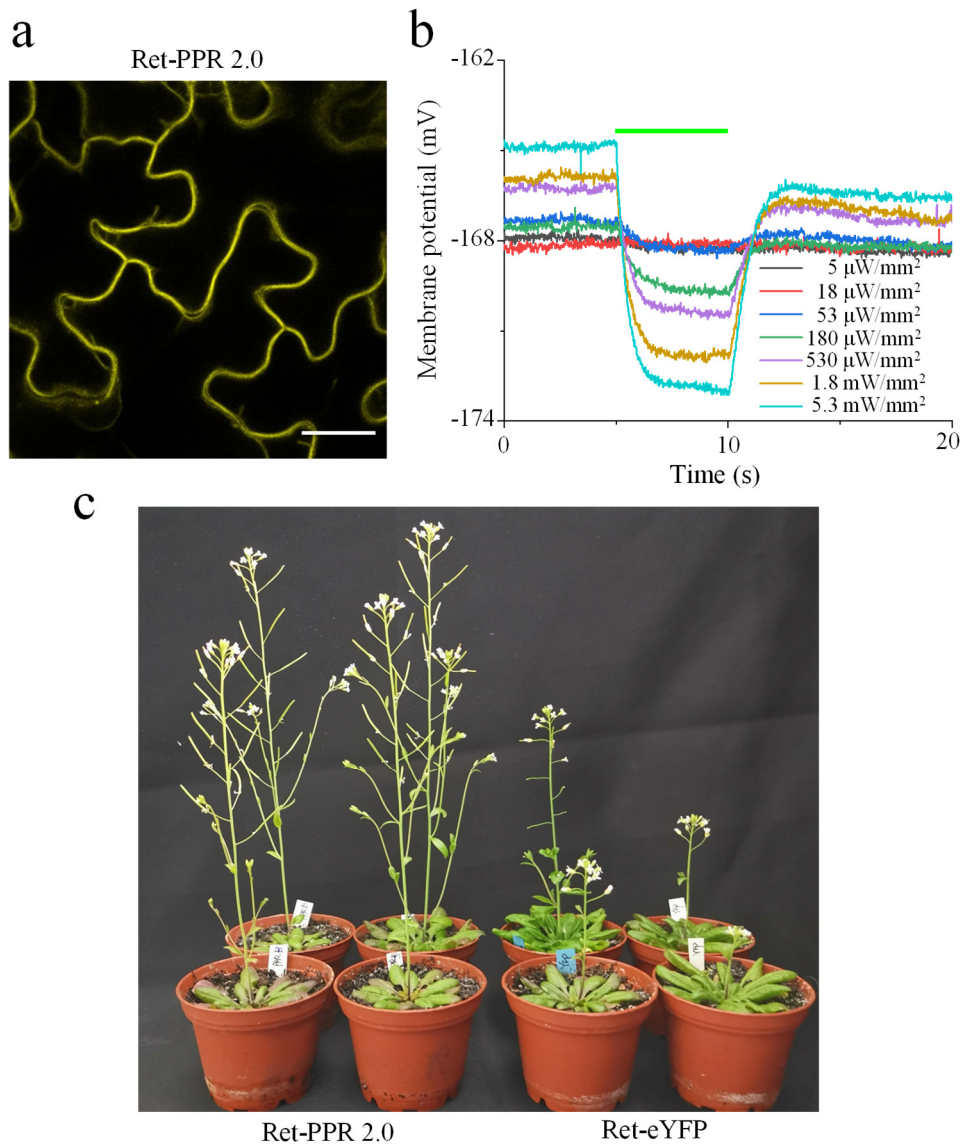
Suppl figure. 13. The representative confocal images of *N. benthamiana* epidermal cells transiently expressing Ret-eYFP and Ret-ACR1 2.0 which drove under 35S promoter, and the images were taken on the third day after agro-infiltration, scale bar = 200 μ m



Suppl figure. 14. Expression and function of Ret-ACR1 2.0 in transgenic *A. thaliana*. **a**, Representative confocal images of *A. thaliana* leaf epidermal cells expressing Ret-ACR1 2.0 stably, scale bar = 200 μm; **b**, Membrane potential recording of mesophyll cells from *A. thaliana* expressing Ret-ACR1 2.0 in different green light (532 nm) intensity; **c**, Comparison on the phenotype of *A. thaliana* expressing Ret-eYFP and Ret-ACR1 2.0 in different light conditions, up to white schema shows the position for the down images of Ret-eYFP and Ret-ACR1 2.0-expressing *A. thaliana*.



Suppl figure. 15. Expression and function of Ret-XXM 2.0 in transgenic *A. thaliana*. **a**, Representative confocal images of *A. thaliana* leaf epidermal cells expressing Ret-XXM 2.0 stably, scale bar = 200 μm; **b**, Membrane potential recording of transgenic *A. thaliana* mesophyll cells expressing Ret-XXM 2.0 in different green (532 nm) and blue (473 nm) light intensity for 5 s; **c**, Comparison on the phenotype of *A. thaliana* expressing Ret-eYFP and Ret-XXM 2.0 in different light conditions.



Suppl. figure. 15. Functional characterization of Ret-PPR 2.0 in transgenic *A. thaliana*
a, Representative confocal images of *A. thaliana* leaf epidermal cells expressing Ret-PPR 2.0 stably, scale bar = 200 μm . **b**, Membrane potential recording on mesophyll cells of transgenic *A. thaliana* expressing Ret-PPR 2.0 in different green (532 nm) light intensity for 5 s. **c**, The phenotype of Ret-PPR 2.0-expressing *A. thaliana* in white light for 45 days.

Suppl table 1. The opsins' information screened in this study

Abbreviation	Type	Species	Reference
<i>Cation Channelrhodopsin</i>			
ChR1	Channelrhodopsin	<i>Chlamydomonas reinhardtii</i>	[13]
ChR2	Channelrhodopsin	<i>Chlamydomonas reinhardtii</i>	[14]
PsChR2	Channelrhodopsin	<i>Pleodorina starrii</i>	[127]
Cheriff	Channelrhodopsin	<i>Scherffelia</i>	[128]
Chrimson	Channelrhodopsin	<i>Chlamydomonas noctigama</i>	[129]
Chronos	Channelrhodopsin	<i>S. helveticum</i>	[129]
<i>Anion Channelrhodopsin</i>			
GtACR1	Channelrhodopsin	<i>Guillardia theta</i>	[20]
GtACR2	Channelrhodopsin	<i>Guillardia theta</i>	[130]
ZipACR	Channelrhodopsin	<i>Proteomonas sulcata</i>	[131]
<i>Pump</i>			
PPR (PPR)	rhodopsin	<i>Chlorella vulgaris</i>	[72]
NpHR	rhodopsin	<i>Natronomonas pharaonis</i>	[59]
KR2	rhodopsin	<i>Krokinobacter eikastus</i>	[56]
Jaws	rhodopsin	<i>Haloarcula (Halobacterium) salinarum</i>	[132]
ArCh	rhodopsin	<i>archaea genera Halobacterium and Halorubrum.</i>	[69]

Suppl table 2: Information of primers used in this study

Primers	Sequences (5' to 3')
MbDioxyn BhKz5F	CGCGGATCCGCCACCATGGGACTCATGCTCATCGATTGGTGCGCTCTTGCTCTC GTGGTTTTTCATTGGAC
MbDioxyn StopSpHd3R	TGCCCAAGCTTACTAGTTCTTAATCTTGATCCTGCTGCTGTGCGGCCTGAAGAT GAAGTCGATAAGGATCATATGC
RC2 Bh5F	CGGGATCCAACATGGCTCCAAGTGTAATGGCCTCTTCCGCGACTACCGTCGCAC CATTTCAGGGACTGAAATCCACGGCGGGCATGCCGGTTGCTCGAA
RC2 SalNc3R	CATGCCATGGAGTCGACCATACATCGAATCCTTCCCTCCGTTACTAACATTTCCAA AGGATGAGTTGCCTAAGGGTGGTAAATACGACAGAGTCTCGAACTTC
2aMbDioxy sal5F	ACGCGTCGACGGATCAGGGGCGCGACAAACTTTAGCTTGCTGAAGCAAGCTG GTGACGTTGAGGAGAATCCCGGACCAATGGGACTCATGCTCATCGA
MbDioxy Hd3R	CCCAAGCTTAGTTCTTAATCTTGATCCTGC
UBQ10 toBh 5F	CGGGATCGCTGAGGCTTAATGGATCC
MbDio to2a 3R	TCACCAGCTTGCTTCAGCAAGCTAAAGTTTGTGCGGCCACCTGACCCTCCGTTCT TAATCTTGATCCTGCTGCTGTG
ACR to2a 5F	CTTTAGCTTGCTGAAGCAAGCTGGTGACGTTGAGGAGAATCCCGGACCAATGAG CAGCATTACCTGCG
ChR to2a 5F	CTTTAGCTTGCTGAAGCAAGCTGGTGACGTTGAGGAGAATCCCGGACCAATGGA TTATGGAGGCGCCCTGA
YFPstop to RBC 3R	CGAACGAAAGCTGCTGAGGTTTAATAAGCTTACTTGTACAGCTCGTCCATG
ACR toUBQ10 5F	CGGGATCGCTGAGGCTTAATGGATCCACCATGAGCAGCATTACCTGCG
ChR2 toUBQ10 5F	CGGGATCGCTGAGGCTTAATGGATCCACCATGGATTATGGAGGCGCCC
YFP to2a 3R	TCACCAGCTTGCTTCAGCAAGCTAAAGTTTGTGCGGCCACCTGACCCTCCCTTG TACAGCTCGTCCATG
RC2 to2a 5F	CTTTAGCTTGCTGAAGCAAGCTGGTGACGTTGAGGAGAATCCCGGACCAATGG CTCCAAGTGTAATGGC
Hd to RBC 3R	CGAACGAAAGCTGCTGAGGTTTAATAAGCTT
MbDio +120R	GCAAGTCTAGCGATCCTCT
RC2 pKzBg5F	GAAGATCTAACAAAAATGGCTCCAAGTGTAATGGC
P2A BhHd3R	CCCAAGCTTACGCGGATCCTGGTCCGGGATTCTCCTCA

ChR-11 Bh5F	GAGGATCCGGTGTAACGAACCCAGTAGTCG
ChR-13 Bh5F	CGGGATCCGGTCTGCTATTTGTAACGAACCCAG
ChR-13+C10 Bh5F	CGGGATCCGGTATGGCTGTGCACCAGATTGGA GAAGGCGGACTGCTATTTGTAACGAACCCAG
ChR-17 Bh5F	CGGGATCCGGTACGAACCCAGTAGTCGTCA
ChR-19 Bh5F	CGGGATCCGGTCCAGTAGTCGTCAATGGCT
YFP Bh5F	CGGGATCCATGGTGAGCAAGGGCGAGGA
ChR2 Bh5F	CGGGATCCATGGATTATGGAGGCGCCCT

5. Materials and Methods

5.1. Molecular cloning

With the traditional gene cloning method, the sequences of beta-carotene 15, 15' - dioxygenase was amplified by PCR from the reported gene of an unculturable marine bacterium. The chloroplast targeting signal (RC2) was fused in the N-terminal of beta-carotene 15, 15'- dioxygenase. The same method was used to get DNA fragments of opsins and then cloned them into plant expression binary vectors pCAMBIA-3300 which was driven by the UBQ10 promoter. The gene of enhanced yellow fluorescent protein --eYFP was fused in the C-terminal of the rhodopsin. The trafficking signal was inverted in the N-terminal of YFP, and the ER export/retention signal was fused in the C-terminal of YFP. The LR membrane targeting peptides were fused in the N-terminal of rhodopsin. P2A peptide gene derived from porcine teschovirus was taken as a linker to connect the genes producing beta-carotene and genes rhodopsin combining signal peptides in N/C-terminals. All constructs were verified by sequencing. The primers used in the research are listed in **suppl table 2**. The plasmids were amplified in *E. coli* and purified using the QIAprep[®] Spin MiniPrep 250 Kit (QIAGEN) and PureLink[™] HiPure Plasmid Filter Midiprep Kit (Invitrogen by Thermo Fisher Scientific) following the manufacturer's instructions.

5.2 Agrobacterium transformation

Agrobacterium tumefaciens GV3101 were transformed by electroporation protocol [133] with the plant expression plasmids described above. Colonies were selected on LB-agar plates with 100 µg/ml kanamycin, 25 µg/ml gentamycin, and 10 µg/ml rifampicin at 28 °C. The positive colonies were identified by PCR amplification of the inserted genes in 1% agarose gel.

Table 1: The component of 50 ml 1% agarose gel (pH=8.3)

Concentration	Components
40 mM	Tris
20 mM	Acetic Acid
1 mM	EDTA
0.5 g	Agarose

Table 2: PCR amplification system

Volume (μ l)	Components
1	Template
11.5	HGD buffer
2	dNTPs
2	Primer 1
2	Primer 2
0.5	Phusion DNA polymerase
31	ddH ₂ O

5.3 Protoplast isolation and transformation

Mesophyll protoplasts were isolated from 4-6-week-old *N. benthamiana* or *Arabidopsis thaliana* plants. Two leaves were cut into 0.5-1 mm strips with fresh razor blades. The leaf strips were then immediately incubated in the enzyme solution (1.5% cellulase R10, 0.4% macerozyme R10, 0.4 M mannitol, 20 mM KCl, 20 mM pH 5.7 MES-Tris, 10 mM CaCl₂, 0.1% BSA) for 3 h in the dark. The digested leaf slices were filtered into a 50 ml tube with a 50 mm nylon mesh and washed with W5 solution (154 mM NaCl, 125 mM CaCl₂, 5 mM KCl, 2 mM pH 5.7 MES-Tris). The protoplasts were pelleted down carefully by centrifugation at 100 × g without brakes for 2 min. After removing the supernatant, the isolated protoplasts were incubated with 2 ml W5 solution on ice for 30 min. Protoplasts will descend and W5 could be replaced by 2-3 ml MMG solution (4 mM pH 5.7 MES-Tris, 0.4 M mannitol, 15 mM MgCl₂).

For transformation, 200 μ l protoplast solution, 20 μ g plasmid DNA, and 220 μ l 40% PEG solution (4 g PEG 4000, 200 mM Mannitol, and 100 mM CaCl₂) were added in order, then mixed gently and incubated at room temperature for 15 min. After adding 0.8 ml W5 solution, the mixture was centrifuged at 100 \times g without brakes for 1 min. The pelleted protoplasts were resuspended in 2-3 ml W5 solution carefully and kept in the dark at room temperature for 1-2 days [134]. Subcellular localization of the YFP fluorescence was observed with a confocal laser scanning microscope (TCS SP5 II; Leica Microsystems, Wetzlar, Germany). The following tables are the solution involved in the experiment:

Mother solution

Volume	Concentration	Components
500 ml	0.5M	MES pH 5.7 (Tris)
100 ml	0.8M	Mannitol
50 ml	2M	KCl
50 ml	1M	CaCl ₂
50 ml	5M	NaCl

Enzyme solution

Concentration	Components
20 mM	MES-Tris pH 5.7
0.4 M	Mannitol
20 mM	KCl
1.5%	Cellulase R10
0.4%	Macerozyme R10

Preheat 10 min in the water at 55 °C, cooled to room temperature (RT), added the following chemicals

Concentration	Components
10 mM	CaCl ₂
0.1%	BSA

40% PEG solution

Concentration/Weight	Components
4g	PEG 4000
200 mM	Mannitol
100 mM	CaCl ₂
	dd H ₂ O

W5 solution

Concentration	Components
154 ml	NaCl
125 ml	CaCl ₂
5 mM	KCl
2 mM	MES-Tris, pH 5.7

MMG solution

Concentration	Components
0.4 mM	Mannitol
15 mM	MgCl ₂
4 mM	MES-Tris, pH 5.7

5.4 Transient expression in *N. benthamiana*

4-6-week-old *N. benthamiana* plants were picked and transiently expressed with fluorescent constructs following the protocol of Xiyan Li [135]. Briefly, the *A. tumefaciens* was cultured overnight in lysogeny broth medium (LB, with 150 μ M

acetosyringone) at 28 °C. Then the cultured *A. tumefaciens* was pelleted and washed thrice with infiltration buffer (10 mM MgCl₂, 10 mM pH 5.6 MES-K, 150 μM acetosyringone). The concentration was adjusted to OD₆₀₀ = 0.4. The resuspended bacteria were then infiltrated into the leaves through the abaxial epidermal via a 1 ml syringe.

5.5 Aequorin-based Luminescence measurements

According to the method of transient expression in the plant, the prepared agrobacterium solution was co-infiltrated into the leaves of 4-week-old *N. Benthamiana* with 10 μM of coelenterazine (PJK Biotech, Germany). After in red light for 2 days, aequorin light emission was measured by a digital luminometer. One leaf infiltrated was picked to put under the camera and the signal which was evoked by green/blue light illumination was recorded.

The preparation of 10mM coelenterazine:

1. Prepared the mix buffer: 1 ml ethanol + 20 μl 3M HCl (37% w/w HCl is about 12 mol/L)
2. 1mg coelenterazine + 236 μl mix buffer which is equal to 10 mM
3. Avoid light, mix completely at low temperature (on ice), store in -80 °C.
4. When using the prepared coelenterazine, 1:2000, or 1:1000 for infiltration in double-distilled H₂O (ddH₂O), it could mix with the agrobacterium solution and infiltrate together.

5.6 Agrobacterium-mediated transformation of *N. tabacum*

Tobacco (*Nicotiana tabacum* cultivars Petit Havana SR1) seeds were sterilized by 6% NaOCl for 5 min. Deionized water was used to wash away the remaining NaOCl. Sterile seeds were placed in 500 ml sterile plastic boxes on the surface of plant growth medium (Murashige & Skoog Medium incl. Vitamins and MES (Duchefa Biochemie), 3% sucrose, 0.8% Gelzan (Sigma-Aldrich), pH 5.8 with KOH). The boxes were placed in a growth chamber with a stable culture condition 14 h light + 26 °C /10 h dark + 16 °C

cycles. Transformation of tobacco was performed as described previously [136, 137] with some minor modifications using *Agrobacterium tumefaciens* strain GV3101 harboring the modified pCAMBIA-3300 vector conferring BASTA resistance.

All the pieces of leaves, explant, and calli were cultured on the calli induction medium (Murashige & Skoog Medium incl. Vitamins and MES (Duchefa Biochemie), 3% sucrose, 0.8% Gelzan, pH 5.8 with KOH, 20 µg/mL DL-Phosphinothricin (Duchefa Biochemie), 500 µg/mL Ticarcillin disodium (Duchefa Biochemie), 100 mg/L Myo-inositol, 1 mg/L Thiamine hydrochloride, 1 mg/L 6-Benzylaminopurine, 100 µg/L 1-Naphthaleneacetic acids (Sigma-Aldrich)) under 650 nm LED red light with the light intensity of ~30 µW/mm² in the growth chamber. And the shoots generated from the calli were moved onto root generation medium (Murashige & Skoog Medium incl. Vitamins and MES (Duchefa Biochemie), 3% sucrose, 0.8% Gelzan, pH 5.8 with KOH, 20 µg/mL DL-Phosphinothricin (Duchefa Biochemie), 500 µg/mL Ticarcillin disodium (Duchefa Biochemie), 100 mg/L Myo-inositol, 1 mg/L Thiamine hydrochloride). BASTA-resistant transformants with well-developed roots were transferred to pots containing soil and grown in 650 nm red light culture room (light intensity of ~30 µW/mm², 14 h light + 26 °C /10 h dark + 16 °C cycles). The expression of the target genes in the transformants was verified by eYFP fluorescence in leaves or pollen tubes. The transformants with high eYFP fluorescence and high PM depolarization response to the certain green light were selected as the candidates. Seeds of the individual plant from every generation were collected and selected on the BASTA resistance selection medium (Murashige & Skoog Medium incl. Vitamins and MES (Duchefa Biochemie), 3% sucrose, 0.8% Gelzan, pH 5.8 with KOH, 20 µg/mL DL-Phosphinothricin (Duchefa Biochemie)).

5.7 Growth conditions for transgenic *N. tabacum*

Tobacco plants were grown in the greenhouse and red-light conditions (650 nm, ~30 µW/mm², and 14 h light + 26 °C /10 h dark + 16 °C cycles) in parallel. In the greenhouse,

incident light was supplemented by high-pressure sodium lamps (Hortilux Schreder, HPS 400 Watt) and shading nets to maintain light conditions between 40 kilolux and 60 kilolux from 8 am to 8 pm, and the temperature was maintained at 24 °C - 26 °C through the heating and ventilation system. The phenotype of WT, Ret-eYFP, and Ret-ACR1 2.0 transgenic tobacco plants growing under different conditions were compared at three different growth stages. a) 25 days in red light + 25-26 days in the greenhouse, b) 48 days in red light + 2-3 days in the greenhouse and c) 50 days in red light. The growth of plants under different conditions was compared.

5.8 Confocal Microscopy and Image Processing

To observe the localization of rhodopsin in plant cells, images were taken with a confocal laser scanning microscope (Leica SP5, Leica Microsystems CMS, Mannheim, Germany). eYFP was excited at 496 nm and fluorescence was captured between 520 to 580 nm. To observe the subcellular localization of rhodopsin, *N. benthamiana* and *N. tabacum* leaf discs placed upside down were observed with a dipping 25 × HCX IRAPO 925/0.95 and 40 × water immersion HC PL FLUOTAR 910/0.3 objective the 40. ImageJ software was used for image processing.

5.9 All-trans-retinal and carotenoids measurement

Five-week-old *N. benthamiana* were infiltrated with *A. tumefaciens* carrying different constructs and grown in red light condition. After 3 days' infiltration with *Agrobacterium*, 200 mg leave material was collected as one sample for retinal and carotenoids measurements. The leaves infiltrated with empty *Agrobacterium* or without infiltration were collected as controls. For transgenic *N. tabacum* plants, samples were collected after 45 days' growth in red light. Ground plant material was extracted with 500 µl of chloroform using a mixer mill MM400 (Retsch, Germany) for 3 min. The extract was centrifuged at 14 000 rpm for 5 min at room temperature, 50 µl of the organic phase was evaporated under reduced pressure and dissolved in 50 µl of a mixture of ethanol and chloroform (V: V, 1:1). 5 µl samples were analyzed by UPLC

combined with UV- and MS/MS-detection using a Waters Acquity ultra-high-performance liquid chromatography system coupled to a Waters Quattro Premier triple quadrupole mass spectrometer (Milford, MA, USA) equipped with an electrospray interface (ESI). The separation was carried out by reversed-phase chromatography using an Acquity BEH C18 column (50 × 2.1 mm, 1.7 μm particle size with a 5 × 2.1 mm guard column; Waters; Milford, MA, USA) and a solvent system consisting of water containing 0.1% formic acid (solvent A) and 0.1% formic acid in acetonitrile (solvent B). Gradient elution was performed at a flow rate of 0.25 ml min⁻¹ and a column temperature of 40 °C starting from 75% to 85% solvent B within 4 min, from 85% to 100% within 1 min, followed by 7 min at 100% solvent B. Compounds were determined by a Waters 996 PDA detector from 200 to 800 nm (max = 380 nm for retinal, max = 450 nm for carotenoids) and by MS/MS using multiple reaction monitoring (MRM). Instrument parameters for ionization and collision-induced dissociation (CID) were optimized by flow injection of retinal and carotenoids. The ESI source was operated in positive mode at a source temperature of 120 °C and a capillary voltage of 2.5 kV. Nitrogen was used as desolvation and cone gas with flow rates of 750 L/h at 400 °C and 50 L/h. The cone voltage was adjusted to 16 V for retinal and 25 V for carotenoids. Fragmentation was carried out using argon as collision gas at a flow rate of 0.3 mL/min. Two specific fragments were monitored for each compound with a dwell time of 50 ms per MRM transition, for retinal m/z 285.1 > 161.1 and m/z 285.1 > 175.1 using a collision energy (CE) of 11 eV, and for carotenoids m/z 536.4 > 346.3 and m/z 536.4 > 444.3 collision energy (CE) of 22 eV with a CE of 16 eV.

5.10 Chlorophylls extraction

Transgenic *N. tabacum* leaves were washed with double-distilled water and cut into ~2 mm slices. The slices were put into 100 ml flasks and soaked with 20 ml mixture of acetone (99.5%, PanReac Applichem) and ethanol (≥99.8%, SIGMA) (V: V, 2:1). After 18 h incubation, the OD value of soaking solution was detected with a nanophotometer (Implen GmbH, Germany), with 663 nm as the index for chlorophyll an (A₆₆₃) and 645

nm for chlorophyll b (A_{645}) [138, 139].

The concentration of chlorophyll a/b was calculated with the Arnon formula:

$$Ca \text{ (mg/g)} = (12.72A_{663} - 2.59A_{645}) V / (1000 * W)$$

$$Cb \text{ (mg/g)} = (22.88 A_{645} - 4.67 A_{663}) V / (1000 * W)$$

$$Ca+b \text{ (mg/g)} = (20.29 A_{645} + 8.05 A_{663}) V / (1000 * W)$$

“Ca” is the concentration of chlorophyll a, “Cb” is the concentration of chlorophyll b, “Ca+b” is the total concentration of chlorophyll a and b, A_{645} represented the absorbance value at wavelength 645 nm and A_{663} represented the absorbance value at wavelength 663 nm. “V” is the volume of soaking solution, “W” is the fresh weight of leaf.

5.11 Plant growth experiment

For the comparison in the greenhouse, the seeds were sowed in the pots with the same soil type, when the plants were 2-week-old, the plants with the same height and amount of leaves were picked to put in the greenhouse, keeping all the pots in the same setting including temperature, lighting, humidity, pests to minimize any variation in environmental factors.

For the comparison on MS solid medium, the seeds were sterilized with 70% ethanol for 2 min and then soaked in 10% bleach for 15 min, following rinsed in sterilized water a few times to remove the bleach. 8 - 10 seeds were picked to put on the MS solid medium, and then the plates were sealed with laboratory parafilm. The whole process was finished on a clean bench. The plates were put in different light conditions vertically under keeping the same environmental factors.

5.12 Cuticular wax analysis

Ret-eYFP and Ret-ACR1 2.0 transgenic tobacco plants were grown in red light for 25 days, then moved to the greenhouse for 25 days. Cuticular waxes were extracted successively by dipping whole leaves (except the petiole cuts) twice in

trichloromethane (Roth) at room temperature for 45 s. Derivatization and gas chromatographic analysis of cuticular waxes were performed according to [140].

5.13 Agrobacterium-mediated transformation of *A. thaliana*

The seed of *Arabidopsis thaliana* (Col-0) was kept in darkness for 2 - 3 days at 4°C and then spread the seeds on wet soil in the little pots. when the plant began to bolt and produce floral inflorescences, using the floral dip method, the *Arabidopsis* flower buds were simply dipped in an *Agrobacterium* cell suspension containing 5% sucrose (wt/vol) and 0.01 – 0.05% Silwet L-77 (vol/vol) to allow uptake of the *agrobacterium* into female gametes. After that, the plant was kept in darkness for one day, then moved to the greenhouse. Repeating this procedure another twice every 7 days to make sure enough flower buds to uptake the *agrobacterium* into female gametes [141].

5.14 Membrane voltage recordings in mesophyll cells

5-week-old plants (*N. benthamiana* or *N. tabacum*) were suitable for mesophyll cell impalement. The lower epidermal of fresh leaves were peeled off and leaf discs with a diameter of ~0.5 cm were glued upside down on custom-made chambers with Medical adhesive (ULRICH Swiss). And the leaf samples were submerged in bath solution (1 mM KCl, 1 mM CaCl₂, 10 mM MES/BTP, pH 6.0) overnight at room temperature before the measurement. Microelectrodes for mesophyll cell impalement were pulled from borosilicate glass capillaries (inner diameter 0.58 mm, outer diameter 1.0 mm, Hilgenberg GmbH) using a flaming/brown micropipette laser puller (P97, Sutter Instrument Co.). The single microelectrode was filled with 300 mM KCl and connected by Ag/AgCl wires to the microelectrode amplifier (Axon geneclamp 500). The reference electrode was filled with 300 mM KCl and plugged with 2% agar in 300 mM KCl. The microelectrode with a resistance of 60-200 MΩ was used for impalement. Data were digitized using a NA USB-6221 interface (National Instruments). Current clamp protocols were applied with the WinWCP V5.3.4 software (University of Strathclyde, UK).

5.15 Chlorophyll fluorescence measurements

Tobacco plants were used to quantify photosynthesis utilizing a PAM (Pulse Amplitude Modulation) fluorometer. WT, Ret-eYFP, and Ret-ACR1 2.0 transgenic tobacco plants were grown in red light from the very beginning. Plants from three different growth conditions (as indicated in the growth condition section) were compared. The fourth or fifth leaf was fixed and monitored with a Maxi PAM fluorometer (AVT 033), chlorophyll fluorescence measurements were recorded with IMAGING WIN v.2.41a FW MULTI RGB (Walz, Effeltrich, Germany). The actinic light applied to drive photosynthesis was set as intensity 7 (FAR as $146 \mu\text{mol m}^{-2} \text{s}^{-1}$). Fluorescence parameters, photochemical quenching (qP), and nonphotochemical quenching (qN and NPQ) were recorded. Fluorescence yield measured briefly before the onset of last saturation pulse (F) and fluorescence yield reached during last saturation pulse (Fm') were measured to calculate the effective quantum yield of photochemical energy conversion at PS II reaction centers calculated according to the equation: Yield = (Fm'-F)/Fm'.

5.16 Significance analysis

All the figures were made by the GraphPad Prism (version 8.0.2), Origin 2018, or Microsoft Excel. Significance was determined by the Student's t-test and one-way analysis of Variance (ANOVA). Significance analysis among more than three groups is performed with one-way ANOVA using IBM SPSS statistics (version 26.0). For the labelling in the figures: *, $P \leq 0.05$; **, $P \leq 0.01$; ***, $P \leq 0.001$; NS: not significant.

6. Reference

1. Appasani, K., *Optogenetics: From Neuronal Function to Mapping and Disease Biology*. 2017: Cambridge University Press.
2. Crick, F.H.C., *Thinking About the Brain*. Scientific American, 1979. **241**(3): p. 219-&.
3. Callaway, E.M. and L.C. Katz, *Photostimulation using caged glutamate reveals functional circuitry in living brain slices*. Proceedings of the National Academy of Sciences of the United States of America, 1993. **90**(16): p. 7661-7665.
4. Hoffmann, A., et al., *Photoactive mitochondria: in vivo transfer of a light-driven proton pump into the inner mitochondrial membrane of *Schizosaccharomyces pombe**. Proceedings of the National Academy of Sciences of the United States of America, 1994. **91**(20): p. 9367-9371.
5. Nagel, G., et al., *Functional expression of bacteriorhodopsin in oocytes allows direct measurement of voltage dependence of light induced H⁺ pumping*. FEBS Lett, 1995. **377**(2): p. 263-6.
6. Zemelman, B.V., et al., *Selective photostimulation of genetically ChARGed neurons*. Neuron, 2002. **33**(1): p. 15-22.
7. Zemelman, B.V., et al., *Photochemical gating of heterologous ion channels: remote control over genetically designated populations of neurons*. Proc Natl Acad Sci U S A, 2003. **100**(3): p. 1352-7.
8. Arenkiel, B.R., et al., *Genetic control of neuronal activity in mice conditionally expressing TRPV1*. Nat Methods, 2008. **5**(4): p. 299-302.
9. Guler, A.D., et al., *Transient activation of specific neurons in mice by selective expression of the capsaicin receptor*. Nat Commun, 2012. **3**: p. 746.
10. Wang, M., et al., *Synaptic modifications in the medial prefrontal cortex in susceptibility and resilience to stress*. J Neurosci, 2014. **34**(22): p. 7485-92.
11. Oesterhelt, D. and W. Stoerkenius, *Functions of a new photoreceptor membrane*. Proc Natl Acad Sci U S A, 1973. **70**(10): p. 2853-7.
12. Matsuno-Yagi, A. and Y. Mukohata, *Two possible roles of bacteriorhodopsin; a comparative study of strains of *Halobacterium halobium* differing in pigmentation*. Biochem Biophys Res Commun, 1977. **78**(1): p. 237-43.
13. Nagel, G., et al., *Channelrhodopsin-1: a light-gated proton channel in green algae*. Science, 2002. **296**(5577): p. 2395-8.
14. Nagel, G., et al., *Channelrhodopsin-2, a directly light-gated cation-selective membrane channel*. Proc Natl Acad Sci U S A, 2003. **100**(24): p. 13940-5.
15. Boyden, E.S., et al., *Millisecond-timescale, genetically targeted optical control of neural activity*. Nat Neurosci, 2005. **8**(9): p. 1263-8.
16. Bi, A., et al., *Ectopic expression of a microbial-type rhodopsin restores visual responses in mice with photoreceptor degeneration*. Neuron, 2006. **50**(1): p. 23-33.
17. Li, X., et al., *Fast noninvasive activation and inhibition of neural and network activity by vertebrate rhodopsin and green algae channelrhodopsin*. Proc Natl

- Acad Sci U S A, 2005. **102**(49): p. 17816-21.
18. Nagel, G., et al., *Light activation of channelrhodopsin-2 in excitable cells of Caenorhabditis elegans triggers rapid behavioral responses*. Curr Biol, 2005. **15**(24): p. 2279-84.
 19. Zhang, F., et al., *Multimodal fast optical interrogation of neural circuitry*. Nature, 2007. **446**(7136): p. 633-9.
 20. Govorunova, E.G., et al., *Natural light-gated anion channels: A family of microbial rhodopsins for advanced optogenetics*. Science, 2015. **349**(6248): p. 647-650.
 21. Schroder-Lang, S., et al., *Fast manipulation of cellular cAMP level by light in vivo*. Nat Methods, 2007. **4**(1): p. 39-42.
 22. Gao, S., et al., *Optogenetic manipulation of cGMP in cells and animals by the tightly light-regulated guanylyl-cyclase opsin CyclOp*. Nat Commun, 2015. **6**: p. 8046.
 23. Bando, Y., et al., *Genetic voltage indicators*. BMC Biology, 2019. **17**(1).
 24. Bando, Y., et al., *Comparative Evaluation of Genetically Encoded Voltage Indicators*. Cell Reports, 2019. **26**(3): p. 802-+.
 25. Hashemi, N.A., et al., *Rhodopsin-based voltage imaging tools for use in muscles and neurons of Caenorhabditis elegans*. Proceedings of the National Academy of Sciences of the United States of America, 2019. **116**(34): p. 17051-17060.
 26. Leong, L.M., B.E. Kang, and B. Baker, *Improving the flexibility of Genetically Encoded Voltage Indicators via intermolecular FRET*. bioRxiv, 2020.
 27. Spudich, J.L., et al., *Retinylidene proteins: Structures and functions from archaea to humans*. Annual Review of Cell and Developmental Biology, 2000. **16**: p. 365-+.
 28. Kuhne, J., et al., *Early formation of the ion-conducting pore in channelrhodopsin-2*. Angew Chem Int Ed Engl, 2015. **54**(16): p. 4953-7.
 29. Shichida, Y. and T. Matsuyama, *Evolution of opsins and phototransduction*. Philos Trans R Soc Lond B Biol Sci, 2009. **364**(1531): p. 2881-95.
 30. Kateriya, S., et al., *"Vision" in single-celled algae*. News Physiol Sci, 2004. **19**: p. 133-7.
 31. Nagel, G., et al., *Channelrhodopsins: directly light-gated cation channels*. Biochem Soc Trans, 2005. **33**(Pt 4): p. 863-6.
 32. Berndt, A., et al., *High-efficiency channelrhodopsins for fast neuronal stimulation at low light levels*. Proceedings of the National Academy of Sciences of the United States of America, 2011. **108**(18): p. 7595-7600.
 33. Schroll, C., et al., *Light-induced activation of distinct modulatory neurons triggers appetitive or aversive learning in Drosophila larvae*. Current Biology, 2006. **16**(17): p. 1741-1747.
 34. Ullrich, S., R. Gueta, and G. Nagel, *Degradation of channelrhodopsin-2 in the absence of retinal and degradation resistance in certain mutants*. Biological Chemistry, 2013. **394**(2): p. 271-280.
 35. Pulver, S.R., et al., *Temporal Dynamics of Neuronal Activation by Channelrhodopsin-2 and TRPA1 Determine Behavioral Output in Drosophila*

- Larvae*. Journal of Neurophysiology, 2009. **101**(6): p. 3075-3088.
36. Ljaschenko, D., N. Ehmann, and R.J. Kittel, *Hebbian Plasticity Guides Maturation of Glutamate Receptor Fields In Vivo*. Cell Reports, 2013. **3**(5): p. 1407-1413.
 37. Nuwal, N., et al., *Avoidance of Heat and Attraction to Optogenetically Induced Sugar Sensation as Operant Behavior in Adult Drosophila*. Journal of Neurogenetics, 2012. **26**(3-4): p. 298-305.
 38. Suh, G.S.B., et al., *Light activation of an innate olfactory avoidance response in Drosophila*. Current Biology, 2007. **17**(10): p. 905-908.
 39. Liang, L., et al., *GABAergic Projection Neurons Route Selective Olfactory Inputs to Specific Higher-Order Neurons*. Neuron, 2013. **79**(5): p. 917-931.
 40. Lin, J.Y., et al., *ReaChR: a red-shifted variant of channelrhodopsin enables deep transcranial optogenetic excitation*. Nature Neuroscience, 2013. **16**(10): p. 1499-+.
 41. Dawydow, A., et al., *Channelrhodopsin-2-XXL, a powerful optogenetic tool for low-light applications*. Proceedings of the National Academy of Sciences of the United States of America, 2014. **111**(38): p. 13972-13977.
 42. Scholz, N., et al., *Mechano-dependent signaling by Latrophilin/CIRL quenches cAMP in proprioceptive neurons*. Elife, 2017. **6**.
 43. Duan, X.D., G. Nagel, and S.Q. Gao, *Mutated Channelrhodopsins with Increased Sodium and Calcium Permeability*. Applied Sciences-Basel, 2019. **9**(4).
 44. Maurice, N., et al., *Striatal Cholinergic Interneurons Control Motor Behavior and Basal Ganglia Function in Experimental Parkinsonism*. Cell Reports, 2015. **13**(4): p. 657-666.
 45. Parker, K.L., et al., *Optogenetic approaches to evaluate striatal function in animal models of Parkinson disease*. Dialogues in Clinical Neuroscience, 2016. **18**(1): p. 99-107.
 46. Arguello, A.A., et al., *Role of a Lateral Orbital Frontal Cortex-Basolateral Amygdala Circuit in Cue-Induced Cocaine-Seeking Behavior*. Neuropsychopharmacology, 2017. **42**(3): p. 727-735.
 47. Wietek, J., et al., *Conversion of Channelrhodopsin into a Light-Gated Chloride Channel*. Science, 2014. **344**(6182): p. 409-412.
 48. Berndt, A., et al., *Structure-Guided Transformation of Channelrhodopsin into a Light-Activated Chloride Channel*. Science, 2014. **344**(6182): p. 420-424.
 49. Wietek, J., et al., *An improved chloride-conducting channelrhodopsin for light-induced inhibition of neuronal activity in vivo*. Scientific Reports, 2015. **5**.
 50. Berndt, A., et al., *Structural foundations of optogenetics: Determinants of channelrhodopsin ion selectivity*. Proceedings of the National Academy of Sciences of the United States of America, 2016. **113**(4): p. 822-829.
 51. Mohammad, F., et al., *Optogenetic inhibition of behavior with anion channelrhodopsins*. Nature Methods, 2017. **14**(3): p. 271-+.
 52. Govorunova, E.G., et al., *Anion channelrhodopsins for inhibitory cardiac optogenetics*. Scientific Reports, 2016. **6**.

53. Govorunova, E.G., et al., *The Expanding Family of Natural Anion Channelrhodopsins Reveals Large Variations in Kinetics, Conductance, and Spectral Sensitivity*. Scientific Reports, 2017. **7**.
54. Graves, A.R., et al., *Hippocampal Pyramidal Neurons Comprise Two Distinct Cell Types that Are Countermodulated by Metabotropic Receptors*. Neuron, 2012. **76**(4): p. 776-789.
55. Oesterhelt, D. and W. Stoeckenius, *Rhodopsin-like protein from the purple membrane of Halobacterium halobium*. Nat New Biol, 1971. **233**(39): p. 149-52.
56. Inoue, K., et al., *A light-driven sodium ion pump in marine bacteria*. Nat Commun, 2013. **4**: p. 1678.
57. Schobert, B. and J.K. Lanyi, *Halorhodopsin Is a Light-Driven Chloride Pump*. Journal of Biological Chemistry, 1982. **257**(17): p. 306-313.
58. Ernst, O.P., et al., *Microbial and Animal Rhodopsins: Structures, Functions, and Molecular Mechanisms*. Chemical Reviews, 2014. **114**(1): p. 126-163.
59. Lanyi, J.K., et al., *The Primary Structure of a Halorhodopsin from Natronobacterium-Pharaonis - Structural, Functional and Evolutionary Implications for Bacterial Rhodopsins and Halorhodopsins*. Journal of Biological Chemistry, 1990. **265**(3): p. 1253-1260.
60. Tsunematsu, T., et al., *Acute Optogenetic Silencing of Orexin/Hypocretin Neurons Induces Slow-Wave Sleep in Mice*. Journal of Neuroscience, 2011. **31**(29): p. 10529-10539.
61. Gradinaru, V., K.R. Thompson, and K. Deisseroth, *eNpHR: a Natronomonas halorhodopsin enhanced for optogenetic applications*. Brain Cell Biol, 2008. **36**(1-4): p. 129-39.
62. Gradinaru, V., et al., *Molecular and cellular approaches for diversifying and extending optogenetics*. Cell, 2010. **141**(1): p. 154-165.
63. Arrenberg, A.B., et al., *Optogenetic Control of Cardiac Function*. Science, 2010. **330**(6006): p. 971-974.
64. Zhang, C.Q., et al., *Optimized photo-stimulation of halorhodopsin for long-term neuronal inhibition*. BMC Biology, 2019. **17**(1).
65. Wietek, J. and M. Prigge, *Enhancing Channelrhodopsins: An Overview*. Methods Mol Biol, 2016. **1408**: p. 141-65.
66. Henderson, R. and P.N.T. Unwin, *3-Dimensional Model of Purple Membrane Obtained by Electron-Microscopy*. Nature, 1975. **257**(5521): p. 28-32.
67. Khorana, H.G., et al., *Amino-Acid Sequence of Bacteriorhodopsin*. Proceedings of the National Academy of Sciences of the United States of America, 1979. **76**(10): p. 5046-5050.
68. Schulten, K., S. Hayashi, and E. Tajkhorshid, *Molecular dynamics simulation of bacteriorhodopsin's photoisomerization using ab initio forces for the excited chromophore*. Abstracts of Papers of the American Chemical Society, 2003. **226**: p. U339-U339.
69. Chow, B.Y., et al., *High-performance genetically targetable optical neural silencing by light-driven proton pumps*. Nature, 2010. **463**(7277): p. 98-102.

70. Han, X., et al., *A high-light sensitivity optical neural silencer: development and application to optogenetic control of non-human primate cortex*. Front Syst Neurosci, 2011. **5**: p. 18.
71. Flytzanis, N.C., et al., *Archaeorhodopsin variants with enhanced voltage-sensitive fluorescence in mammalian and Caenorhabditis elegans neurons*. Nat Commun, 2014. **5**: p. 4894.
72. Zhang, F., et al., *The microbial opsin family of optogenetic tools*. Cell, 2011. **147**(7): p. 1446-57.
73. Schneider, F., *Design and electrophysiological characterization of rhodopsin-based optogenetic tools*. 2014.
74. Shevchenko, V., et al., *Inward H⁺ pump xenorhodopsin: Mechanism and alternative optogenetic approach*. Science Advances, 2017. **3**(9).
75. Inoue, K., et al., *A natural light-driven inward proton pump*. Nature Communications, 2016. **7**.
76. Kato, H.E., et al., *Structural basis for Na⁽⁺⁾ transport mechanism by a light-driven Na⁽⁺⁾ pump*. Nature, 2015. **521**(7550): p. 48-53.
77. Kato, H.E., et al., *Structural basis for Na⁺ transport mechanism by a light-driven Na⁺ pump*. Nature, 2015. **521**(7550): p. 48-53.
78. Gushchin, I., et al., *Structure of the light-driven sodium pump KR2 and its implications for optogenetics*. FEBS J, 2016. **283**(7): p. 1232-8.
79. Balashov, S.P., et al., *Light-driven Na⁺ pump from Gillisia limnaea: a high-affinity Na⁺ binding site is formed transiently in the photocycle*. Biochemistry, 2014. **53**(48): p. 7549-7561.
80. Yoshizawa, S., et al., *Functional characterization of flavobacteria rhodopsins reveals a unique class of light-driven chloride pump in bacteria*. Proc Natl Acad Sci U S A, 2014. **111**(18): p. 6732-7.
81. Bertsova, Y., A. Bogachev, and V. Skulachev, *Proteorhodopsin from Dokdonia sp. PRO95 is a light-driven Na⁺-pump*. Biochemistry (Moscow), 2015. **80**(4): p. 449-454.
82. Braam, J., *In touch: plant responses to mechanical stimuli*. New Phytol, 2005. **165**(2): p. 373-89.
83. Lautner, S., et al., *Characteristics of electrical signals in poplar and responses in photosynthesis*. Plant Physiol, 2005. **138**(4): p. 2200-9.
84. Stahlberg, R., R. Cleland, and E. Van Volkenburgh, *Communication in Plants: Neuronal Aspects of Plant Life*. 2006.
85. Trebacz, K., H. Dziubinska, and E. Krol, *Electrical signals in long-distance communication in plants*, in *Communication in plants*. 2006, Springer. p. 277-290.
86. Fromm, J., *Long-distance electrical signaling and physiological functions in higher plants*, in *Plant electrophysiology*. 2006, Springer. p. 269-285.
87. Fromm, J. and S. Lautner, *Characteristics and functions of phloem-transmitted electrical signals in higher plants*, in *Communication in Plants*. 2006, Springer. p. 321-332.
88. White, P.J., et al., *Advanced patch-clamp techniques and single-channel*

- analysis*. Journal of Experimental Botany, 1999. **50**: p. 1037-1054.
89. Krol, E. and K. Trebacz, *Ways of ion channel gating in plant cells*. Annals of Botany, 2000. **86**(3): p. 449-469.
 90. Kong, S.G. and K. Okajima, *Diverse photoreceptors and light responses in plants*. Journal of Plant Research, 2016. **129**(2): p. 111-114.
 91. Banerjee, S. and D. Mitra, *Structural Basis of Design and Engineering for Advanced Plant Optogenetics*. Trends in Plant Science, 2020. **25**(1): p. 35-65.
 92. Ochoa-Fernandez, R., et al., *Optogenetics in plants: Red/far-red light control of gene expression*, in *Optogenetics*. 2016, Springer. p. 125-139.
 93. Chatelle, C., et al., *A Green-Light-Responsive System for the Control of Transgene Expression in Mammalian and Plant Cells*. ACS Synth Biol, 2018. **7**(5): p. 1349-1358.
 94. Nash, A.I., et al., *Structural basis of photosensitivity in a bacterial light-oxygen-voltage/helix-turn-helix (LOV-HTH) DNA-binding protein*. Proc Natl Acad Sci U S A, 2011. **108**(23): p. 9449-54.
 95. Ochoa-Fernandez, R., et al., *Optogenetic control of gene expression in plants in the presence of ambient white light*. Nat Methods, 2020. **17**(7): p. 717-725.
 96. Cosentino, C., et al., *Optogenetics. Engineering of a light-gated potassium channel*. Science, 2015. **348**(6235): p. 707-10.
 97. Papanatsiou, M., et al., *Optogenetic manipulation of stomatal kinetics improves carbon assimilation, water use, and growth*. Science, 2019. **363**(6434): p. 1456-+.
 98. Reyer, A., et al., *Channelrhodopsin-mediated optogenetics highlights a central role of depolarization-dependent plant proton pumps*. Proc Natl Acad Sci U S A, 2020. **117**(34): p. 20920-20925.
 99. Kim, Y.S., et al., *In Vitro Characterization of a Recombinant Blh Protein from an Uncultured Marine Bacterium as a beta-Carotene 15,15'-Dioxygenase*. Journal of Biological Chemistry, 2009. **284**(23): p. 15781-15793.
 100. Shen, B.R., et al., *An optimized transit peptide for effective targeting of diverse foreign proteins into chloroplasts in rice*. Scientific Reports, 2017. **7**.
 101. Kim, J.H., et al., *High Cleavage Efficiency of a 2A Peptide Derived from Porcine Teschovirus-1 in Human Cell Lines, Zebrafish and Mice*. Plos One, 2011. **6**(4).
 102. Wang, Y.C., et al., *2A self-cleaving peptide-based multi-gene expression system in the silkworm Bombyx mori*. Scientific Reports, 2015. **5**.
 103. Stockklauser, C., et al., *A sequence motif responsible for ER export and surface expression of Kir2.0 inward rectifier K⁺ channels*. Febs Letters, 2001. **493**(2-3): p. 129-133.
 104. Lynch, V.H. and C.S. French, *Beta-Carotene, an Active Component of Chloroplasts*. Archives of Biochemistry and Biophysics, 1957. **70**(2): p. 382-391.
 105. Kim, Y.S., C.S. Park, and D.K. Oh, *Retinal production from beta-carotene by beta-carotene 15,15'-dioxygenase from an unculturable marine bacterium*. Biotechnology Letters, 2010. **32**(7): p. 957-961.

106. Michniewicz, M., E.M. Frick, and L.C. Strader, *Gateway-compatible tissue-specific vectors for plant transformation*. BMC Res Notes, 2015. **8**: p. 63.
107. Klapoetke, N.C., et al., *Independent optical excitation of distinct neural populations*. Nat Methods, 2014. **11**(3): p. 338-46.
108. Mikosch, M., et al., *Diacidic motif is required for efficient transport of the K⁺ channel KAT1 to the plasma membrane*. Plant Physiology, 2006. **142**(3): p. 923-930.
109. Yamada, K., Y. Osakabe, and K. Yamaguchi-Shinozaki, *A C-terminal motif contributes to the plasma membrane localization of Arabidopsis STP transporters*. Plos One, 2017. **12**(10).
110. Vert, G., et al., *IRT1, an Arabidopsis transporter essential for iron uptake from the soil and for plant growth*. Plant Cell, 2002. **14**(6): p. 1223-1233.
111. Chen, J.G., et al., *A seven-transmembrane RGS protein that modulates plant cell proliferation*. Science, 2003. **301**(5640): p. 1728-1731.
112. Lin, P.J.C., et al., *Secretory carrier membrane proteins interact and regulate trafficking of the organellar (Na⁺,K⁺)/H⁺ exchanger NHE7*. Journal of Cell Science, 2005. **118**(9): p. 1885-1897.
113. Li, C., H.M. Wu, and A.Y. Cheung, *FERONIA and Her Pals: Functions and Mechanisms*. Plant Physiology, 2016. **171**(4): p. 2379-2392.
114. Hematy, K., et al., *A receptor-like kinase mediates the response of Arabidopsis cells to the inhibition of cellulose synthesis*. Current Biology, 2007. **17**(11): p. 922-931.
115. Barbier-Brygoo, H., et al., *Anion channels in higher plants: functional characterization, molecular structure and physiological role*. Biochim Biophys Acta, 2000. **1465**(1-2): p. 199-218.
116. Shepard, B.D., et al., *A cleavable N-terminal signal peptide promotes widespread olfactory receptor surface expression in HEK293T cells*. PLoS One, 2013. **8**(7): p. e68758.
117. Kumari, A., et al., *Arabidopsis H⁽⁺⁾-ATPase AHAI controls slow wave potential duration and wound-response jasmonate pathway activation*. Proc Natl Acad Sci U S A, 2019. **116**(40): p. 20226-20231.
118. Battle, M.W., F. Vegliani, and M.A. Jones, *Shades of green: untying the knots of green photoperception*. J Exp Bot, 2020. **71**(19): p. 5764-5770.
119. Ishizaki, H. and T. Akiya, *Effects of Chlorine on Growth and Quality of Tobacco*. Jarq-Japan Agricultural Research Quarterly, 1978. **12**(1): p. 1-6.
120. Franco-Navarro, J.D., et al., *Chloride regulates leaf cell size and water relations in tobacco plants*. J Exp Bot, 2016. **67**(3): p. 873-91.
121. Gaxiola, R.A., M.G. Palmgren, and K. Schumacher, *Plant proton pumps*. FEBS Lett, 2007. **581**(12): p. 2204-14.
122. Grefen, C., et al., *A ubiquitin-10 promoter-based vector set for fluorescent protein tagging facilitates temporal stability and native protein distribution in transient and stable expression studies*. Plant J, 2010. **64**(2): p. 355-65.
123. Khadilkar, A.S., et al., *Constitutive and Companion Cell-Specific Overexpression of AVPI, Encoding a Proton-Pumping Pyrophosphatase,*

- Enhances Biomass Accumulation, Phloem Loading, and Long-Distance Transport*. Plant Physiol, 2016. **170**(1): p. 401-14.
124. Pizzio, G.A., et al., *Arabidopsis Type I Proton-Pumping Pyrophosphatase Expresses Strongly in Phloem, Where It Is Required for Pyrophosphate Metabolism and Photosynthate Partitioning*. Plant Physiology, 2015. **167**(4): p. 1541-U676.
 125. Wang, Y., M.R. Blatt, and Z.H. Chen, *Ion transport at the plant plasma membrane*. eLS, 2018: p. 1-16.
 126. Geibel, S., et al., *The voltage-dependent proton pumping in bacteriorhodopsin is characterized by optoelectric behavior*. Biophysical Journal, 2001. **81**(4): p. 2059-2068.
 127. Szundi, I., R. Bogomolni, and D.S. Kliger, *Platymonas subcordiformis Channelrhodopsin-2 (PsChR2) Function: II. RELATIONSHIP OF THE PHOTOCHEMICAL REACTION CYCLE TO CHANNEL CURRENTS*. J Biol Chem, 2015. **290**(27): p. 16585-94.
 128. Hochbaum, D.R., et al., *All-optical electrophysiology in mammalian neurons using engineered microbial rhodopsins*. Nature methods, 2014. **11**(8): p. 825-833.
 129. Inagaki, H.K., et al., *Optogenetic control of Drosophila using a red-shifted channelrhodopsin reveals experience-dependent influences on courtship*. Nature Methods, 2014. **11**(3): p. 325-U311.
 130. Govorunova, E.G., et al., *NEUROSCIENCE. Natural light-gated anion channels: A family of microbial rhodopsins for advanced optogenetics*. Science, 2015. **349**(6248): p. 647-50.
 131. Govorunova, E.G., et al., *The Expanding Family of Natural Anion Channelrhodopsins Reveals Large Variations in Kinetics, Conductance, and Spectral Sensitivity*. Sci Rep, 2017. **7**: p. 43358.
 132. Chuong, A.S., et al., *Noninvasive optical inhibition with a red-shifted microbial rhodopsin*. Nat Neurosci, 2014. **17**(8): p. 1123-9.
 133. Main, G.D., S. Reynolds, and J.S. Gartland, *Electroporation protocols for Agrobacterium*. Methods Mol Biol, 1995. **44**: p. 405-12.
 134. Li, X., *A transient expression assay using Arabidopsis mesophyll protoplasts*. Bio-Protocol, 2011. **1**: p. e70.
 135. Li, X., *Infiltration of Nicotiana benthamiana protocol for transient expression via Agrobacterium*. Bio-protocol, 2011. **1**(e95).
 136. Science, A.A.f.t.A.o., *A simple and general method for transferring genes into plants*. Science, 1985. **227**(4691): p. 1229-1231.
 137. Rosales-Campos, A.L., A. Gutiérrez-Ortega, and D.d.E.d.J. Guadalajara, *Agrobacterium-mediated Transformation of Nicotiana tabacum cv. Xanthi Leaf Explants*. 2019.
 138. Lichtenthaler, H.K., *Chlorophylls and Carotenoids - Pigments of Photosynthetic Biomembranes*. Methods in Enzymology, 1987. **148**: p. 350-382.
 139. Kaleniecka, A. and P.K. Zarzycki, *Degradation Studies of Selected Bisphenols in the Presence of β -Cyclodextrin and/or Duckweed Water Plant*. Journal of

- AOAC International, 2020. **103**(2): p. 439-448.
140. Bueno, A., et al., *Cuticular wax coverage and its transpiration barrier properties in Quercus coccifera L. leaves: does the environment matter?* Tree physiology, 2020. **40**(7): p. 827-840.
 141. Zhang, X.R., et al., *Agrobacterium-mediated transformation of Arabidopsis thaliana using the floral dip method.* Nature Protocols, 2006. **1**(2): p. 641-646.

Declaration of independence

Three Ph.D. students (Meiqi Ding, Jing Yu-Strzelczyk, and me) take part in this study. Meiqi Ding mainly takes charge of the preparation of transgenic *Nicotiana tabacum*, research on tobacco pollen tubes. Jing Yu-Strzelczyk provided the results of membrane potential recording in the process of screening interest opsins and a part of data for the voltage changes in transgenic *N. tabacum*. In fact, we all participated in each other's work during the research, so there was no obvious boundary in our work.

I hereby declare that my thesis entitled:

The exploitation of opsin-based optogenetic tools for application in higher plants

Except for the help from my colleagues in the same project, I did not receive any help or support from commercial consultants. All sources and/or materials applied are listed and specified in the thesis.

Furthermore, our work on the ACR1 was published in *Nature Plants* with the title “Optogenetic control of plant growth by a microbial rhodopsin”, but the work on XXM and PPR has not been submitted as part of another examination process neither in identical nor in a similar form.

Wuerzburg

Date:

Signature:

Yang Zhou

Acknowledgments

In the project, I appreciate Prof. Dr. Georg Nagel (Physiological Institute, Wuerzburg), Dr. Shiqiang Gao (Physiological Institute, Wuerzburg), and Dr. Kai Konrad (Institute for Molecular Plant Physiology and Biophysics, Wuerzburg) for their guidance and support in my work. Prof. Dr. Georg Nagel provides the fund and much constructive suggestion in the research, Dr. Shiqiang Gao presented the idea which produced retinal in plants and designed the whole project with Prof. Dr. Georg Nagel. Dr. Kai Konrad gave us much valuable advice in the experiment about plants. Besides, I express my thanks to Prof. Dr. Wolfgang Dröge-Laser (department of Pharmaceutical Biology, Wuerzburg) for his help and advice during my research. Especially, I do appreciate Meiqi Ding and Jing Yu-Strzelczyk for their work and help in this study. Without their contribution, this project could not be promoted smoothly. Besides, I am grateful to Dr. Markus Krischke (Pharmaceutical Biology, Wuerzburg) who detected the concentration of retinal and β -carotene, and Dr. Jana Leide (Department of Botany II, Wuerzburg) did the leaf cuticular waxes and sucrose esters detection. Also, I give my thanks to my colleagues for their help in my work and life. Especially, thank my family for their support. At last, thanks a lot for the financial support from Prof. Georg Nagel, the China scholarship council, and DAAD.

Curriculum Vitae

Personal information

Name: Yang Zhou
Birth: 02.06.1985 in Henan, China
Current Address: Frankfurter Str. 17, 97082, Wuerzburg
E-mail: yang.zhou@nui-wuerzburg.de zhouyang198562@126.com

Education

10/2016—04.2021	Wuerzburg University, Germany	Ph.D. in optogenetics
09/2012--07/2015	Zhengzhou University, China	M.S in Biochemistry and Molecular Biology
09/2005--07/2009	Zhengzhou University, China	B.S in Bio-engineering

Publications

Yang Zhou, Meiqi Ding, Jing Yu-Strzelczyk, et al., Optogenetic control of plant growth by a microbial rhodopsin, *Nature plants*, 7, 144-151 (2021).

Yang Zhou, Meiqi Ding, Xiaodong Duan, et al., "Extending the Anion Channelrhodopsin-Based Toolbox for Plant Optogenetics" *Membranes*, 11, no. 4: 287 (2021).

Pinging Li, **Yang Zhou**, Qian Li, et al. Extending the linker region increases the activity of the Bacillus subtilis cellulase Cell15. *Biotechnol Lett*, 38, 1587–1593 (2016).

Haonan Chang, Bei-Yuan Liu, Yunkun Qi, **Yang Zhou**, et al, Blocking of the PD-1/PD-L1 Interaction by a d-Peptide Antagonist for Cancer Immunotherapy, *Angew. Chem. Int. Ed*, 54, 1-6 (2015)

Date:

Signature: